



Search for pair production of squarks or gluinos decaying via sleptons or weak bosons in final states with two same-sign or three leptons with the ATLAS detector

The ATLAS Collaboration

A search for pair production of squarks or gluinos decaying via sleptons or weak bosons is reported. The search targets a final state with exactly two leptons with same-sign electric charge or at least three leptons without any charge requirement. The analysed data set corresponds to an integrated luminosity of 139 fb^{-1} of proton–proton collisions collected at a centre-of-mass energy of 13 TeV with the ATLAS detector at the LHC. Multiple signal regions are defined, targeting several SUSY simplified models yielding the desired final states. A single control region is used to constrain the normalisation of the $WZ + \text{jets}$ background. No significant excess of events over the Standard Model expectation is observed. The results are interpreted in the context of several supersymmetric models featuring R-parity conservation or R-parity violation, yielding exclusion limits surpassing those from previous searches. In models considering gluino (squark) pair production, gluino (squark) masses up to 2.2 (1.7) TeV are excluded at 95% confidence level.

Contents

| | | |
|-----------|---|-----------|
| 1 | Introduction | 2 |
| 2 | ATLAS detector | 3 |
| 3 | Signal models | 5 |
| 4 | Data and samples of simulated events | 7 |
| 5 | Object selection | 8 |
| 6 | Event selection | 10 |
| 6.1 | RPC SRs | 10 |
| 6.2 | RPV SRs | 12 |
| 7 | Background estimation | 13 |
| 7.1 | SM processes with prompt same-sign leptons | 13 |
| 7.2 | Electrons with incorrect charge | 13 |
| 7.3 | Fake and non-prompt leptons | 14 |
| 7.4 | Validation of the background estimates | 15 |
| 8 | Systematic uncertainties | 15 |
| 9 | Statistical analysis | 17 |
| 10 | Results | 19 |
| 11 | Conclusion | 26 |

1 Introduction

The ATLAS experiment [1] at the Large Hadron Collider (LHC) [2] probes the electroweak sector of the Standard Model (SM) at the TeV scale. The presence of prompt electrons or muons (collectively referred to as leptons) in reconstructed events provides one of the main experimental signatures to isolate processes mediated by electroweak, scalar or exotic couplings, from the large QCD multijet background produced in proton–proton (pp) collisions. The production of pairs of leptons with the same electric charge (also referred to as ‘same-sign leptons’) is particularly rare in the SM, with an inclusive cross section of about 1 pb [3] for centre-of-mass energies around 13 TeV. In contrast, it may occur frequently in scenarios with physics beyond the SM (BSM physics) [4–6], and therefore searches for anomalous production of same-sign leptons have been integral parts of the LHC and Tevatron experimental programmes [7–9].

Extensions of the SM introducing invariance under supersymmetric transformations [10–15] (SUSY) provide many such possibilities. Even minimal realisations such as the Minimal Supersymmetric Standard Model (MSSM) [16, 17] contain SUSY partners for all SM fields as well as members of an extended Higgs sector [18] that may decay in complex cascades involving leptons. In the MSSM, SUSY transformations relate each of the Weyl components of a fundamental SM chiral fermion f to a new scalar field, \tilde{f}_L or \tilde{f}_R ,

with identical gauge charges. The quarks and leptons thus lead to 12 physical squarks (\tilde{q}) and 9 sleptons ($\tilde{\ell}$, $\tilde{\nu}$). Gluinos \tilde{g} are the spin-1/2 Majorana fermionic partners of SM gluons. The partners of electroweak and Higgs bosons mix to form spin-1/2 mass eigenstates referred to as neutralinos $\tilde{\chi}_i^0$ ($i = 1, \dots, 4$, ordered by increasing mass) for the neutral ones, and as charginos $\tilde{\chi}_j^\pm$ ($j = 1, 2$) for the others. Depending on the dominant components of the admixtures, they might be described as bino-, wino- or higgsino-like, with important consequences for the mass spectrum and main decay channels [19].

By assuming an ad hoc discrete symmetry, the R-parity [20], the lightest SUSY particle (LSP) becomes stable and may contribute to dark matter [21, 22]. In many models the LSP is the lightest neutralino $\tilde{\chi}_1^0$, which interacts weakly and thus leaves missing transverse momentum as its characteristic signature in the detector. Other phenomenological consequences in R-parity-conserving (RPC) models include SUSY partners always being produced in pairs, with cascade decays into a final state of LSPs and SM particles. On the other hand, R-parity-violating (RPV) models [23] may allow non-conservation of baryon number or lepton number, potentially necessary for grand unification [24] or neutrino flavour mixing. Detector signatures in such models are highly variable since they depend on the nature and strength of the non-zero RPV couplings, and can significantly enhance the production of multilepton final states at the LHC.

A search for pair production of gluinos or squarks with the ATLAS experiment is presented in the following. Different types of cascade decays are considered, arising in either RPC or RPV SUSY scenarios, which lead to final states with either two same-sign leptons or three leptons, several jets and, in many cases, missing transverse momentum. The analysis makes use of the full set of data collected during Run 2 of the LHC. The results complement and improve upon those from an earlier search [25] performed on the same data set, yielding increased sensitivity for two benchmark scenarios while also providing new tailored search regions for processes or decay modes not considered in Ref. [25], such as the production of first- or second-generation squarks. A search with a similar purpose was performed by the CMS experiment [26]. Models with squark production were probed previously by ATLAS during Run 1 [27].

The paper is organised as follows. An overview of the ATLAS detector is provided in Section 2, followed in Section 3 by descriptions of the different SUSY processes of relevance. Details of the recorded data used for the analysis, and of the simulated Monte Carlo (MC) samples, are given in Section 4, while the reconstruction of different types of high-level objects from those inputs is described in Section 5. The definitions of several search regions used to look for the chosen SUSY processes are motivated in Section 6. The estimation of SM backgrounds is described in Section 7, followed by a summary of the sources of systematic uncertainty affecting background or signal predictions in Section 8. The various estimates are compared with observations in control and signal regions by using a coherent statistical framework described in Section 9, providing the results listed in Section 10 and used to perform signal-strength hypothesis tests for the various SUSY benchmarks. Concluding remarks are provided in Section 11.

2 ATLAS detector

The ATLAS detector [1] at the LHC covers nearly the entire solid angle around the collision point.¹ It consists of an inner tracking detector surrounded by a thin superconducting solenoid, electromagnetic and

¹ ATLAS uses a right-handed coordinate system with its origin at the nominal interaction point (IP) in the centre of the detector and the z -axis along the beam pipe. The x -axis points from the IP to the centre of the LHC ring, and the y -axis points upwards. Cylindrical coordinates (r, ϕ) are used in the transverse plane, ϕ being the azimuthal angle around the z -axis. The pseudorapidity is defined in terms of the polar angle θ as $\eta = -\ln \tan(\theta/2)$. Angular distance is measured in units of $\Delta R \equiv \sqrt{(\Delta\eta)^2 + (\Delta\phi)^2}$.

hadron calorimeters, and a muon spectrometer incorporating three large superconducting air-core toroidal magnets.

The inner-detector system (ID) is immersed in a 2 T axial magnetic field and provides charged-particle tracking in the range $|\eta| < 2.5$. The high-granularity silicon pixel detector covers the vertex region and typically provides four measurements per track, the first hit normally being in the insertable B-layer installed before Run 2 [28, 29]. It is followed by the silicon microstrip tracker, which usually provides eight measurements per track. These silicon detectors are complemented by the transition radiation tracker (TRT), which enables radially extended track reconstruction up to $|\eta| = 2.0$. The TRT also provides electron identification information based on the fraction of hits (typically 30 in total) above a higher energy-deposit threshold corresponding to transition radiation.

The calorimeter system covers the pseudorapidity range $|\eta| < 4.9$. Within the region $|\eta| < 3.2$, electromagnetic calorimetry is provided by barrel and endcap high-granularity lead/liquid-argon (LAr) calorimeters, with an additional thin LAr presampler covering $|\eta| < 1.8$ to correct for energy loss in material upstream of the calorimeters. Hadron calorimetry is provided by the steel/scintillator-tile calorimeter, segmented into three barrel structures within $|\eta| < 1.7$, and two copper/LAr hadron endcap calorimeters. The solid angle coverage is completed with forward copper/LAr and tungsten/LAr calorimeter modules optimised for electromagnetic and hadronic energy measurements respectively.

The muon spectrometer (MS) comprises separate trigger and high-precision tracking chambers measuring the deflection of muons in a magnetic field generated by the superconducting air-core toroidal magnets. The field integral of the toroids ranges between 2.0 and 6.0 T m across most of the detector. Three layers of precision chambers, each consisting of layers of monitored drift tubes, cover the region $|\eta| < 2.7$, complemented by cathode-strip chambers in the forward region, where the background is highest. The muon trigger system covers the range $|\eta| < 2.4$ with resistive-plate chambers in the barrel, and thin-gap chambers in the endcap regions.

Interesting events are selected by the first-level trigger system implemented in custom hardware, followed by selections made by algorithms implemented in software in the high-level trigger [30]. The first-level trigger accepts events from the 40 MHz bunch crossings at a rate below 100 kHz, which the high-level trigger further reduces in order to record events to disk at about 1 kHz.

An extensive software suite [31] is used in data simulation, in the reconstruction and analysis of real and simulated data, in detector operations, and in the trigger and data acquisition systems of the experiment.

3 Signal models

This analysis considers experimental signatures arising from the production of either gluino pairs or squark–antisquark pairs $\tilde{q}\tilde{q}^*$ (with $q = u, d, s, c$). Several gluino and squark decay modes are investigated, and these are summarised in Figure 1: in most cases the first step of the decay chain is to a non-stable neutralino or chargino $\tilde{\chi}$ and SM quark(s) of first or second generation. Various $\tilde{\chi}$ decay modes may lead to final states featuring two same-sign leptons or three leptons. Amongst those possibilities, this analysis searches especially for the following sources of electrons and muons:

- $\tilde{\chi}$ decays into SM gauge bosons and $\tilde{\chi}_1^0$ LSPs; although the direct decays $\tilde{\chi}_1^\pm \rightarrow W^\pm \tilde{\chi}_1^0$ and $\tilde{\chi}_2^0 \rightarrow Z \tilde{\chi}_1^0$ are most efficiently probed with other experimental signatures [32–34], more favourable branching ratios to same-sign leptons are found for cascade decays such as $\tilde{\chi}_1^\pm \rightarrow \tilde{\chi}_2^0 W^\pm \rightarrow \tilde{\chi}_1^0 Z W^\pm$, as illustrated in Figures 1(a) and 1(b), which are thus the focus here.
- $\tilde{\chi}$ decays into sleptons and subsequently into SM leptons and $\tilde{\chi}_1^0$ LSPs, such as $\tilde{\chi}_1^\pm (\rightarrow \tilde{\ell} \tilde{\nu}) \rightarrow \ell \nu \tilde{\chi}_1^0$ or $\tilde{\chi}_2^0 (\rightarrow \tilde{\ell} \tilde{\ell}) \rightarrow \ell^+ \ell^- \tilde{\chi}_1^0$, as illustrated in Figures 1(c) and 1(d).
- direct $\tilde{\chi}_1^0$ decay into SM leptons and quarks, $\tilde{\chi}_1^0 \rightarrow u \bar{d} \ell^+$, via a non-zero RPV coupling λ' as illustrated in Figure 1(e).
- $\tilde{g} \rightarrow \tilde{t} \bar{t} \rightarrow \bar{t} b q$ decays via a non-zero RPV coupling λ'' , shown in Figure 1(f).

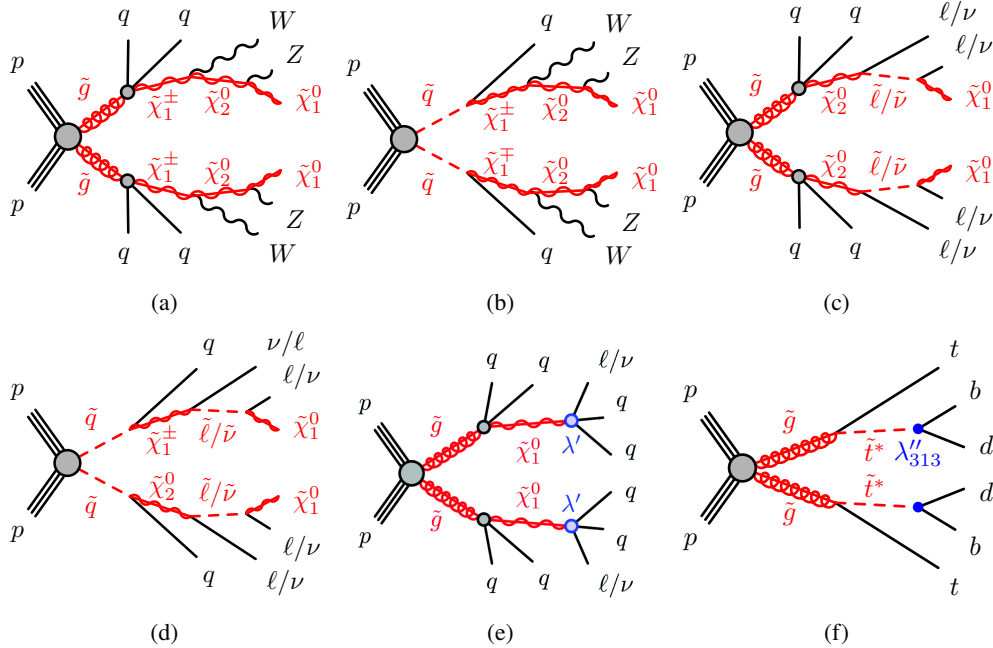


Figure 1: Examples of sources of same-sign leptons which may arise in supersymmetric processes and are targeted by the search regions of the analysis.

The experimental sensitivity to such processes is assessed in simplified models [35–37] where only the superpartners directly involved in the process of interest are considered, alternative production and decay modes are ignored, and masses and mixings of superpartners are either varied freely or fixed to chosen values.

For the cascade decays of charginos into pairs of SM bosons (Figures 1(a) and 1(b)), the gluino (or squark) and $\tilde{\chi}_1^0$ LSP masses are varied independently to generate different scenarios. The masses of intermediate superpartners are then set halfway in between, i.e. $m(\tilde{\chi}_1^\pm) = (m(\tilde{g}/\tilde{q}) + m(\tilde{\chi}_1^0))/2$ and $m(\tilde{\chi}_2^0) = (m(\tilde{\chi}_1^\pm) + m(\tilde{\chi}_1^0))/2$. The decay of $\tilde{\chi}_1^\pm$ and $\tilde{\chi}_2^0$ to leptons takes place through real or virtual W/Z bosons, depending on the mass difference from the LSP. Quarks produced in the first step of the gluino decay chain are assumed to be u, d, s or c with equal probability. Due to the small Yukawa couplings for the first two quark generations, the decays $\tilde{g} \rightarrow qq\tilde{\chi}_1^\pm$ and $\tilde{q} \rightarrow q\tilde{\chi}_1^\pm$ are only relevant for a wino-like chargino [38], so only production of left-handed squarks is considered. In minimal models with a neutralino LSP [38], such chargino cascade decays and a non-degenerate mass hierarchy may occur when neutralinos are non-trivial admixtures, but these would compete with several other, generally more favourable, decay modes [19]. In gauge-mediated [39–41] SUSY breaking models, however, this can be a more natural mode in the alternative form $\tilde{\chi}_1^\pm \rightarrow W^\pm\tilde{\chi}_1^0 \rightarrow W^\pm Z\tilde{G}$ where the gravitino \tilde{G} is the LSP. Previous ATLAS searches using various signatures [25, 27, 42, 43] probed gluino masses up to 2 TeV and squark masses up to 630 GeV with these decay modes.

Similarly, for the decays of charginos and neutralinos into sleptons (Figures 1(c) and 1(d)), gluino (or squark) and $\tilde{\chi}_1^0$ LSP masses are varied independently, while the masses of intermediate superpartners are set to $m(\tilde{\chi}_1^\pm/\tilde{\chi}_2^0) = (m(\tilde{g}/\tilde{q}) + m(\tilde{\chi}_1^0))/2$ and $m(\tilde{\ell}/\tilde{\nu}) = (m(\tilde{\chi}_1^\pm/\tilde{\chi}_2^0) + m(\tilde{\chi}_1^0))/2$. Such scenarios arise in the mass spectra of models where sleptons are light, and thus were searched for in early LHC analyses [44–46]. Gluinos are chosen to decay only into $\tilde{\chi}_2^0$ while squarks are equally likely to decay into either $\tilde{\chi}_1^\pm$ or $\tilde{\chi}_2^0$. In both cases, the neutralino or chargino subsequently decays in an equiprobable way into any of the six SM leptons, together with the left-handed slepton appropriate for charge and lepton number conservation. The latter decays exclusively into its SM partner and the LSP. Previous ATLAS searches [25, 27, 42, 43] probed gluino masses up to 2.2 TeV and squark masses up to 850 GeV. The intermediate charginos or sleptons are also constrained by previous analyses [47–50], but for these particles the present analysis can probe masses higher than those excluded by the direct-production searches, thanks to their higher production rate in the cascade decays of gluinos or squarks.

Finally, event kinematics in the case of neutralino decays via λ' RPV couplings (Figure 1(e)) are completely determined by the gluino and $\tilde{\chi}_1^0$ LSP masses, which again are varied independently to generate different scenarios. Without choosing explicit values, it is assumed that the relevant λ' couplings can be large enough to allow prompt $\tilde{\chi}_1^0$ decay into $\ell^-u\bar{d}$ or $\nu_\ell d\bar{d}$ ($\ell = e, \mu$), or their charge conjugates, with equal probabilities, while evading low-energy experimental bounds [51]. The $\tilde{\chi}_1^0$ natural width also depends on the mass of virtual squarks mediating the decay and is set to 100 MeV. For such a scenario, current experimental sensitivity [52] excludes gluino masses up to 2.2 TeV.

An additional scenario exemplified in Figure 1(f) is considered, in which pair-produced gluinos decay into the lightest top squark (and a SM top quark) which itself decays via a suitable λ'' RPV coupling into a pair of quarks, leading in half of the cases to a final state with two same-sign top quarks and up to four jets. Such scenarios were highlighted in Ref. [53] especially, and searches have been performed in the $t\bar{t}bbqq$ [25, 26, 52] and $t\bar{t}qqqq$ [54] final states. In the present analysis, only the former case is addressed, as it yields a clearer experimental signature; for this scenario, Ref. [52] excluded gluino masses up to 1.8 TeV for top squark masses around 1 TeV. A set of benchmark models is generated by varying the gluino and top squark masses independently, the latter being bounded from below by existing constraints on $t\bar{t}^*$ production [55]. The top squarks are assumed to decay promptly. A new set of search regions allows the sensitivity to be extended beyond that reached in Ref. [25] with the same data.

4 Data and samples of simulated events

The results presented here are obtained by analysing proton–proton collision data collected during Run 2 of the LHC at a centre-of-mass energy of 13 TeV. The number of simultaneous inelastic interactions averages to 33.7 for the entire data set [56], but exceeds 70 in a small fraction of the data. Events recorded when parts of the detector were not functional or reserved for detector commissioning or calibration purposes are subsequently ignored, leaving 95.6% of the recorded data [56] available for analysis. The integrated luminosity of this data set amounts to 139 fb^{-1} , with an uncertainty of 1.7%. The latter is obtained [57] using the LUCID-2 detector [58] for the primary luminosity measurements.

Large samples of simulated events are also employed, mainly to predict contributions from SM processes with prompt² leptons to the search regions used in this analysis, as well as those from hypothetical SUSY signal processes. Other usages include validating assumptions employed in data-based background estimation methods and, more generally, assessing systematic uncertainties. Those samples were obtained by simulating individual proton–proton collisions for hard-interaction processes of interest with the different combinations of MC event generators described below. The events were then processed through a detailed simulation of the ATLAS detector [59] based on GEANT4 [60]. In some cases, notably for BSM signal samples, a faster simulation which relies on a parameterisation of the calorimeter response [61] was used instead. At this stage, additional minimum-bias interactions generated by PYTHIA 8.186 were simulated separately and overlaid on each simulated hard-interaction event to account for pile-up effects. The response of the detector and its electronic readout chain is then emulated [59], also accounting for effects from interactions in the previous and following bunch-crossings. Reconstructed events are reweighted to reproduce the measured distributions of the number of simultaneous interactions in different data-taking periods and the measured effects of various sources of reconstruction inefficiency, for example in the application of electron identification algorithms. Specific kinematic variables, such as lepton momenta, are smeared to reproduce the measured detector resolution.

The MC generators used to simulate the main SM processes of interest are summarised in Table 1, together with the selected parton shower algorithms, the sets of tuned parameters (tunes), and the sets of parton distribution functions (PDF). When PYTHIA was used, the decays of bottom and charm hadrons were simulated with the EVTGEN program [62]. Diboson processes [63] include all resonant and non-resonant $pp \rightarrow 3\ell\nu/4\ell/\ell^\pm\ell^\pm\nu\nu$ processes of order α^4 in the fine-structure constant, including Higgs boson contributions, as well as the vector-boson scattering/fusion processes at order α^6 . Triboson processes similarly include all the relevant resonant and non-resonant processes with up to six charged leptons in the final state at order α^6 . The associated production of $t\bar{t}$ and an on-shell W boson includes a complementary sample generated at leading order (LO) in QCD with the matrix elements of order α^3 . Associated production of $t\bar{t}$ and a pair of same-flavour opposite-sign (SFOS) leptons was generated for dilepton invariant masses as low as 1 GeV. Other processes not identified individually in the table but included in the background estimates comprise associated production of $t\bar{t}$ and two vector or Higgs bosons, associated production of single top quarks with one or two vector or Higgs bosons, and production of three top quarks. Fast detector simulation was employed for the $4t$, tH , tWH , $t\bar{t}ZZ$, $t\bar{t}WH$, $t\bar{t}HH$ processes.

The SUSY signal samples were generated with MG5_AMC@NLO 2.6.2 [3] and the NNPDF2.3LO PDF, except for the $\tilde{g} \rightarrow q\bar{q}WZ\tilde{\chi}_1^0$ and $\tilde{g} \rightarrow t\bar{b}\bar{q}$ samples, for which the NNPDF3.0LO PDF was used. The

² Prompt leptons are defined as those produced neither in the decay of a hadron, nor radiatively in the fragmentation of quarks and gluons, nor in the conversion of a photon not originating from the electromagnetic shower of a charged lepton. They may originate from the leptonic decay of a prompt τ -lepton.

Table 1: List of Monte Carlo event generators and their settings for the main simulated samples of SM processes. When no reference is provided for the cross-section normalisation, the one computed by the generator is used. LO and NLO denote leading-order and next-to-leading-order calculations, respectively; in some cases (indicated), matrix elements are used with different accuracies depending on the number of additional parton emissions.

| Process | Generator | Computation order | Parton shower | Cross-section normalisation | PDF set | Set of tuned parameters |
|---|--|---|--|-----------------------------------|---------------------------------------|-------------------------|
| $t\bar{t}W$ [64] | SHERPA 2.2.10 [65] + OPENLOOPS [68–70] | NLO 0-1j + LO 2j + LO $O(\alpha^3 \alpha_s)$ | CSShower [66] | NLO | NNPDF3.0NLO [67] | default |
| $t\bar{t}\ell^+\ell^-$ [64] $1 < m_{\ell\ell} < 5$ GeV | SHERPA 2.2.1 [65] MG5_AMC@NLO 2.3.3 [3] | NLO | CSShower [66, 71] | NLO | NNPDF3.0NLO [67] | default |
| $t\bar{t}H$ [74] | POWHEG BOX v2 [65] | NLO | PYTHIA 8.230 [72] | NLO [75] | NNPDF3.0NLO [67] | A14 [73] |
| $t\bar{t}t\bar{t}$ [64] | MG5_AMC@NLO 2.3.3 [3] + MADSPIN [76, 77] | NLO | PYTHIA 8.230 [72] | NLO | NNPDF3.1NLO [67] | A14 [73] |
| Other $t/\bar{t} + X$ [64] | MG5_AMC@NLO 2.3.3 [3] | NLO or LO | PYTHIA 8.210-230 [72] | NLO or LO | NNPDF3.0/3.1NLO [67] | A14 [73] |
| Diboson [63] | SHERPA 2.2.2 [65] + OPENLOOPS [68–70] | NLO 0-1j + LO 2-3j | CSShower [66, 71] | NLO | NNPDF3.0NLO [67] | default |
| Triboson [63] | SHERPA 2.2.1 [65] | LO 0-1j | CSShower [66, 71] | NLO | NNPDF3.0NNLO [67] | default |
| $t\bar{t}$ [78] | POWHEG BOX v2 [79–82] | NLO | PYTHIA 8.230 [83] | NNLO [78] | NNPDF3.0NLO [67] | A14 [73] |
| Single top (s -, t -channel) (tW) | POWHEG BOX v2 [80–82, 84] SHERPA 2.2.7 [65] | NLO | PYTHIA 8.230 [83] CSShower [66, 71] | NNLO [85, 86] NNLO + NNLL [87] | NNPDF3.0NLO [67] NNPDF3.0NNLO [67] | A14 [73] default |
| $W \rightarrow \ell\nu, Z/\gamma^* \rightarrow \ell\ell$ [88] | SHERPA 2.2.11 [65] | NLO 0-2j + LO 3-4j | CSShower [66, 71] | NNLO [88, 89] | NNPDF3.0NNLO [67] | default |

pair production of gluinos and squarks was simulated at LO, complemented by matrix elements for up to two extra parton emissions. Superpartners not involved in the model of interest were decoupled by being assigned unreachable masses. The decays of gluinos or squarks were factored out of the hard interaction and simulated with PYTHIA 8.235 [83], which was also used for the subsequent stages of the event generation with the A14 tune [73]. The matching between matrix elements and parton showers followed the CKKW-L prescription [90], with a matching scale set to one quarter of the gluino or squark mass. For all models, the fast simulation was used to process the generated events. Signal cross sections are calculated to approximate next-to-next-to-leading order in the strong coupling constant, adding the resummation of soft gluon emission at next-to-next-to-leading-logarithm accuracy (approximate NNLO+NNLL) [91–98]. The nominal cross section and its uncertainty are derived using the PDF4LHC15_mc PDF set, following the recommendations of Ref. [99].

5 Object selection

Charged-particle tracks with $|\eta| < 2.5$ are reconstructed [100–102] in the ID and combined to form primary vertex candidates [103–105]. The vertex with the largest $\sum (p_T^{\text{track}})^2$ formed by at least two tracks is taken to be the primary vertex and position of the hard-scattering interaction. The transverse and longitudinal impact parameters of the tracks, denoted by d_0 and z_0 respectively, are measured at their point of closest approach to the beam line [106]. Requirements placed on the ratio $|d_0^{\text{sig}}|$ of d_0 to its estimated uncertainty $\sigma(d_0)$ and on the value of $|z_0 \sin(\theta)|$ with respect to the primary vertex are stated below.

Jets with $|\eta| < 4.5$ are reconstructed with the FASTJET implementation [107] of the anti- k_t algorithm [108], with radius parameter $R = 0.4$, out of particle-flow objects [109, 110] combining calorimeter energy deposits [111] and ID tracks. The jet’s p_T , energy and mass are calibrated to the particle level [109], and only jets with $p_T > 20$ GeV are retained. Those originating from pile-up interactions, according to a track-based discriminant [112], are rejected. For selection criteria referring to the number of jets, only jets with $|\eta| < 2.8$ are counted. Around 0.5% of the selected events are discarded due to the presence of jets from sources [113] other than pp interactions. Within the ID acceptance, jets containing bottom hadrons (referred to as b -jets) are identified with the DL1r tagging algorithm [114], which exploits the properties

of reconstructed tracks and secondary vertices. The analysis selects true b -jets with an estimated 70% efficiency in $t\bar{t}$ events while rejecting 99.8% of other jets free of charm hadrons or τ -leptons [114].

Muons with $|\eta| < 2.5$ and $p_T > 10$ GeV are used. They are obtained [115] from an iterated track fit of ID and MS hits. Momentum corrections [116] compensate for detector misalignments. The ‘Medium’ quality criteria defined in Ref. [115] are applied, and pile-up muons are rejected by requiring $|z_0 \sin(\theta)| < 0.5$ mm. The candidates satisfying these requirements are referred to as baseline muons. Around 0.1% of events contain a muon from a cosmic-ray shower or with poor expected momentum resolution, and are rejected. Prompt muons are further distinguished from background sources with a requirement $|d_0^{\text{sig}}| < 3$ and an isolation criterion [115] consisting of an upper bound of 6%, relative to the muon p_T , on the summed $|p_T|$ of suitable ID tracks³ within $\Delta R < \min(0.3, 10 \text{ GeV}/p_T(\mu))$. They are referred to as signal muons.

Electrons with $|\eta| < 2.47$ and $p_T > 10$ GeV are used. They are reconstructed [117] from clustered energy deposits in the electromagnetic calorimeter matched to an ID track re-fitted to account for bremsstrahlung losses. Their momentum is determined by a calibration procedure [117, 118] based on boosted decision trees (BDTs). Electrons within the calorimeter’s barrel-to-endcap transition region $1.37 < |\eta| < 1.52$ are not considered. Electrons from most background sources are rejected with a likelihood discriminant [117] built from information about the development of the electron shower in the calorimeter, its compatibility with the matched track, and particle identification in the TRT detector. Electrons with $|z_0 \sin(\theta)| > 0.5$ mm are rejected. The candidates satisfying these requirements are referred to as baseline electrons. Non-prompt or fake electrons are further suppressed by keeping only electrons within $|\eta| < 2.0$, imposing the tighter ‘MediumLH’ identification criteria [117], a combination of track-based and calorimeter-based isolation criteria [117], and requiring $|d_0^{\text{sig}}| < 5$. The first isolation criterion is similar to the one used for muons, while the other consists of an upper bound of 6%, relative to the electron p_T , on the sum of other calorimeter energy deposits within $\Delta R < 0.2$. Electrons very likely to have a wrongly assigned charge are identified and then rejected using the ECIDS discriminant [117], a BDT which is based on the properties of the electron track and which accepts 98% of simulated $Z \rightarrow ee$ decay electrons while rejecting 90% of those with the wrong charge. The remaining candidates are referred to as signal electrons.

An overlap removal procedure is applied to baseline lepton candidates and jets to avoid treating the same detector signals as multiple objects. Jets close to electrons ($\Delta R < 0.2$) are removed, unless they are classified as b -jets with $p_T < 100$ GeV, and so are jets close to muons ($\Delta R < 0.2$ or sharing an ID track) if they have less than three associated ID tracks. Leptons close to remaining jets ($\Delta R < \min(0.4, 0.1 + 9.6 \text{ GeV}/p_T(\ell))$) are removed, as they are likely to be fake or non-prompt; the ΔR bound is smaller at high p_T to retain leptons from boosted top quark or $\tilde{\chi}_1^0$ decays. Electrons close to muons ($\Delta R < 0.01$) or to higher- p_T electrons ($\Delta R < 0.05$) are removed. Throughout this procedure, ΔR is calculated with the rapidity y rather than the pseudorapidity η .

The missing transverse momentum $\mathbf{p}_T^{\text{miss}}$ and its magnitude E_T^{miss} are reconstructed [119] from selected electrons, muons and jets prior to overlap removal, together with reconstructed photons ($p_T > 25$ GeV, $|\eta| < 2.37$) satisfying ‘Tight’ identification criteria [117] and a track-based ‘soft term’ consisting of softer contributions associated with the primary vertex but not included in aforementioned objects. The E_T^{miss} reconstruction employs its own overlap removal procedure.

³ These have $p_T > 1$ GeV, originate from the primary vertex, and exclude the muon’s own track; more details can be found in Ref. [115].

6 Event selection

Events with $E_T^{\text{miss}} < 250$ GeV were selected using dilepton triggers [120, 121]. Since the luminosity increased during Run 2, the lepton p_T thresholds were raised in steps to a maximum of 24 GeV for triggers requiring two electrons, 22 GeV for triggers requiring two muons, and 17 GeV (14 GeV) for the electron (muon) in different-flavour dilepton triggers. For events with $E_T^{\text{miss}} > 250$ GeV, a logical OR of these dilepton triggers and E_T^{miss} triggers [122] was used. Events are preselected by requiring exactly two signal leptons with the same electric charge or at least three signal leptons⁴ without any charge requirement.

Multiple signal regions (SRs) were defined with the goal of maximising the sensitivity to the signal models shown in Figure 1. These SRs are not exclusive and can overlap. They are primarily built on requirements placed on the number of signal ($n_{\text{Sig}}(\ell)$) and/or baseline ($n_{\text{BL}}(\ell)$) leptons and their relative charges, the number of b -jets ($n_{b\text{-jets}}$) with $p_T > 20$ GeV, the number of jets (n_{jets}) with p_T above 25, 40 or 50 GeV, regardless of their flavour, and also apply independent selections to a series of observables sensitive to kinematic differences between signal and background events. For each SR, numerous candidate observables were assessed, but only those bringing the best sequential improvement in expected sensitivity were retained; this explains the variability in the chosen selection variables for the different SRs. One of the most sensitive observables used across all SRs is the effective mass, m_{eff} , which aids in establishing the mass scale of the processes being probed, and is defined as the scalar sum of the p_T of the jets and leptons and the E_T^{miss} of the event,

$$m_{\text{eff}} = \sum p_T^{\text{jet}} + \sum p_T^\ell + E_T^{\text{miss}}. \quad (1)$$

6.1 RPC SRs

SRs targeting the RPC models are shown in Tables 2–5. Depending on the model, RPC SRs can require events with at least two leptons with the same electric charge, or three or more leptons. SRs with a three-lepton selection accept any charge combination for the three leptons. A veto on b -tagged jets is imposed in order to reduce SM backgrounds with top quarks. For those signal models not involving the presence of a Z boson in the final state (Figures 1(c) and 1(d)), events in which the invariant mass of any pair of two same-flavour opposite-sign leptons is compatible with the Z boson mass ($m_{\text{SFOS}} \in [81, 101]$ GeV) are vetoed.

SRs targeting the benchmark models where pair production of gluinos (Figure 1(a)) and squarks (Figure 1(b)) leads to cascade decays of charginos into pairs of SM bosons are named SRGGWZ and SRSSWZ, respectively. Multiple SRs are defined for each benchmark model, specifically tailored to target the different neutralino and gluino (or squark) mass-splitting scenarios. Those different scenarios are identified by a suffix ‘-L’, ‘-M’, or ‘-H’ –standing for low, medium and high mass splitting– in the SR name, with ‘H’ being the scenario where $m_{\tilde{g}(\tilde{q})} \gg m_{\tilde{\chi}_1^0}$, ‘L’ denoting the scenario where $m_{\tilde{g}(\tilde{q})} \approx m_{\tilde{\chi}_1^0}$, and ‘M’ referring to the SR defined for the intermediate phase space between ‘L’ and ‘H’. For those benchmark models where squarks are pair produced, the SR ‘-M’ is further split into a region in the intermediate phase space close to the low mass splitting, ‘-ML’, and another one close to the high mass splitting, ‘-MH’. Requirements are placed on the jet multiplicity, E_T^{miss} , m_{eff} or $\sum p_T^{\text{jet}}$, depending on the kinematics of the objects generated in the different mass-splitting scenarios. Additional selection criteria are applied to other observables that were

⁴ In the following, unless otherwise stated, ‘leptons’ refers to signal leptons.

found to discriminate strongly between signal and background events. Those variables are the ratios of the different terms present in Eq. (1), i.e. $E_T^{\text{miss}}/\sum p_T^{\text{jet}}$, $E_T^{\text{miss}}/m_{\text{eff}}$, $E_T^{\text{miss}}/\sum p_T^\ell$, $m_{\text{eff}}/\sum p_T^\ell$, $\sum p_T^\ell/\sum p_T^{\text{jet}}$; the azimuthal separation between the system formed by the two leading leptons and the direction of the missing transverse momentum of the event, $\Delta\phi(\ell 1\ell 2, \mathbf{p}_T^{\text{miss}})$; and the E_T^{miss} significance, $\mathcal{S}(E_T^{\text{miss}})$ [123].

Table 2: Definition of the signal regions used for the RPC model shown in Figure 1(a), where pair production of gluinos leads to cascade decays of charginos into pairs of SM bosons.

| SR name | $n_{\text{Sig}}(\ell)$ ($n_{\text{BL}}(\ell)$) | $n_{b\text{-jets}}$ | n_{jets} | p_T^{jet} [GeV] | E_T^{miss} [GeV] | m_{eff} [GeV] | $\Delta\phi(\ell 1\ell 2, \mathbf{p}_T^{\text{miss}})$ | $\mathcal{S}(E_T^{\text{miss}})$ |
|----------|--|---------------------|-------------------|--------------------------|---------------------------|----------------------------|--|----------------------------------|
| SRGGWZ-L | ≥ 2 (≥ 3) | = 0 | ≥ 6 | > 25 | > 200 | $> 8 \times \sum p_T^\ell$ | > 0.2 | > 6 |
| SRGGWZ-M | ≥ 2 (-) | | ≥ 6 | > 40 | > 190 | > 1300 | > 0.8 | - |
| SRGGWZ-H | ≥ 2 (-) | | ≥ 6 | > 40 | > 150 | > 2100 | - | - |

Table 3: Definition of the signal regions used for the RPC model shown in Figure 1(b), where pair production of squarks leads to cascade decays of charginos into pairs of SM bosons.

| SR name | $n_{\text{Sig}}(\ell)$ | $n_{b\text{-jets}}$ | n_{jets} | p_T^{jet} [GeV] | E_T^{miss} [GeV] | m_{eff} [GeV] | $E_T^{\text{miss}}/\sum p_T^\ell$ | $\sum p_T^\ell/\sum p_T^{\text{jet}}$ | $n_{Z \rightarrow \ell^+\ell^-}$ |
|-----------|------------------------|---------------------|-------------------|--------------------------|-------------------------------|------------------------|-----------------------------------|---------------------------------------|----------------------------------|
| SRSSWZ-L | ≥ 3 | = 0 | ≥ 4 | > 25 | $> 0.2 \times m_{\text{eff}}$ | - | - | < 0.2 | $= 0^\dagger$ |
| SRSSWZ-ML | | | ≥ 6 | > 25 | > 150 | > 800 | > 1.2 | < 0.3 | $\geq 1^\dagger$ |
| SRSSWZ-MH | | | ≥ 5 | > 40 | > 200 | > 900 | > 1.1 | < 0.4 | $\geq 1^\dagger$ |
| SRSSWZ-H | | | ≥ 5 | > 40 | > 250 | > 1500 | > 0.3 | < 0.7 | - |

† : based on number of SFOS pairs with $81 < m_{\text{SFOS}} < 101$ GeV

SRs targeting the benchmark models where pair production of gluinos (Figure 1(c)) and squarks (Figure 1(d)) leads to decays of charginos and neutralinos into sleptons are named SRGGSlep and SRSSSlep, respectively. Multiple SRs are defined for the different mass-splitting scenarios and named as per the convention described previously. An extra SR (SRSSSlep-H (loose)) is defined for the RPC model shown in Figure 1(d), using the same selection criteria as for SRSSSlep-H, but with the m_{eff} requirement relaxed to 1 TeV to allow for a binned fit in the model-dependent interpretation (see Section 9). SRs are defined in terms of the variables previously described, with requirements also placed on the p_T of the leading and sub-leading leptons, denoted by $p_T^{\ell 1}$ and $p_T^{\ell 2}$ respectively, and on the angular distance between the two leading leptons, $\Delta R(\ell 1, \ell 2)$.

Table 4: Definition of the signal regions used for the RPC model shown in Figure 1(c), where pair production of gluinos leads to decays of charginos and neutralinos into sleptons.

| SR name | $n_{\text{Sig}}(\ell)$ | $n_{b\text{-jets}}$ | n_{jets} | p_T^{jet} [GeV] | E_T^{miss} [GeV] | $E_T^{\text{miss}}/\sum p_T^{\text{jet}}$ | $p_T^{\ell 2}$ [GeV] | Other |
|------------|------------------------|---------------------|-------------------|--------------------------|---------------------------|---|----------------------|--|
| SRGGSlep-L | $\geq 3^\dagger$ | = 0 | ≥ 4 | ≥ 40 | - | > 0.4 | > 30 | $E_T^{\text{miss}}/\sum p_T^\ell > 1.4$ |
| SRGGSlep-M | | | | | > 150 | > 0.3 | > 70 | $\Delta\phi(\ell 1\ell 2, \mathbf{p}_T^{\text{miss}}) > 0.7$ |
| SRGGSlep-H | | | | | > 100 | - | - | $\sum p_T^{\text{jet}} > 1200$ GeV |

† : SFOS pairs with $81 < m_{\text{SFOS}} < 101$ GeV are not allowed

Table 5: Definition of the signal regions used for the RPC model shown in Figure 1(d), where pair production of squarks leads to decays of charginos and neutralinos into sleptons. Requirements on p_T^ℓ apply to all three leptons.

| SR name | $n_{\text{Sig}}(\ell)$ | p_T^ℓ [GeV] | $n_{b\text{-jets}}$ | n_{jets} | p_T^{jet} [GeV] | E_T^{miss} [GeV] | m_{eff} [GeV] | $\Delta\phi(\ell_1\ell_2, \mathbf{p}_T^{\text{miss}})$ |
|--------------------|--|------------------|---------------------|-------------------|--------------------------|---------------------------|------------------------|--|
| | other requirements | | | | | | | |
| SRSSSlep-L | = 3* | < 60 | = 0 | ≥ 3 | > 60, 60, 25 | > 100 | > 600 | > 1.4 |
| | $\sum p_T^\ell / \sum p_T^{\text{jet}} < 0.6$ | | | | | | | |
| SRSSSlep-ML | = 3* | > 30 | = 0 | ≥ 3 | > 60, 60, 25 | > 100 | > 700 | > 1.4 |
| | $E_T^{\text{miss}} / \sum p_T^\ell > 0.7, \quad \sum p_T^\ell / \sum p_T^{\text{jet}} < 0.6$ | | | | | | | |
| SRSSSlep-MH | = 3* | > 40 | = 0 | ≥ 2 | > 60 | > 200 | > 1000 | > 0.5 |
| | $E_T^{\text{miss}} / \sum p_T^\ell > 0.7, \quad \Delta R(\ell_1, \ell_2) > 0.2$ | | | | | | | |
| SRSSSlep-H | = 3* | > 40 | = 0 | ≥ 2 | > 60 | > 200 | > 2000 | > 0.3 |
| | $\Delta R(\ell_1, \ell_2) > 0.5$ | | | | | | | |
| SRSSSlep-H (loose) | = 3* | > 40 | = 0 | ≥ 2 | > 60 | > 200 | > 1000 | > 0.3 |
| | $\Delta R(\ell_1, \ell_2) > 0.5$ | | | | | | | |

*: additional baseline leptons are not allowed, nor SFOS pairs with $81 < m_{\text{SFOS}} < 101$ GeV

6.2 RPV SRs

SRs targeting the RPV models are shown in Tables 6 and 7. The SRs are named SRLQD and SRUDD, where the former corresponds to the SR defined for the model where the neutralino decays via the λ' RPV coupling of LQD type (Figure 1(e)), and the latter to the SRs defined for the model where gluinos decay via top squarks and the λ'' RPV coupling of UDD type (Figure 1(f)). For the latter, the suffix appended to the SR name indicates the requirement on the number of b -jets. Those SRs require exactly two leptons with the same electric charge, high jet multiplicity, and high $\sum p_T^{\text{jet}}$ or high m_{eff} . No requirement is placed on the E_T^{miss} as no neutralinos are expected in the final state of RPV model events.

Table 6: Definition of the signal region used for the RPV model shown in Figure 1(e), where the neutralino decays via the λ' RPV coupling of LQD type.

| SR name | $n_{\text{Sig}}(\ell)$ | $n_{b\text{-jets}}$ | n_{jets} | p_T^{jet} [GeV] | m_{eff} [GeV] |
|---------|------------------------|---------------------|-------------------|--------------------------|------------------------|
| SRLQD | = 2 | – | ≥ 5 | > 50 | > 2600 |

Table 7: Definition of the signal regions used for the RPV model shown in Figure 1(f), where gluinos decay via top squarks and the λ'' RPV coupling of UDD type.

| SR name | $n_{\text{Sig}}(\ell)$ | $n_{b\text{-jets}}$ | n_{jets} | p_T^{jet} [GeV] | m_{eff} [GeV] | $\sum p_T^{\text{jet}}$ [GeV] |
|------------|------------------------|---------------------|-------------------|--------------------------|------------------------|-------------------------------|
| SRUDD-1b | = 2 | = 1 | ≥ 6 | > 50 | – | > 1600 |
| SRUDD-2b | | = 2 | ≥ 2 | > 25 | – | > 1700 |
| SRUDD-ge2b | | ≥ 2 | ≥ 5 | > 50 | – | > 1600 |
| SRUDD-ge3b | | ≥ 3 | ≥ 4 | > 50 | > 1600 | – |

7 Background estimation

Background contributions to the search regions can be divided into three categories, consisting in SM processes with genuine same-sign leptons in the final state, and other SM processes forming same-sign lepton pairs because of the incorrect reconstruction of an electron’s charge or the presence of fake or non-prompt (F/NP) leptons. The following three sub-sections detail the estimation method for each category: processes with genuine same-sign leptons are estimated with MC simulations, aided by a single control region in the data, while for the other two, data events with specific lepton selection criteria are exploited. Comparisons between background predictions and observed data in carefully designed validation regions are presented in a fourth sub-section.

7.1 SM processes with prompt same-sign leptons

The largest contribution to the RPC SRs originates from WZ + jets with both bosons decaying into leptons. All these SRs veto events with b -jets, which suppresses processes involving top quarks. For WZ + jets, a control region intermediate in jet multiplicity is employed, referred to as CRWZ2j. It is defined with three signal leptons (and no fourth baseline lepton), two of them forming a SFOS pair with invariant mass in the range $81 < m_{\text{SFOS}} < 101$ GeV. The two same-sign leptons of the triplet must have $p_{\text{T}} > 15$ GeV, and the sum of the three leptons’ p_{T} must exceed 130 GeV. Events must contain either two or three jets with $p_{\text{T}} > 25$ GeV, with no b -jet present. Contributions from hypothetical BSM processes are reduced by requiring $30 < E_{\text{T}}^{\text{miss}} < 150$ GeV and $m_{\text{eff}} < 1.5$ TeV. This selection results in an estimated purity exceeding 85%, with the remainder dominated by other multiboson processes. The overall normalisation of the WZ + jets MC prediction is then treated as a free parameter and set by fitting the observed data yields in CRWZ2j. This is realised with a maximum likelihood fit formed by the joint probability of expected background contributions to CRWZ2j with their uncertainties. In the case of signal-strength hypothesis testing, the joint probability is expanded to include contributions to the signal regions of interest, as well as the tested signal contribution to all regions. The procedure is fully detailed in Section 9. It is found that a scale factor of 0.86 ± 0.05 relative to the MC prediction using the theoretical inclusive NLO cross section best accommodates the observed data in CRWZ2j. This below-unity value is consistent with past observations [124, 125]. In the RPV SRs, no simultaneous CR-SR fit is performed and the WZ + jets normalisation is determined by CRWZ2j alone. This sequential approach does not propagate correlations among the WZ + jets uncertainties for RPV SRs, but this does not affect the results because the WZ + jets background is subdominant in those SRs.

Other SM background processes with prompt same-sign leptons are estimated by normalising the simulated samples to the theoretical cross section. Some weaker sources of same-sign leptons are ignored. Those include radiative top quark decays $t \rightarrow b\ell^+\nu\ell^+\ell^-$ in $t\bar{t}$ events, found to be negligible for the analyses in Refs. [25, 126], and multiple parton scattering, for which similar conclusions were reached in Ref. [25].

7.2 Electrons with incorrect charge

Electrons and positrons are distinguished by the curvature of their ID tracks, which may be error-prone if they start radiating early in the ID. The probability π for signal electrons to exhibit a charge flip is around 0.06% in the validation region with the largest charge-flip contribution. It varies by several orders of magnitude with $|\eta|$ and p_{T} as illustrated in Ref. [117]. Contributions of charge-flip background

to the various analysis regions are estimated by selecting data events with opposite-sign leptons and weighting them according to the known $\pi(|\eta|, p_T)$ values. The latter are measured in simulated $t\bar{t}$ events, and multiplied by factors $\gamma(|\eta|, p_T)$ correcting the known mismodelling. The factors γ , assumed to be process-independent, are determined [117] from the rates of opposite- and same-sign dielectron pairs observed in $Z \rightarrow ee$ decays in data and MC events. They are found to be within 20% of unity.

The dominant uncertainties in the predicted charge-flip yields are those arising from the measurement of the γ corrections, which is statistically limited and affected by a significant background. The predicted yields suffer from a typical uncertainty of 50%, which, however, does not impact the results of the present analysis since they represent at most 7% of the total background in any of the SRs.

7.3 Fake and non-prompt leptons

Non-prompt leptons arising from hadron decays or photon conversions, as well as hadrons misreconstructed as electrons, may survive the identification criteria in Section 5 at a low rate. When combined with a prompt lepton in an event, they may form a same-sign lepton pair. This source of background is estimated primarily with the matrix method summarised in the following paragraphs, and its prediction is then compared with that of a corrected simulation [54, 127].

The matrix method [128] exploits the different efficiency of the identification and isolation requirements when applied to F/NP leptons. In a given region of interest, data events are selected by applying lepton selection criteria that are looser than those defining signal leptons, and then categorising those events according to the number of actual signal leptons. A fully determined system of linear equations can then be constructed, relating the numbers of such categorised events to the unknown numbers of events with only prompt leptons, or exactly one F/NP lepton, etc., where the coefficients are functions of the probabilities ε and ζ for loose prompt leptons or F/NP leptons to also satisfy the nominal criteria. This can be illustrated for events with a single lepton by the matrix equation:

$$\begin{pmatrix} n_{\text{signal}} \\ n_{\text{all}} \end{pmatrix} = \begin{pmatrix} 1 & 1 \\ \varepsilon^{-1} & \zeta^{-1} \end{pmatrix} \cdot \begin{pmatrix} n_{\text{signal, prompt}} \\ n_{\text{signal, F/NP}} \end{pmatrix}.$$

The desired estimate $n_{\text{signal, F/NP}}$ can then be obtained easily. This approach can be readily extended to final states with multiple leptons. The general method is described in detail in Ref. [129], and the present analysis relies upon the software implementation referenced therein. The sample of loosely selected leptons comprises the subset of baseline leptons after overlap removal, which for muons satisfy $|d_0^{\text{sig}}| < 7$, and for electrons satisfy the ECIDS requirement in Section 5 and are restricted to $|\eta| < 2.0$. The estimated contribution of charge-flip electrons is subtracted from all terms.

The probabilities $\varepsilon(|\eta|, p_T)$ are calculated with simulated $t\bar{t}$ decays to leptons. The probabilities $\zeta(p_T)$ are measured in data [25] within the range $10 < p_T < 75$ GeV in regions enriched in $t\bar{t}$ events with one or two prompt leptons and one F/NP lepton forming a same-sign pair, which is also the leading contributor of F/NP leptons to the SRs. Separate measurements are made depending on the number of b -jets in the event (≤ 1 or ≥ 2) and whether the electron satisfies the criteria [120] to trigger the event recording. The undesirable contributions of $WZ + \text{jets}$ and $t\bar{t}W$ to these measurement regions, estimated with MC samples, are scaled by correction factors of 0.84 and 1.19 respectively, based on observed data in CRWZ2j and the region VRTTV defined in Table 8. For muons, ε is found to increase with p_T from 75% at 10 GeV to 98% at 70 GeV, while ζ varies between 10% and 15% in the most relevant range, $10 < p_T < 40$ GeV, reaching

its lowest values at around 20 GeV. For electrons, ε also increases with p_T , from 50% at 10 GeV to 97% at 100 GeV, while ζ varies between 5% and 10% in the aforementioned p_T range. When the electron satisfies the trigger criteria, ζ values can be up to twice as large. Over the whole measurement range and for both lepton flavours, ε is always found to be much larger than ζ , a necessary condition for the applicability of the matrix method [129]. In the SRGGWZ-L region, which only selects events containing a third baseline lepton in addition to the pair of same-sign signal leptons, the estimate is calculated with the reasonable assumption that the F/NP lepton is part of the latter pair.

The same conservative systematic uncertainties as in Ref. [25] are used to account for contamination from prompt same-sign lepton processes in the measurement regions and for the assumption that ε and ζ can be used outside of the regions in which they are measured. The latter is assessed primarily with $t\bar{t}$ simulation, such that the uncertainties cover the effects of having unknown relative contributions of different sources of F/NP leptons and residual variations of the probabilities as function of the environment that are not captured by the parameterisation as function of p_T . This procedure leads to uncertainties in ζ ranging from 30% at lower p_T for both flavours, up to 80% for high- p_T muons. Combined with statistical uncertainties in the ζ measurements, these translate for example into systematic uncertainties in the predicted F/NP yields of 44% and 75% in the SRSSWZ-L and SRUDD-ge2b signal regions, respectively, which contain a significant F/NP contribution. They are in most cases comparable in size to the corresponding statistical uncertainties in the predicted F/NP SR yields.

The SR yields predicted with the matrix method were cross-checked against those predicted by MC simulations of $t\bar{t}$ and W/Z + jets processes. For the latter, simulated events with F/NP leptons are weighted by three correction factors extracted from fits to data in appropriate regions: one for F/NP electrons, one for non-prompt muons from bottom hadron decays, and one for other sources of non-prompt muons. The estimates are compatible within uncertainties with the ones obtained with the matrix method.

7.4 Validation of the background estimates

The WZ + jets, $t\bar{t}W$ and $t\bar{t}\ell^+\ell^-$ background predictions are checked in the validation regions (VRs) defined in Table 8. The purity in the targeted SM process is expected to range from 70% to 80% for the two VRWZ regions, and from 30% to 55% for the four VRTTV/VRTTW regions, while the expected contributions from SUSY signal processes remain small. The VRs are designed to be orthogonal to the SRs, with the exception of VRWZ4j and VRWZ6j, which partially overlap with four of the SRGGWZ and SRSSWZ regions. However, for each of those, the expected number shared SM background events does not exceed 3% of the total number of events in the VR. The background predictions and the observed numbers of events in CRWZ2J and in the VRs are illustrated in Figure 2. The data and the background expectation in all VRs agree within uncertainties. The largest tension occurs in VRWZ6j, but it was checked that in this region the level of agreement doesn't become poorer as a function of m_{eff} or E_T^{miss} .

8 Systematic uncertainties

The predicted background yields in the SRs are affected by several sources of systematic and statistical uncertainty. The systematic uncertainties are grouped into experimental and theoretical ones, as well as those arising from the data-driven methods described above, normalisation, and MC statistics.

Table 8: The definitions of validation regions used to check the accuracy of the SM background predictions. Requirements are placed on signal leptons, jets, and some of the event-level variables defined in Section 6.

| | $n_{\text{Sig}}(\ell)$ | $n_{b\text{-jets}}$ | n_{jets} | $p_{\text{T}}^{\text{jet}}$ [GeV] | m_{eff} [GeV] | $E_{\text{T}}^{\text{miss}}$ [GeV] |
|-----------|---|---------------------|-------------------|-----------------------------------|------------------------|------------------------------------|
| | other requirements | | | | | |
| VRWZ4j | = 3* | = 0 | ≥ 4 | > 25 | [600, 1500] | [30, 250] |
| | $E_{\text{T}}^{\text{miss}}/m_{\text{eff}} < 0.2$, $81 < m_{\text{SFOS}} < 101$ GeV | | | | | |
| VRWZ6j | = 3* | = 0 | ≥ 6 | > 25 | [400, 1500] | [30, 250] |
| | $E_{\text{T}}^{\text{miss}}/m_{\text{eff}} < 0.15$, $81 < m_{\text{SFOS}} < 101$ GeV | | | | | |
| VRTTV | ≥ 2 | ≥ 1 | ≥ 3 | > 40 | [600, 1500] | [30, 250] |
| | $p_{\text{T}} > 30$ GeV for the two leading- p_{T} same-sign leptons, $\Delta R > 1.1$ between the leading- p_{T} lepton and any jet, $\sum p_{\text{T}}^{b\text{-jet}}/\sum p_{\text{T}}^{\text{jet}} > 0.4$, $E_{\text{T}}^{\text{miss}}/m_{\text{eff}} > 0.1$ | | | | | |
| VRTTV1b6j | ≥ 2 | ≥ 1 | ≥ 6 | > 40 | < 1500 | [30, 250] |
| | $p_{\text{T}} > 30$ GeV for the two leading- p_{T} same-sign leptons, $E_{\text{T}}^{\text{miss}}/m_{\text{eff}} < 0.15$ | | | | | |
| VRTTW | = 2* ($\mu^{\pm}\mu^{\pm}$) | ≥ 2 | ≥ 2 | > 25 | < 1500 | [30, 250] |
| | both leptons with $p_{\text{T}} > 25$ GeV, one with $p_{\text{T}} > 40$ GeV | | | | | |
| VRTTW3j | = 2* ($e^{\pm}\mu^{\pm}$) | ≥ 2 | ≥ 3 | > 25 | < 1500 | [30, 250] |
| | both leptons with $p_{\text{T}} > 25$ GeV | | | | | |

*: additional baseline leptons are not allowed

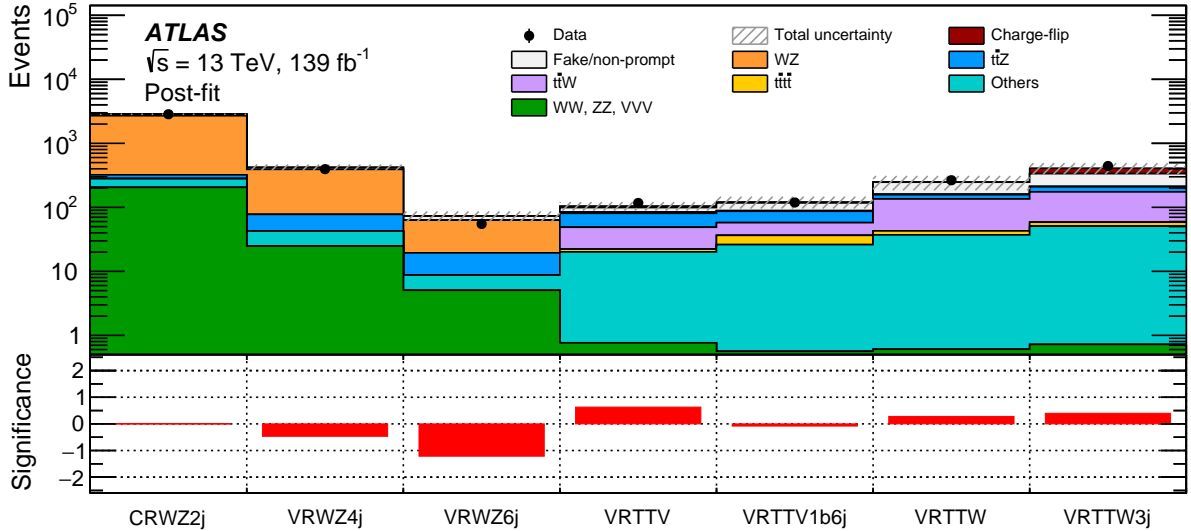


Figure 2: Data and post-fit background comparison in CRWZ2j and the VRs. The total uncertainties in the expected event yields are shown as the hatched bands. The bottom panel shows the significance [130] quantifying the deviation of the observed yields from the background expectation.

The experimental uncertainties come from the possible differences between the data and simulations in elements of this analysis and the uncertainties in the data taken from the operating detectors. They are related to luminosity, pile-up, triggers, and the reconstructed objects. For luminosity, a 1.7% relative uncertainty [58]

is applied. For pile-up, the uncertainty is computed by increasing and decreasing the weights associated with the mean number of simultaneous interactions by 4%. For leptons, uncertainties are computed for reconstruction efficiencies [117], identification efficiencies [115, 131], isolation efficiencies [132], energy scales and resolutions [116, 117], and trigger efficiencies [120–122] using various methods. For jets, uncertainties are considered for the jet vertex tagger (JVT) [133], jet energy scale (JES) [134] and jet energy resolution (JER) [109], and flavour tagging [135–137]. For the E_T^{miss} , uncertainties are estimated by propagating the uncertainties in the energy and momentum scale of each of the objects entering the calculation, and the uncertainties in the soft term’s resolution and scale [119].

The theoretical uncertainties come from the MC modelling of the relevant SM and SUSY processes, including cross sections, choice of scales, the PDF and α_s . The theoretical uncertainties from the dominant background processes in the signal regions, such as WZ , $W^\pm W^\pm$, and $t\bar{t}V$ (as well as $t\bar{t}\bar{t}\bar{t}$ for RPV signal regions), are computed in detail. Uncertainties from the choice of renormalisation scales, factorisation scales, resummation scales, merging scales and the recoil schemes, are evaluated by using the varied scales instead of the chosen scales and comparing the results. The impact of the choice of PDF is evaluated by symmetrising the event count variations seen when using the MMHT2014 [138], CT14 [139], and NNPDF [140] PDF sets. The total cross-section uncertainty is not applied to the WZ process because this process is normalised to data in the CRWZ2j control region. For the remaining rarer processes listed in Table 1, an overall 50% uncertainty is assigned. While some of the SRs are divided into several bins of a particular observable, the theory uncertainties are assumed to affect all bins uniformly. The impact of this simplification upon exclusion limits presented in the following sections was found to be acceptably small.

For the purpose of defining correlations, the different processes are grouped into nine categories: WZ , $t\bar{t}W$, $t\bar{t}\ell\ell$, $t\bar{t}\bar{t}\bar{t}$, other multiboson processes, other processes with top quarks, F/NP leptons, charge-flip electrons, and SUSY signal. Within each group, every source of uncertainty is treated as fully correlated, including across the different regions involved in the simultaneous fit. Experimental uncertainties are also treated as correlated between the different groups, while all other uncertainties are assumed to be uncorrelated. The total uncertainty and the separate contributions from each source are shown in Figure 3 and Figure 4 for CR/VRs and SRs separately. The total uncertainties vary from 2% (CRWZ2j) to 31% (SRSSSlep-H). The dominant contributions come from the F/NP-lepton background estimate, and the MC statistics in the SRs. The total uncertainty in CRWZ2j is smaller than the sum in quadrature of the individual components because of the anti-correlation between the normalisation and modelling uncertainties.

9 Statistical analysis

The expected SM backgrounds are determined with a profile likelihood fit [141], referred to as a background-only fit. The fit strategy differs between the RPC and RPV searches. For the RPC searches, the background-only fit uses the observed event yield in CRWZ2j as a constraint to adjust the normalisation of the WZ + jets background assuming that no signal is present. The inputs to the background-only fit include the number of events observed in CRWZ2j, and the number of events predicted in CRWZ2j, and in the SR(s) of interest, for all background processes. Both the observed and predicted numbers of events are described by Poisson statistics. The systematic uncertainties are included in the fit as nuisance parameters. They are constrained by Gaussian distributions with widths corresponding to the sizes of the uncertainties and are treated as correlated, when appropriate, between the various regions. The product of the various probability density functions forms the likelihood, which the fit maximises by adjusting the normalisation of the WZ + jets background and the nuisance parameters. For the RPV searches, CRWZ2j

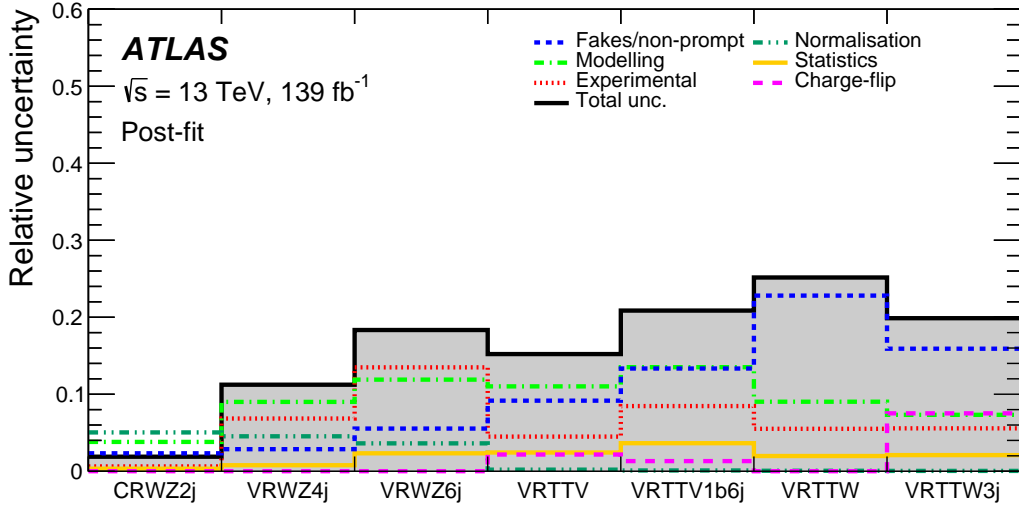


Figure 3: Relative contributions from different categories of uncertainties in CRWZ2j and the VRs. Correlations between different sources of systematic uncertainty are considered, so the total uncertainty does not necessarily match the quadrature summation of the components.

is not included in the fit, and the likelihood fit is used just to constrain the nuisance parameters associated with the systematic uncertainties. In both cases, the results of the background-only fit are used to test the compatibility of the observed data and the background estimates in the SRs.

In the absence of a significant excess over the SM expectation, two levels of interpretation are provided for BSM physics scenarios: model-independent exclusion limits and model-dependent exclusion limits set on the SUSY benchmark models illustrated in Figure 1. The CL_s method [142, 143] is used to derive the confidence level (CL) of the exclusion for a particular signal model. A signal model with a CL_s value below 0.05 is excluded at 95% CL.

Model-independent exclusion fits are used to set 95% CL upper limits on the possible BSM contributions to the SRs. This fit proceeds in the same way as the background-only fit, with CRWZ2j (for RPC searches) and the SRs both participating in a simultaneous likelihood fit, and the likelihood function including an additional parameter-of-interest to describe the potential signal contribution. Signal contamination in CRWZ2j is assumed to be zero. The hypothesis tests are performed for each of the SRs independently. The limits were evaluated using pseudo-experiments.

Model-dependent exclusion fits are used to set 95% CL exclusion limits on the masses of gluinos and squarks for the SUSY benchmark models considered in this paper. The fit proceeds similarly to the model-independent fit, except that both the signal yield in the SRs and the signal contamination in CRWZ2j expected from the model are taken into account, and the SRs are usually binned. For the models shown in Figures 1(d) and 1(f), only the SRs with the best expected sensitivity are considered. Table 9 shows the SRs used for each benchmark model and the fitted observable in each SR. The observable providing the best sensitivity for each SR is chosen as the fitted variable. The binning of each observable was optimised to provide the best sensitivity for the benchmark model of interest, while keeping enough events in each bin of the fitted SR. This multi-bin approach was found to enhance the sensitivity for all the SUSY scenarios considered in this search. In this model-dependent fit, the CL_s value is computed using the asymptotic

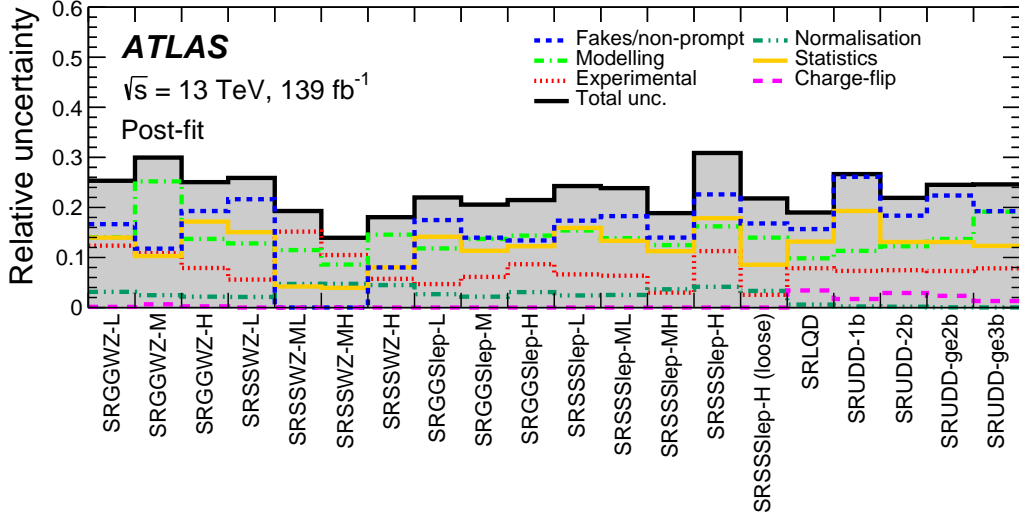


Figure 4: Relative contributions from different categories of uncertainties in the signal regions. Correlations between different sources of systematic uncertainty are considered, so the total uncertainty does not necessarily match the quadrature summation of the components.

approximation [144]. For some selected points a comparison with ‘toy’ experiments was performed, and the exclusion mass limits are overestimated by a maximum of 2%.

Table 9: Fit configuration used to obtain the exclusion limits for each benchmark model. The targeted signal model is shown in the first column. The second and third columns show the signal regions and the fitted variable in each signal region, respectively. A statistical combination of signal regions is represented by the symbol ‘&’, while ‘||’ means that for each point of the $\{m_{\tilde{g}(\tilde{q})}, m_{\tilde{\chi}_1^0}\}$ parameter space, the signal region with the best expected sensitivity is chosen.

| Model | Signal region(s) | Variable |
|---|--|---|
| $\tilde{g} \rightarrow qq'WZ\tilde{\chi}_1^0$ Figure 1(a) | SRGGWZ-L SRGGWZ-M SRGGWZ-H | single-bin, m_{eff} , single-bin |
| $\tilde{q} \rightarrow q'WZ\tilde{\chi}_1^0$ Figure 1(b) | SRSSWZ-L SRSSWZ-ML SRSSWZ-MH SRSSWZ-H | $E_{\text{T}}^{\text{miss}}$, $E_{\text{T}}^{\text{miss}}$, m_{eff} , m_{eff} |
| $\tilde{g} \rightarrow q\tilde{q}(\ell\ell/\nu\nu)\tilde{\chi}_1^0$ Figure 1(c) | SRGGSlep-L SRGGSlep-M SRGGSlep-H | $E_{\text{T}}^{\text{miss}}/\sum p_{\text{T}}^{\ell}$, $E_{\text{T}}^{\text{miss}}$, $E_{\text{T}}^{\text{miss}}$ |
| $\tilde{q} \rightarrow q(\ell\nu/\ell\ell/\nu\nu)\tilde{\chi}_1^0$ Figure 1(d) | SRSSSlep-L SRSSSlep-ML SRSSSlep-MH SRSSSlep-H (loose) | m_{eff} |
| $\tilde{g} \rightarrow q\tilde{q}\tilde{\chi}_1^0, \tilde{\chi}_1^0 \rightarrow \ell qq$ Figure 1(e) | SRLQD | m_{eff} |
| $\tilde{g} \rightarrow \tilde{t}\tilde{t}, \tilde{t} \rightarrow b\bar{d}$ Figure 1(f) | SRUDD-1b & SRUDD-ge2b | $\sum p_{\text{T}}^{\text{jet}}$ |

10 Results

The observed number of events in each SR along with the background expectations and uncertainties are summarised in Figure 5, and shown in detail in Tables 10–12. The background prediction corresponds to the estimate after the background-only fit described in Section 9. The overall excess (less than 2 standard

deviations) observed in SRSSWZ-ML, SRSSWZ-MH, and SRSSWZ-H, is due to the overlap among these regions, which have three data events in common. Overlap among the remaining SRs is also observed, but in a smaller proportion. The contribution from WZ + jets dominates in the SRs with no b -jets, while the production of fake/non-prompt leptons and processes involving the top quark dominate in the SRs where the veto on b -jets is not applied. No significant excess of events above the SM prediction is observed in any of the SRs. The highest significance corresponds to SRSSlep-L with 2.2 standard deviations (with the calculation of Table 13). The distributions of the most discriminating variable for some of the SRs, with the signal region requirement on the displayed variable removed, are shown in Figure 6.

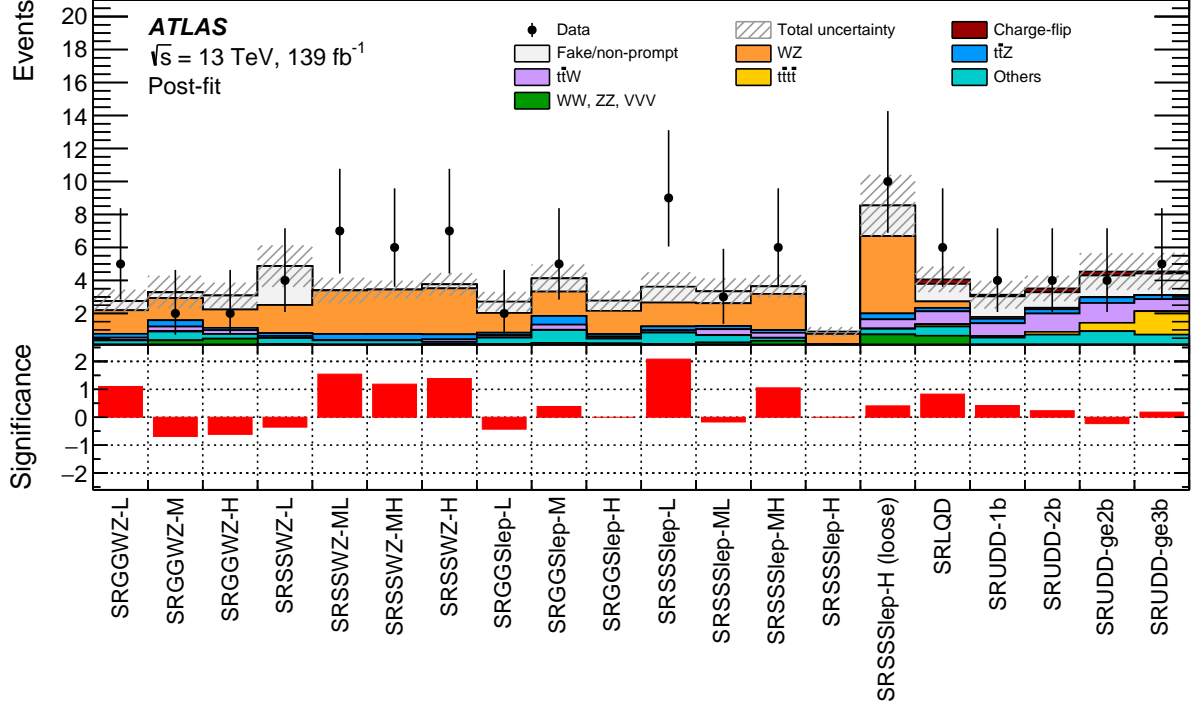


Figure 5: Data and post-fit background comparison in all SRs. The total uncertainties in the expected event yields are shown as the hatched bands. The bottom panel shows the significance [130] quantifying the deviation of the observed yields from the background expectation.

In the absence of a significant deviation from the SM prediction, the results are interpreted in terms of model-independent upper limits on possible BSM contributions to the SRs, as well as exclusion limits on the masses of the SUSY particles in the benchmark scenarios shown in Figure 1. The 95% CL upper limits on the number of BSM events, S^{95} , that may contribute to the SRs are shown in Table 13. Normalising these by the integrated luminosity L of the data sample, they can be interpreted as upper limits on the visible BSM cross section (σ_{vis}), defined as $\sigma_{\text{vis}} = \sigma_{\text{prod}} \times \mathcal{A} \times \epsilon = S^{95}/L$, where σ_{prod} is the production cross section for an arbitrary BSM signal process, and \mathcal{A} and ϵ are the corresponding acceptance and reconstruction efficiency for the relevant SR. The probability of the observations being compatible with the SM-only hypothesis is quantified by the p -values displayed in the last column of Table 13. For SRs where the data yield is smaller than expected, the p -value is capped at 0.50.

Exclusion limits at 95% CL are also set on the masses of the superpartners involved in the SUSY benchmark scenarios considered. Figure 6 shows the fitted variable's distribution for each displayed SR. The bins

Table 10: The number of observed data events and expected background contributions in signal regions defined for the RPC models shown in Figures 1(a) and 1(b). Backgrounds shown with a ‘-’ do not contribute to that region. The displayed yields include all statistical and systematic uncertainties. The individual uncertainties can be correlated or anticorrelated and therefore do not necessarily add in quadrature to equal the total uncertainty.

| | SRGGWZ-L | SRGGWZ-M | SRGGWZ-H | SRSSWZ-L | SRSSWZ-ML | SRSSWZ-MH | SRSSWZ-H |
|------------------------|-----------------|-----------------|-----------------|-----------------|-----------------|-----------------|-----------------|
| Observed | 5 | 2 | 2 | 4 | 7 | 6 | 7 |
| Total background | 2.8 ± 0.7 | 3.3 ± 1.0 | 3.1 ± 0.8 | 4.9 ± 1.3 | 3.4 ± 0.8 | 3.4 ± 0.6 | 3.8 ± 0.7 |
| WZ | 1.4 ± 0.4 | 1.3 ± 0.8 | 1.1 ± 0.4 | 1.7 ± 0.6 | 2.6 ± 0.7 | 2.7 ± 0.5 | 2.8 ± 0.6 |
| $ZZ, W^\pm W^\pm, VVV$ | 0.09 ± 0.05 | 0.37 ± 0.11 | 0.47 ± 0.11 | 0.14 ± 0.07 | 0.09 ± 0.06 | 0.11 ± 0.07 | 0.15 ± 0.07 |
| $t\bar{t}W$ | 0.15 ± 0.09 | 0.26 ± 0.12 | 0.22 ± 0.07 | 0.12 ± 0.07 | < 0.05 | < 0.05 | 0.14 ± 0.04 |
| $t\bar{t}Z$ | 0.24 ± 0.08 | 0.38 ± 0.22 | 0.15 ± 0.10 | 0.18 ± 0.10 | 0.38 ± 0.14 | 0.38 ± 0.12 | 0.31 ± 0.10 |
| $t\bar{t}t\bar{t}$ | 0.02 ± 0.01 | 0.04 ± 0.02 | < 0.02 | < 0.02 | < 0.02 | < 0.02 | < 0.02 |
| Other SM processes | 0.26 ± 0.18 | 0.53 ± 0.28 | 0.28 ± 0.15 | 0.36 ± 0.20 | 0.28 ± 0.31 | 0.25 ± 0.21 | 0.12 ± 0.10 |
| Fake/non-prompt | 0.56 ± 0.46 | 0.3 ± 0.4 | 0.9 ± 0.6 | 2.4 ± 1.1 | < 0.3 | < 0.3 | 0.24 ± 0.27 |
| Charge-flip | < 0.02 | 0.03 ± 0.02 | < 0.02 | - | - | - | - |

Table 11: The number of observed data events and expected background contributions in signal regions defined for the RPC models shown in Figures 1(c) and 1(d). Backgrounds shown with a ‘-’ do not contribute to that region. The displayed yields include all statistical and systematic uncertainties. The individual uncertainties can be correlated or anticorrelated and therefore do not necessarily add in quadrature to equal the total uncertainty.

| | SRGGSlep-L | SRGGSlep-M | SRGGSlep-H | SRSSSlep-L | SRSSSlep-ML | SRSSSlep-MH | SRSSSlep-H | SRSSSlep-H (loose) |
|------------------------|-----------------|-----------------|-----------------|-----------------|-----------------|-----------------|-----------------|--------------------|
| Observed | 2 | 5 | 0 | 9 | 3 | 6 | 0 | 10 |
| Total background | 2.7 ± 0.6 | 4.1 ± 0.9 | 2.8 ± 0.6 | 3.6 ± 0.9 | 3.3 ± 0.8 | 3.6 ± 0.7 | 0.89 ± 0.28 | 8.5 ± 1.9 |
| WZ | 1.19 ± 0.27 | 1.5 ± 0.4 | 1.4 ± 0.4 | 1.4 ± 0.4 | 1.4 ± 0.4 | 2.2 ± 0.4 | 0.61 ± 0.17 | 4.7 ± 1.1 |
| $ZZ, W^\pm W^\pm, VVV$ | 0.14 ± 0.08 | 0.21 ± 0.11 | 0.18 ± 0.09 | 0.13 ± 0.07 | 0.23 ± 0.12 | 0.34 ± 0.17 | 0.04 ± 0.03 | 0.7 ± 0.4 |
| $t\bar{t}W$ | 0.15 ± 0.08 | 0.31 ± 0.09 | 0.11 ± 0.05 | 0.14 ± 0.08 | 0.35 ± 0.08 | 0.30 ± 0.07 | < 0.05 | 0.55 ± 0.29 |
| $t\bar{t}Z$ | 0.15 ± 0.08 | 0.53 ± 0.17 | 0.15 ± 0.09 | 0.23 ± 0.13 | 0.19 ± 0.08 | 0.16 ± 0.09 | 0.05 ± 0.03 | 0.36 ± 0.22 |
| $t\bar{t}t\bar{t}$ | < 0.02 | 0.02 ± 0.01 | 0.02 ± 0.01 | < 0.02 | < 0.02 | < 0.02 | < 0.02 | 0.02 ± 0.01 |
| Other SM processes | 0.39 ± 0.23 | 0.8 ± 0.4 | 0.29 ± 0.18 | 0.7 ± 0.4 | 0.44 ± 0.25 | 0.17 ± 0.09 | 0.02 ± 0.03 | 0.34 ± 0.18 |
| Fake/non-prompt | 0.7 ± 0.5 | 0.8 ± 0.6 | 0.6 ± 0.4 | 1.0 ± 0.6 | 0.7 ± 0.6 | 0.5 ± 0.5 | 0.14 ± 0.20 | 1.9 ± 1.4 |
| Charge-flip | - | - | - | - | - | - | - | - |

displayed above the SR requirement correspond to the binning used in the exclusion fit. For illustration purposes, only one SR per benchmark model is shown. Figure 7 shows the exclusion limits obtained for the RPC models shown in Figure 1. For each point of the $\{m_{\tilde{g}(\tilde{q})}, m_{\tilde{\chi}_1^0}\}$ parameter space, the SR with the best expected sensitivity is chosen. Figures 7(a) and 7(b) show the mass limits on gluinos and squarks, respectively, for the cascade decays of charginos into pairs of SM bosons. The mass limits on gluinos are up to 400 GeV higher than the previously obtained limits and exclude gluinos with masses up to 2 TeV. The improvement over Ref. [25] is achieved mostly by using a looser SR selection to increase signal acceptance, and by benefiting from the high discriminating power of the m_{eff} shape in SRGGWZ-M. For squarks, the mass limits surpass the prior results by around 600 GeV and exclude squarks with masses up to 1.2 TeV.

Figures 7(c) and 7(d) show the mass limits on gluinos and squarks, respectively, for the decays of charginos and neutralinos into sleptons. The mass limits on gluinos extend up to 2.2 TeV for a massless neutralino, while in a very compressed scenario, the limits on the neutralino mass surpass the previous ones by around 200 GeV. For the model where squarks are pair produced, the mass limits on squarks are up to 850 GeV

Table 12: The number of observed data events and expected background contributions in signal regions defined for the RPV models shown in Figures 1(e) and 1(f). The displayed yields include all statistical and systematic uncertainties. The individual uncertainties can be correlated or anticorrelated and therefore do not necessarily add in quadrature to equal the total uncertainty.

| | SRLQD | SRUDD-1b | SRUDD-2b | SRUDD-ge2b | SRUDD-ge3b |
|------------------------|-----------------|-----------------|-----------------|-----------------|-----------------|
| Observed | 6 | 4 | 4 | 4 | 5 |
| Total background | 4.1 ± 0.8 | 3.1 ± 0.8 | 3.5 ± 0.8 | 4.5 ± 1.1 | 4.6 ± 1.1 |
| WZ | 0.40 ± 0.14 | 0.11 ± 0.06 | 0.10 ± 0.10 | 0.03 ± 0.02 | < 0.02 |
| $ZZ, W^\pm W^\pm, VVV$ | 0.65 ± 0.22 | 0.06 ± 0.03 | 0.08 ± 0.05 | 0.05 ± 0.03 | < 0.02 |
| $t\bar{t}W$ | 0.78 ± 0.23 | 0.78 ± 0.24 | 1.11 ± 0.27 | 1.20 ± 0.30 | 0.7 ± 0.4 |
| $t\bar{t}Z$ | 0.20 ± 0.08 | 0.27 ± 0.17 | 0.26 ± 0.13 | 0.34 ± 0.19 | 0.24 ± 0.11 |
| $t\bar{t}t\bar{t}$ | 0.14 ± 0.09 | 0.10 ± 0.06 | 0.17 ± 0.11 | 0.51 ± 0.30 | 1.4 ± 0.7 |
| Other SM processes | 0.56 ± 0.27 | 0.47 ± 0.23 | 0.63 ± 0.31 | 0.9 ± 0.5 | 0.7 ± 0.4 |
| Fake/non-prompt | 1.1 ± 0.6 | 1.3 ± 0.8 | 0.9 ± 0.6 | 1.3 ± 1.0 | 1.3 ± 0.9 |
| Charge-flip | 0.27 ± 0.14 | 0.11 ± 0.05 | 0.24 ± 0.10 | 0.24 ± 0.11 | 0.13 ± 0.06 |

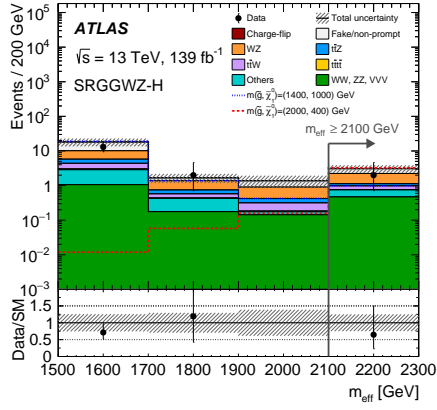
Table 13: Upper limits at 95% CL on the visible cross section (σ_{vis}), on the number of signal events (S_{obs}^{95}), and on the number of signal events given the expected number of background events and its $\pm 1\sigma$ variations, (S_{exp}^{95}). The last two columns indicate the CL_b value, i.e. the confidence level observed for the background-only hypothesis, the discovery p -value ($p(s=0)$) and its associated significance Z .

| SR | σ_{vis} [fb] | S_{obs}^{95} | S_{exp}^{95} | CL_b | $p(s=0)$ (Z) |
|--------------------|----------------------------|-----------------------|-----------------------|---------------|------------------|
| SRGGWZ-L | 0.06 | 8.3 | $5.2^{+2.0}_{-1.1}$ | 0.91 | 0.06 (1.59) |
| SRGGWZ-M | 0.03 | 4.8 | $5.2^{+1.9}_{-1.4}$ | 0.38 | 0.50 (0.00) |
| SRGGWZ-H | 0.03 | 4.2 | $4.9^{+2.1}_{-1.1}$ | 0.30 | 0.50 (0.00) |
| SRSSWZ-L | 0.04 | 5.9 | $6.2^{+2.6}_{-1.8}$ | 0.42 | 0.50 (0.00) |
| SRSSWZ-ML | 0.08 | 10.5 | $6.5^{+2.3}_{-1.5}$ | 0.95 | 0.02 (2.07) |
| SRSSWZ-MH | 0.06 | 8.8 | $5.5^{+2.1}_{-1.4}$ | 0.93 | 0.04 (1.80) |
| SRSSWZ-H | 0.06 | 8.8 | $5.5^{+2.3}_{-1.4}$ | 0.91 | 0.10 (1.29) |
| SRGGSlep-L | 0.03 | 4.1 | $4.8^{+2.0}_{-1.1}$ | 0.34 | 0.50 (0.00) |
| SRGGSlep-M | 0.04 | 6.2 | $5.7^{+2.4}_{-1.4}$ | 0.60 | 0.42 (0.19) |
| SRGGSlep-H | 0.02 | 2.9 | $4.5^{+2.0}_{-0.9}$ | 0.01 | 0.40 (0.26) |
| SRSSSlep-L | 0.08 | 11.8 | $6.0^{+2.3}_{-1.8}$ | 0.98 | 0.01 (2.23) |
| SRSSSlep-ML | 0.04 | 4.9 | $5.1^{+2.4}_{-1.0}$ | 0.45 | 0.50 (0.00) |
| SRSSSlep-MH | 0.06 | 8.0 | $5.6^{+2.3}_{-1.7}$ | 0.85 | 0.16 (1.01) |
| SRSSSlep-H | 0.02 | 2.5 | $3.5^{+1.3}_{-0.4}$ | 0.00 | 0.40 (0.25) |
| SRSSSlep-H (loose) | 0.07 | 10.0 | $8.2^{+3.5}_{-2.2}$ | 0.70 | 0.31 (0.48) |
| SRLQD | 0.06 | 7.6 | $5.8^{+2.2}_{-1.7}$ | 0.81 | 0.22 (0.76) |
| SRUDD-1b | 0.05 | 6.9 | $5.4^{+2.1}_{-1.2}$ | 0.77 | 0.21 (0.80) |
| SRUDD-2b | 0.05 | 6.3 | $5.2^{+2.5}_{-1.2}$ | 0.70 | 0.26 (0.66) |
| SRUDD-ge2b | 0.04 | 5.9 | $6.1^{+2.3}_{-1.4}$ | 0.46 | 0.50 (0.00) |
| SRUDD-ge3b | 0.05 | 6.8 | $6.2^{+2.6}_{-1.6}$ | 0.62 | 0.41 (0.22) |

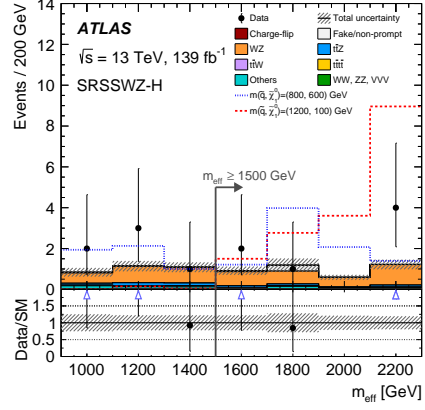
higher than the previous limits and exclude squarks with masses up to 1.7 TeV.

Figure 7(e) shows the mass limits on gluinos for the scenario where the neutralino decays via λ' RPV couplings. Gluinos with masses up to 2.2 TeV are excluded, surpassing the results of the previous search by around 400 GeV. The sensitivity decreases rapidly for low-mass neutralinos because their decay products are very collimated and do not pass the isolation requirements, resulting in very low efficiency. The

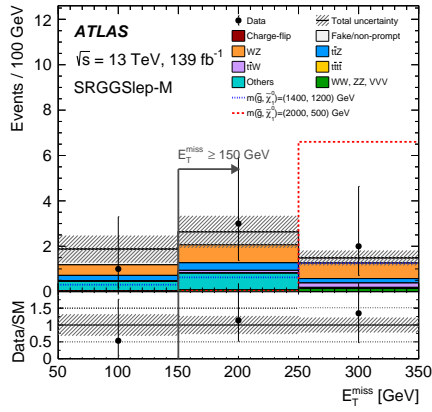
limits in Figure 7(f) are set for pair production of gluinos in the RPV model where gluinos decay via top squarks into tbd final states if λ'' couplings are non-zero. The limits were obtained by using the statistical combination of SRUDD-1b and SRUDD-ge2b, as it was found to provide the best expected sensitivity. Gluinos with masses up to 1.65 TeV are excluded for a top squark with a mass below 1.45 TeV. The improvement over Ref. [25] is in this case driven by the split into SRs of different b -jet multiplicities, together with the binned fits of the $\sum p_T^{\text{jet}}$ distributions.



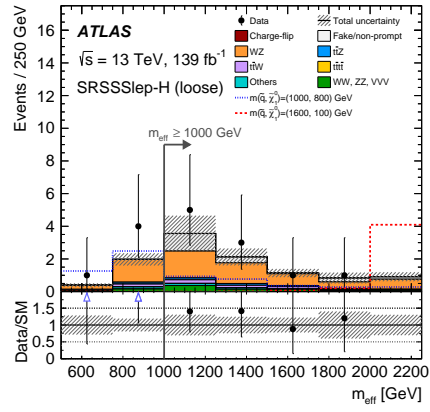
(a) SRGGWZ-H



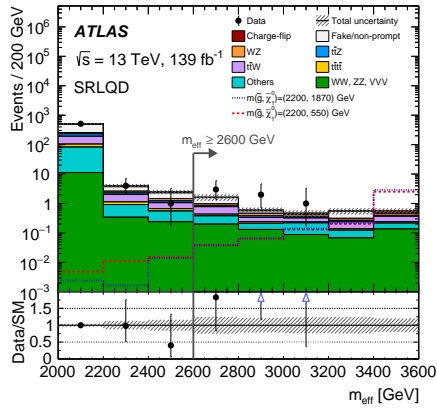
(b) SRSSWZ-H



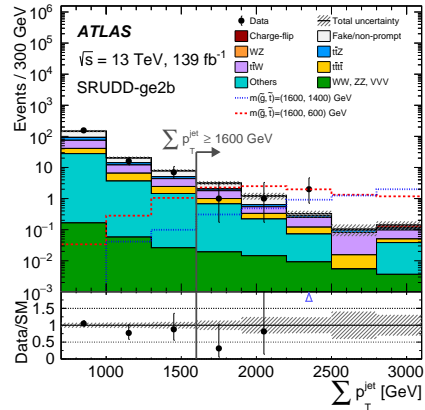
(c) SRGGSlep-M



(d) SRSSSlep-H (loose)

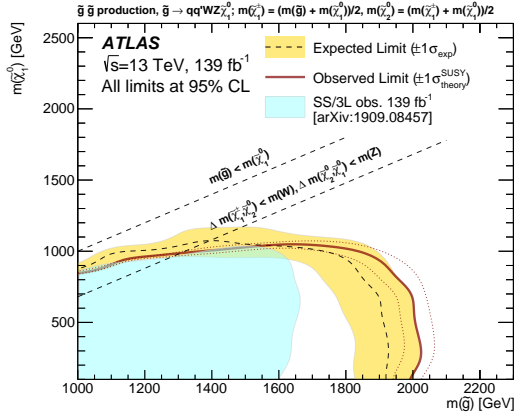


(e) SRLQD

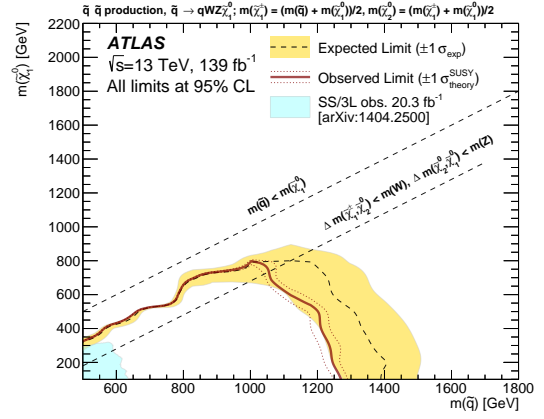


(f) SRUDD-ge2b

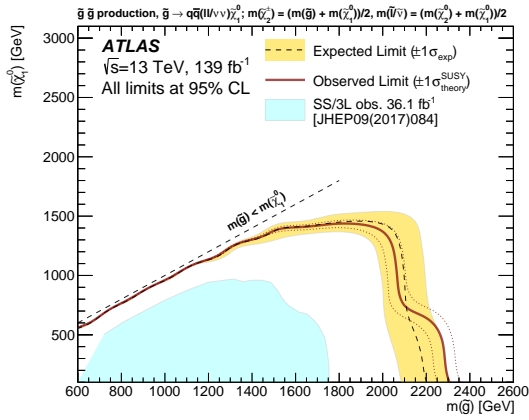
Figure 6: Distributions of the data and estimated background after the background-only fit for the signal regions (a) SRGGWZ-H, (b) SRSSWZ-H, (c) SRGGSlep-M, (d) SRSSSlep-H (loose), (e) SRLQD, and (f) SRUDD-ge2b. All SR selections but the one on the quantity shown are applied. The line with an arrow indicates the requirement used in that signal region. Distributions for two signal hypotheses for the model of interest are also shown. The bins displayed above the signal region requirement correspond to the binning used in the exclusion fit. All uncertainties are included in the uncertainty band. Overflow (underflow) events, where present, are included in the last (first) bin.



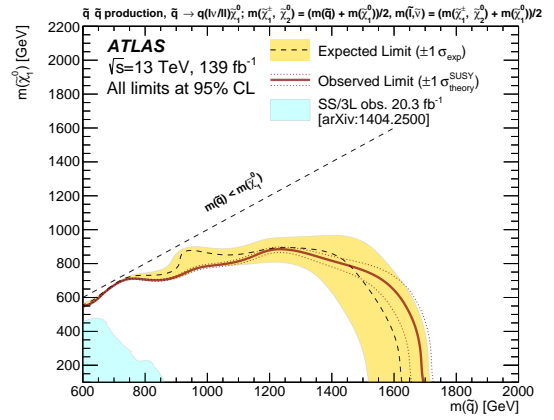
(a) $\tilde{g} \rightarrow qq'WZ\tilde{\chi}_1^0$



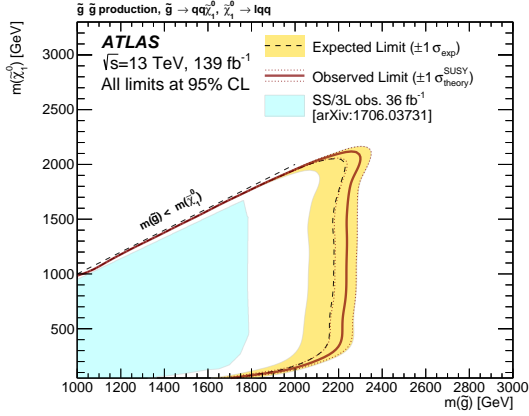
(b) $\tilde{q} \rightarrow q'WZ\tilde{\chi}_1^0$



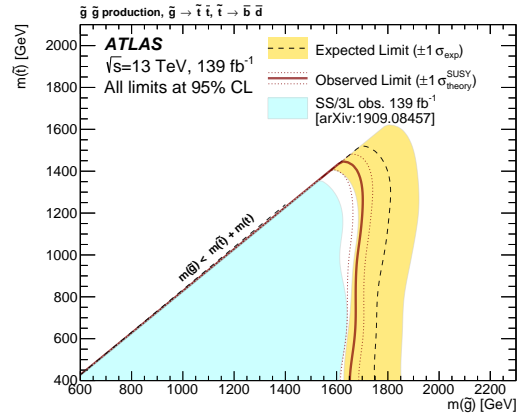
(c) $\tilde{g} \rightarrow qq'(ll/\nu\nu)\tilde{\chi}_1^0$



(d) $\tilde{q} \rightarrow q(lv/ll/\nu\nu)\tilde{\chi}_1^0$



(e) $\tilde{g} \rightarrow qq\tilde{\chi}_1^0, \tilde{\chi}_1^0 \rightarrow lqq$



(f) $\tilde{g} \rightarrow \tilde{t}\tilde{t}, \tilde{t} \rightarrow \tilde{b}\tilde{d}$

Figure 7: Observed (red line) and expected (black dashed line) 95% CL exclusion regions for \tilde{g} , \tilde{q} , $\tilde{\chi}_1^0$ and \tilde{t} masses obtained for the models shown in Figure 1. The yellow band shows the $\pm 1\sigma$ variation of the expected limits. The red dotted lines around the observed limit illustrate the change in the observed limit as the nominal signal cross section is scaled up and down by the theoretical uncertainty. The light blue shaded area indicates the observed limits obtained by previous ATLAS searches.

11 Conclusion

A search for pair production of squarks or gluinos decaying via sleptons or weak bosons in final states with either two same-sign leptons or at least three leptons is presented. The search uses 139 fb^{-1} of proton–proton collision data collected by the ATLAS detector at the LHC at a centre-of-mass energy of 13 TeV.

No significant excess of events over the Standard Model expectation is observed. The results are interpreted in the context of several supersymmetric simplified models featuring gluino or squark pair production in R-parity-conserving and R-parity-violating scenarios. Lower limits on particle masses are derived at 95% confidence level for these models, reaching as high as 2.2 TeV for gluinos and 1.7 TeV for squarks, surpassing the exclusion limits from similar previous searches performed by ATLAS. Improved analysis techniques, the inclusion of a control region for the WZ + jets background, and a significantly larger data set in some cases, contributed to this improvement. Model-independent limits on the cross section of a possible signal contribution to the signal regions defined in this search are also set.

Acknowledgements

We thank CERN for the very successful operation of the LHC, as well as the support staff from our institutions without whom ATLAS could not be operated efficiently.

We acknowledge the support of ANPCyT, Argentina; YerPhI, Armenia; ARC, Australia; BMWFW and FWF, Austria; ANAS, Azerbaijan; CNPq and FAPESP, Brazil; NSERC, NRC and CFI, Canada; CERN; ANID, Chile; CAS, MOST and NSFC, China; Minciencias, Colombia; MEYS CR, Czech Republic; DNRF and DNSRC, Denmark; IN2P3-CNRS and CEA-DRF/IRFU, France; SRNSFG, Georgia; BMBF, HGF and MPG, Germany; GSRI, Greece; RGC and Hong Kong SAR, China; ISF and Benoziyo Center, Israel; INFN, Italy; MEXT and JSPS, Japan; CNRST, Morocco; NWO, Netherlands; RCN, Norway; MEiN, Poland; FCT, Portugal; MNE/IFA, Romania; MESTD, Serbia; MSSR, Slovakia; ARRS and MIZŠ, Slovenia; DSI/NRF, South Africa; MICINN, Spain; SRC and Wallenberg Foundation, Sweden; SERI, SNSF and Cantons of Bern and Geneva, Switzerland; MOST, Taiwan; TENMAK, Türkiye; STFC, United Kingdom; DOE and NSF, United States of America. In addition, individual groups and members have received support from BCKDF, CANARIE, Compute Canada and CRC, Canada; PRIMUS 21/SCI/017 and UNCE SCI/013, Czech Republic; COST, ERC, ERDF, Horizon 2020 and Marie Skłodowska-Curie Actions, European Union; Investissements d’Avenir Labex, Investissements d’Avenir IDEX and ANR, France; DFG and AvH Foundation, Germany; Herakleitos, Thales and Aristeia programmes co-financed by EU-ESF and the Greek NSRF, Greece; BSF-NSF and MINERVA, Israel; Norwegian Financial Mechanism 2014–2021, Norway; NCN and NAWA, Poland; La Caixa Banking Foundation, CERCA Programme Generalitat de Catalunya and PROMETEO and GenT Programmes Generalitat Valenciana, Spain; Göran Gustafssons Stiftelse, Sweden; The Royal Society and Leverhulme Trust, United Kingdom.

The crucial computing support from all WLCG partners is acknowledged gratefully, in particular from CERN, the ATLAS Tier-1 facilities at TRIUMF (Canada), NDGF (Denmark, Norway, Sweden), CC-IN2P3 (France), KIT/GridKA (Germany), INFN-CNAF (Italy), NL-T1 (Netherlands), PIC (Spain), ASGC (Taiwan), RAL (UK) and BNL (USA), the Tier-2 facilities worldwide and large non-WLCG resource providers. Major contributors of computing resources are listed in Ref. [145].

References

- [1] ATLAS Collaboration, *The ATLAS Experiment at the CERN Large Hadron Collider*, [JINST **3** \(2008\) S08003](#).
- [2] L. Evans and P. Bryant, *LHC Machine*, [JINST **3** \(2008\) S08001](#).
- [3] J. Alwall et al., *The automated computation of tree-level and next-to-leading order differential cross sections, and their matching to parton shower simulations*, [JHEP **07** \(2014\) 079](#), arXiv: [1405.0301 \[hep-ph\]](#).
- [4] A. De Simone, O. Matsedonskyi, R. Rattazzi and A. Wulzer, *A first top partner hunter's guide*, [JHEP **04** \(2013\) 004](#), arXiv: [1211.5663 \[hep-ph\]](#).
- [5] B. Fuks, M. Nemevšek and R. Ruiz, *Doubly Charged Higgs Boson Production at Hadron Colliders*, [Phys. Rev. D **101** \(2020\) 075022](#), arXiv: [1912.08975 \[hep-ph\]](#).
- [6] R. M. Barnett, J. F. Gunion and H. E. Haber, *Discovering supersymmetry with like-sign dileptons*, [Phys. Lett. B **315** \(1993\) 349](#), arXiv: [hep-ph/9306204](#).
- [7] ATLAS Collaboration, *Search for anomalous production of prompt like-sign lepton pairs at $\sqrt{s} = 7$ TeV with the ATLAS detector*, [JHEP **12** \(2012\) 007](#), arXiv: [1210.4538 \[hep-ex\]](#).
- [8] CMS Collaboration, *Search for new physics in events with same-sign dileptons and b-tagged jets in pp collisions at $\sqrt{s} = 7$ TeV*, [JHEP **08** \(2012\) 110](#), arXiv: [1205.3933 \[hep-ex\]](#).
- [9] CDF Collaboration, *Inclusive Search for Anomalous Production of High- p_T Like-Sign Lepton Pairs in $p\bar{p}$ Collisions at $\sqrt{s} = 1.8$ TeV*, [Phys. Rev. Lett. **93** \(2004\) 061802](#), URL: <https://link.aps.org/doi/10.1103/PhysRevLett.93.061802>.
- [10] Y. Golfand and E. Likhtman, *Extension of the Algebra of Poincare Group Generators and Violation of P Invariance*, [JETP Lett. **13** \(1971\) 323](#), [[Pisma Zh. Eksp. Teor. Fiz. **13** \(1971\) 452](#)].
- [11] D. Volkov and V. Akulov, *Is the neutrino a goldstone particle?*, [Phys. Lett. B **46** \(1973\) 109](#).
- [12] J. Wess and B. Zumino, *Supergauge transformations in four dimensions*, [Nucl. Phys. B **70** \(1974\) 39](#).
- [13] J. Wess and B. Zumino, *Supergauge invariant extension of quantum electrodynamics*, [Nucl. Phys. B **78** \(1974\) 1](#).
- [14] S. Ferrara and B. Zumino, *Supergauge invariant Yang-Mills theories*, [Nucl. Phys. B **79** \(1974\) 413](#).
- [15] A. Salam and J. Strathdee, *Super-symmetry and non-Abelian gauges*, [Phys. Lett. B **51** \(1974\) 353](#).
- [16] P. Fayet, *Supersymmetry and weak, electromagnetic and strong interactions*, [Phys. Lett. B **64** \(1976\) 159](#).
- [17] P. Fayet, *Spontaneously broken supersymmetric theories of weak, electromagnetic and strong interactions*, [Phys. Lett. B **69** \(1977\) 489](#).
- [18] P. Fayet, *Supergauge Invariant Extension of the Higgs Mechanism and a Model for the Electron and Its Neutrino*, [Nucl. Phys. B **90** \(1975\) 104](#).
- [19] A. Canepa, T. Han and X. Wang, *The Search for Electroweakinos*, [Ann. Rev. Nucl. Part. Sci. **70** \(2020\) 425](#), arXiv: [2003.05450 \[hep-ph\]](#).

- [20] G. R. Farrar and P. Fayet, *Phenomenology of the production, decay, and detection of new hadronic states associated with supersymmetry*, *Phys. Lett. B* **76** (1978) 575.
- [21] H. Goldberg, *Constraint on the Photino Mass from Cosmology*, *Phys. Rev. Lett.* **50** (1983) 1419, Erratum: *Phys. Rev. Lett.* **103** (2009) 099905.
- [22] J. Ellis, J. Hagelin, D. V. Nanopoulos, K. A. Olive and M. Srednicki, *Supersymmetric relics from the big bang*, *Nucl. Phys. B* **238** (1984) 453.
- [23] L. Girardello and M. T. Grisaru, *Soft Breaking of Supersymmetry*, *Nucl. Phys. B* **194** (1982) 65.
- [24] H. K. Dreiner, *An Introduction to explicit R-parity violation*, *Adv. Ser. Direct. High Energy Phys.* **21** (2010) 565, ed. by G. L. Kane, arXiv: [hep-ph/9707435](https://arxiv.org/abs/hep-ph/9707435).
- [25] ATLAS Collaboration, *Search for squarks and gluinos in final states with same-sign leptons and jets using 139fb^{-1} of data collected with the ATLAS detector*, *JHEP* **06** (2020) 046, arXiv: [1909.08457](https://arxiv.org/abs/1909.08457) [[hep-ex](#)].
- [26] CMS Collaboration, *Search for physics beyond the standard model in events with jets and two same-sign or at least three charged leptons in proton–proton collisions at $\sqrt{s} = 13\text{ TeV}$* , *Eur. Phys. J. C* **80** (2020) 752, arXiv: [2001.10086](https://arxiv.org/abs/2001.10086) [[hep-ex](#)].
- [27] ATLAS Collaboration, *Summary of the searches for squarks and gluinos using $\sqrt{s} = 8\text{ TeV}$ pp collisions with the ATLAS experiment at the LHC*, *JHEP* **10** (2015) 054, arXiv: [1507.05525](https://arxiv.org/abs/1507.05525) [[hep-ex](#)].
- [28] ATLAS Collaboration, *ATLAS Insertable B-Layer: Technical Design Report*, ATLAS-TDR-19; CERN-LHCC-2010-013, 2010, URL: <https://cds.cern.ch/record/1291633>, Addendum: ATLAS-TDR-19-ADD-1; CERN-LHCC-2012-009, 2012, URL: <https://cds.cern.ch/record/1451888>.
- [29] B. Abbott et al., *Production and integration of the ATLAS Insertable B-Layer*, *JINST* **13** (2018) T05008, arXiv: [1803.00844](https://arxiv.org/abs/1803.00844) [[physics.ins-det](#)].
- [30] ATLAS Collaboration, *Performance of the ATLAS trigger system in 2015*, *Eur. Phys. J. C* **77** (2017) 317, arXiv: [1611.09661](https://arxiv.org/abs/1611.09661) [[hep-ex](#)].
- [31] ATLAS Collaboration, *The ATLAS Collaboration Software and Firmware*, ATL-SOFT-PUB-2021-001, 2021, URL: <https://cds.cern.ch/record/2767187>.
- [32] ATLAS Collaboration, *Search for squarks and gluinos in final states with jets and missing transverse momentum using 139fb^{-1} of $\sqrt{s} = 13\text{ TeV}$ pp collision data with the ATLAS detector*, *JHEP* **02** (2021) 143, arXiv: [2010.14293](https://arxiv.org/abs/2010.14293) [[hep-ex](#)].
- [33] ATLAS Collaboration, *Search for squarks and gluinos in final states with one isolated lepton, jets, and missing transverse momentum at $\sqrt{s} = 13\text{ TeV}$ with the ATLAS detector*, *Eur. Phys. J. C* **81** (2021) 600, arXiv: [2101.01629](https://arxiv.org/abs/2101.01629) [[hep-ex](#)], Erratum: *Eur. Phys. J. C* **81** (2021) 956.
- [34] ATLAS Collaboration, *Searches for new phenomena in events with two leptons, jets, and missing transverse momentum in 139fb^{-1} of $\sqrt{s} = 13\text{ TeV}$ pp collisions with the ATLAS detector*, (2022), arXiv: [2204.13072](https://arxiv.org/abs/2204.13072) [[hep-ex](#)].
- [35] J. Alwall, M.-P. Le, M. Lisanti and J. G. Wacker, *Searching for directly decaying gluinos at the Tevatron*, *Phys. Lett. B* **666** (2008) 34, arXiv: [0803.0019](https://arxiv.org/abs/0803.0019) [[hep-ph](#)].

- [36] J. Alwall, P. Schuster and N. Toro, *Simplified models for a first characterization of new physics at the LHC*, [Phys. Rev. D **79** \(2009\) 075020](#), arXiv: [0810.3921 \[hep-ph\]](#).
- [37] D. Alves et al., *Simplified models for LHC new physics searches*, [J. Phys. G **39** \(2012\) 105005](#), arXiv: [1105.2838 \[hep-ph\]](#).
- [38] S. P. Martin, *A Supersymmetry Primer*, [Adv. Ser. Direct. High Energy Phys. **18** \(1998\) 1](#), arXiv: [hep-ph/9709356](#).
- [39] M. Dine and W. Fischler, *A phenomenological model of particle physics based on supersymmetry*, [Phys. Lett. B **110** \(1982\) 227](#).
- [40] L. Alvarez-Gaumé, M. Claudson and M. B. Wise, *Low-energy supersymmetry*, [Nucl. Phys. B **207** \(1982\) 96](#).
- [41] C. R. Nappi and B. A. Ovrut, *Supersymmetric extension of the $SU(3) \times SU(2) \times U(1)$ model*, [Phys. Lett. B **113** \(1982\) 175](#).
- [42] ATLAS Collaboration, *Search for squarks and gluinos in events with an isolated lepton, jets, and missing transverse momentum at $\sqrt{s} = 13$ TeV with the ATLAS detector*, [Phys. Rev. D **96** \(2017\) 112010](#), arXiv: [1708.08232 \[hep-ex\]](#).
- [43] ATLAS Collaboration, *Search for new phenomena in final states with large jet multiplicities and missing transverse momentum using $\sqrt{s} = 13$ TeV proton–proton collisions recorded by ATLAS in Run 2 of the LHC*, [JHEP **10** \(2020\) 062](#), arXiv: [2008.06032 \[hep-ex\]](#).
- [44] ATLAS Collaboration, *Further search for supersymmetry at $\sqrt{s} = 7$ TeV in final states with jets, missing transverse momentum and isolated leptons with the ATLAS detector*, [Phys. Rev. D **86** \(2012\) 092002](#), arXiv: [1208.4688 \[hep-ex\]](#).
- [45] ATLAS Collaboration, *Search for supersymmetry with jets, missing transverse momentum and at least one hadronically decaying τ lepton in proton–proton collisions at $\sqrt{s} = 7$ TeV with the ATLAS detector*, [Phys. Lett. B **714** \(2012\) 197](#), arXiv: [1204.3852 \[hep-ex\]](#).
- [46] ATLAS Collaboration, *Search for events with large missing transverse momentum, jets, and at least two tau leptons in 7 TeV proton–proton collision data with the ATLAS detector*, [Phys. Lett. B **714** \(2012\) 180](#), arXiv: [1203.6580 \[hep-ex\]](#).
- [47] ATLAS Collaboration, *Search for electroweak production of charginos and sleptons decaying into final states with two leptons and missing transverse momentum in $\sqrt{s} = 13$ TeV pp collisions using the ATLAS detector*, [Eur. Phys. J. C **80** \(2020\) 123](#), arXiv: [1908.08215 \[hep-ex\]](#).
- [48] ATLAS Collaboration, *Search for direct stau production in events with two hadronic τ -leptons in $\sqrt{s} = 13$ TeV pp collisions with the ATLAS detector*, [Phys. Rev. D **101** \(2020\) 032009](#), arXiv: [1911.06660 \[hep-ex\]](#).
- [49] CMS Collaboration, *Search for supersymmetric partners of electrons and muons in proton–proton collisions at $\sqrt{s} = 13$ TeV*, [Phys. Lett. B **790** \(2019\) 140](#), arXiv: [1806.05264 \[hep-ex\]](#).
- [50] CMS Collaboration, *Search for direct pair production of supersymmetric partners of τ leptons in the final state with two hadronically decaying τ leptons and missing transverse momentum in proton–proton collisions at $\sqrt{s} = 13$ TeV*, (2022), arXiv: [2207.02254 \[hep-ex\]](#).

- [51] R. Barbier et al., *R-parity-violating supersymmetry*, *Phys. Rept.* **420** (2005) 1, arXiv: [hep-ph/0406039](#).
- [52] ATLAS Collaboration, *Search for R-parity-violating supersymmetry in a final state containing leptons and many jets with the ATLAS experiment using $\sqrt{s} = 13$ TeV proton–proton collision data*, *Eur. Phys. J. C* **81** (2021) 1023, arXiv: [2106.09609](#) [[hep-ex](#)].
- [53] B. C. Allanach and B. Gripaios, *Hide and Seek With Natural Supersymmetry at the LHC*, *JHEP* **05** (2012) 062, arXiv: [1202.6616](#) [[hep-ph](#)].
- [54] ATLAS Collaboration, *Search for supersymmetry in final states with two same-sign or three leptons and jets using 36fb^{-1} of $\sqrt{s} = 13$ TeV pp collision data with the ATLAS detector*, *JHEP* **09** (2017) 084, arXiv: [1706.03731](#) [[hep-ex](#)], Erratum: *JHEP* **08** (2019) 121.
- [55] ATLAS Collaboration, *A search for pair-produced resonances in four-jet final states at $\sqrt{s} = 13$ TeV with the ATLAS detector*, *Eur. Phys. J. C* **78** (2018) 250, arXiv: [1710.07171](#) [[hep-ex](#)].
- [56] ATLAS Collaboration, *ATLAS data quality operations and performance for 2015–2018 data-taking*, *JINST* **15** (2020) P04003, arXiv: [1911.04632](#) [[physics.ins-det](#)].
- [57] ATLAS Collaboration, *Luminosity determination in pp collisions at $\sqrt{s} = 13$ TeV using the ATLAS detector at the LHC*, ATLAS-CONF-2019-021, 2019, URL: <https://cds.cern.ch/record/2677054>.
- [58] G. Avoni et al., *The new LUCID-2 detector for luminosity measurement and monitoring in ATLAS*, *JINST* **13** (2018) P07017.
- [59] ATLAS Collaboration, *The ATLAS Simulation Infrastructure*, *Eur. Phys. J. C* **70** (2010) 823, arXiv: [1005.4568](#) [[physics.ins-det](#)].
- [60] S. Agostinelli et al., *GEANT4 – a simulation toolkit*, *Nucl. Instrum. Meth. A* **506** (2003) 250.
- [61] ATLAS Collaboration, *The simulation principle and performance of the ATLAS fast calorimeter simulation FastCaloSim*, ATL-PHYS-PUB-2010-013, 2010, URL: <https://cds.cern.ch/record/1300517>.
- [62] D. J. Lange, *The EvtGen particle decay simulation package*, *Nucl. Instrum. Meth. A* **462** (2001) 152.
- [63] ATLAS Collaboration, *Multi-Boson Simulation for 13 TeV ATLAS Analyses*, ATL-PHYS-PUB-2017-005, 2017, URL: <https://cds.cern.ch/record/2261933>.
- [64] ATLAS Collaboration, *Modelling of rare top quark processes at $\sqrt{s} = 13$ TeV in ATLAS*, ATL-PHYS-PUB-2020-024, 2020, URL: <https://cds.cern.ch/record/2730584>.
- [65] E. Bothmann et al., *Event generation with Sherpa 2.2*, *SciPost Phys.* **7** (2019) 034, arXiv: [1905.09127](#) [[hep-ph](#)].
- [66] S. Schumann and F. Krauss, *A parton shower algorithm based on Catani–Seymour dipole factorisation*, *JHEP* **03** (2008) 038, arXiv: [0709.1027](#) [[hep-ph](#)].
- [67] The NNPDF Collaboration, R. D. Ball et al., *Parton distributions for the LHC run II*, *JHEP* **04** (2015) 040, arXiv: [1410.8849](#) [[hep-ph](#)].
- [68] F. Buccioni et al., *OpenLoops 2*, *Eur. Phys. J. C* **79** (2019) 866, arXiv: [1907.13071](#) [[hep-ph](#)].

- [69] F. Cascioli, P. Maierhöfer and S. Pozzorini, *Scattering Amplitudes with Open Loops*, *Phys. Rev. Lett.* **108** (2012) 111601, arXiv: [1111.5206 \[hep-ph\]](#).
- [70] A. Denner, S. Dittmaier and L. Hofer, *COLLIER: A fortran-based complex one-loop library in extended regularizations*, *Comput. Phys. Commun.* **212** (2017) 220, arXiv: [1604.06792 \[hep-ph\]](#).
- [71] T. Gleisberg and S. Höche, *Comix, a new matrix element generator*, *JHEP* **12** (2008) 039, arXiv: [0808.3674 \[hep-ph\]](#).
- [72] T. Sjöstrand, S. Mrenna and P. Skands, *A brief introduction to PYTHIA 8.1*, *Comput. Phys. Commun.* **178** (2008) 852, arXiv: [0710.3820 \[hep-ph\]](#).
- [73] ATLAS Collaboration, *ATLAS Pythia 8 tunes to 7 TeV data*, ATL-PHYS-PUB-2014-021, 2014, URL: <https://cds.cern.ch/record/1966419>.
- [74] ATLAS Collaboration, *Modelling of the $t\bar{t}H$ and $t\bar{t}V(V = W, Z)$ processes for $\sqrt{s} = 13$ TeV ATLAS analyses*, ATL-PHYS-PUB-2016-005, 2016, URL: <https://cds.cern.ch/record/2120826>.
- [75] D. de Florian et al., *Handbook of LHC Higgs Cross Sections: 4. Deciphering the Nature of the Higgs Sector*, (2016), arXiv: [1610.07922 \[hep-ph\]](#).
- [76] S. Frixione, E. Laenen, P. Motylinski and B. R. Webber, *Angular correlations of lepton pairs from vector boson and top quark decays in Monte Carlo simulations*, *JHEP* **04** (2007) 081, arXiv: [hep-ph/0702198](#).
- [77] P. Artoisenet, R. Frederix, O. Mattelaer and R. Rietkerk, *Automatic spin-entangled decays of heavy resonances in Monte Carlo simulations*, *JHEP* **03** (2013) 015, arXiv: [1212.3460 \[hep-ph\]](#).
- [78] ATLAS Collaboration, *Studies on top-quark Monte Carlo modelling for Top2016*, ATL-PHYS-PUB-2016-020, 2016, URL: <https://cds.cern.ch/record/2216168>.
- [79] S. Frixione, G. Ridolfi and P. Nason, *A positive-weight next-to-leading-order Monte Carlo for heavy flavour hadroproduction*, *JHEP* **09** (2007) 126, arXiv: [0707.3088 \[hep-ph\]](#).
- [80] P. Nason, *A new method for combining NLO QCD with shower Monte Carlo algorithms*, *JHEP* **11** (2004) 040, arXiv: [hep-ph/0409146](#).
- [81] S. Frixione, P. Nason and C. Oleari, *Matching NLO QCD computations with parton shower simulations: the POWHEG method*, *JHEP* **11** (2007) 070, arXiv: [0709.2092 \[hep-ph\]](#).
- [82] S. Alioli, P. Nason, C. Oleari and E. Re, *A general framework for implementing NLO calculations in shower Monte Carlo programs: the POWHEG BOX*, *JHEP* **06** (2010) 043, arXiv: [1002.2581 \[hep-ph\]](#).
- [83] T. Sjöstrand et al., *An introduction to PYTHIA 8.2*, *Comput. Phys. Commun.* **191** (2015) 159, arXiv: [1410.3012 \[hep-ph\]](#).
- [84] E. Re, *Single-top Wt -channel production matched with parton showers using the POWHEG method*, *Eur. Phys. J. C* **71** (2011) 1547, arXiv: [1009.2450 \[hep-ph\]](#).

- [85] J. Campbell, T. Neumann and Z. Sullivan, *Single-top-quark production in the t-channel at NNLO*, *JHEP* **02** (2021) 040, arXiv: [2012.01574 \[hep-ph\]](#).
- [86] R. D. Ball et al., *The PDF4LHC21 combination of global PDF fits for the LHC Run III*, *J. Phys. G* **49** (2022) 080501, arXiv: [2203.05506 \[hep-ph\]](#).
- [87] N. Kidonakis and N. Yamanaka, *Higher-order corrections for tW production at high-energy hadron colliders*, *JHEP* **05** (2021) 278, arXiv: [2102.11300 \[hep-ph\]](#).
- [88] ATLAS Collaboration, *ATLAS simulation of boson plus jets processes in Run 2*, ATL-PHYS-PUB-2017-006, 2017, URL: <https://cds.cern.ch/record/2261937>.
- [89] C. Anastasiou, L. Dixon, K. Melnikov and F. Petriello, *High-precision QCD at hadron colliders: Electroweak gauge boson rapidity distributions at next-to-next-to leading order*, *Phys. Rev. D* **69** (2004) 094008, arXiv: [hep-ph/0312266](#).
- [90] L. Lönnblad and S. Prestel, *Matching tree-level matrix elements with interleaved showers*, *JHEP* **03** (2012) 019, arXiv: [1109.4829 \[hep-ph\]](#).
- [91] W. Beenakker, C. Borschensky, M. Krämer, A. Kulesza and E. Laenen, *NNLL-fast: predictions for coloured supersymmetric particle production at the LHC with threshold and Coulomb resummation*, *JHEP* **12** (2016) 133, arXiv: [1607.07741 \[hep-ph\]](#).
- [92] W. Beenakker et al., *NNLL resummation for squark and gluino production at the LHC*, *JHEP* **12** (2014) 023, arXiv: [1404.3134 \[hep-ph\]](#).
- [93] W. Beenakker et al., *Towards NNLL resummation: hard matching coefficients for squark and gluino hadroproduction*, *JHEP* **10** (2013) 120, arXiv: [1304.6354 \[hep-ph\]](#).
- [94] W. Beenakker et al., *NNLL resummation for squark-antisquark pair production at the LHC*, *JHEP* **01** (2012) 076, arXiv: [1110.2446 \[hep-ph\]](#).
- [95] W. Beenakker et al., *Soft-gluon resummation for squark and gluino hadroproduction*, *JHEP* **12** (2009) 041, arXiv: [0909.4418 \[hep-ph\]](#).
- [96] A. Kulesza and L. Motyka, *Soft gluon resummation for the production of gluino-gluino and squark-antisquark pairs at the LHC*, *Phys. Rev. D* **80** (2009) 095004, arXiv: [0905.4749 \[hep-ph\]](#).
- [97] A. Kulesza and L. Motyka, *Threshold Resummation for Squark-Antisquark and Gluino-Pair Production at the LHC*, *Phys. Rev. Lett.* **102** (2009) 111802, arXiv: [0807.2405 \[hep-ph\]](#).
- [98] W. Beenakker, R. Höpker, M. Spira and P. Zerwas, *Squark and gluino production at hadron colliders*, *Nucl. Phys. B* **492** (1997) 51, arXiv: [hep-ph/9610490](#).
- [99] J. Butterworth et al., *PDF4LHC recommendations for LHC Run II*, *J. Phys. G* **43** (2016) 023001, arXiv: [1510.03865 \[hep-ph\]](#).
- [100] T. Cornelissen et al., *The new ATLAS track reconstruction (NEWT)*, *J. Phys. Conf.: Ser.* **119** (2008) 032014.
- [101] ATLAS Collaboration, *Performance of the ATLAS Inner Detector Track and Vertex Reconstruction in the High Pile-Up LHC Environment*, ATL-CONF-2012-042, 2012, URL: <https://cds.cern.ch/record/1435196>.

- [102] A. Salzburger, *Optimisation of the ATLAS Track Reconstruction Software for Run-2*, *J. Phys.: Conf. Ser.* **664** (2015) 072042, URL: <https://cds.cern.ch/record/2018442>.
- [103] ATLAS Collaboration, *Reconstruction of primary vertices at the ATLAS experiment in Run 1 proton–proton collisions at the LHC*, *Eur. Phys. J. C* **77** (2017) 332, arXiv: [1611.10235](https://arxiv.org/abs/1611.10235) [[hep-ex](#)].
- [104] ATLAS Collaboration, *Vertex Reconstruction Performance of the ATLAS Detector at $\sqrt{s} = 13$ TeV*, ATL-PHYS-PUB-2015-026, 2015, URL: <https://cds.cern.ch/record/2037717>.
- [105] ATLAS Collaboration, *Development of ATLAS Primary Vertex Reconstruction for LHC Run 3*, ATL-PHYS-PUB-2019-015, 2019, URL: <https://cds.cern.ch/record/2670380>.
- [106] ATLAS Collaboration, *Alignment of the ATLAS Inner Detector in Run 2*, *Eur. Phys. J. C* **80** (2020) 1194, arXiv: [2007.07624](https://arxiv.org/abs/2007.07624) [[hep-ex](#)].
- [107] M. Cacciari, G. P. Salam and G. Soyez, *FastJet user manual*, *Eur. Phys. J. C* **72** (2012) 1896, arXiv: [1111.6097](https://arxiv.org/abs/1111.6097) [[hep-ph](#)].
- [108] M. Cacciari, G. P. Salam and G. Soyez, *The anti- k_t jet clustering algorithm*, *JHEP* **04** (2008) 063, arXiv: [0802.1189](https://arxiv.org/abs/0802.1189) [[hep-ph](#)].
- [109] ATLAS Collaboration, *Jet energy scale and resolution measured in proton–proton collisions at $\sqrt{s} = 13$ TeV with the ATLAS detector*, *Eur. Phys. J. C* **81** (2020) 689, arXiv: [2007.02645](https://arxiv.org/abs/2007.02645) [[hep-ex](#)].
- [110] ATLAS Collaboration, *Jet reconstruction and performance using particle flow with the ATLAS Detector*, *Eur. Phys. J. C* **77** (2017) 466, arXiv: [1703.10485](https://arxiv.org/abs/1703.10485) [[hep-ex](#)].
- [111] ATLAS Collaboration, *Topological cell clustering in the ATLAS calorimeters and its performance in LHC Run 1*, *Eur. Phys. J. C* **77** (2017) 490, arXiv: [1603.02934](https://arxiv.org/abs/1603.02934) [[hep-ex](#)].
- [112] ATLAS Collaboration, *Performance of pile-up mitigation techniques for jets in pp collisions at $\sqrt{s} = 8$ TeV using the ATLAS detector*, *Eur. Phys. J. C* **76** (2016) 581, arXiv: [1510.03823](https://arxiv.org/abs/1510.03823) [[hep-ex](#)].
- [113] ATLAS Collaboration, *Selection of jets produced in 13 TeV proton–proton collisions with the ATLAS detector*, ATL-CONF-2015-029, 2015, URL: <https://cds.cern.ch/record/2037702>.
- [114] ATLAS Collaboration, *ATLAS flavour-tagging algorithms for the LHC Run 2 pp collision dataset*, (2022), arXiv: [2211.16345](https://arxiv.org/abs/2211.16345) [[physics.data-an](#)].
- [115] ATLAS Collaboration, *Muon reconstruction and identification efficiency in ATLAS using the full Run 2 pp collision data set at $\sqrt{s} = 13$ TeV*, *Eur. Phys. J. C* **81** (2021) 578, arXiv: [2012.00578](https://arxiv.org/abs/2012.00578) [[hep-ex](#)].
- [116] ATLAS Collaboration, *Studies of the muon momentum calibration and performance of the ATLAS detector with pp collisions at $\sqrt{s} = 13$ TeV*, (2022), arXiv: [2212.07338](https://arxiv.org/abs/2212.07338) [[hep-ex](#)].
- [117] ATLAS Collaboration, *Electron and photon performance measurements with the ATLAS detector using the 2015–2017 LHC proton–proton collision data*, *JINST* **14** (2019) P12006, arXiv: [1908.00005](https://arxiv.org/abs/1908.00005) [[hep-ex](#)].

- [118] ATLAS Collaboration, *Electron and photon energy calibration with the ATLAS detector using 2015–2016 LHC proton–proton collision data*, *JINST* **14** (2019) P03017, arXiv: 1812.03848 [hep-ex].
- [119] ATLAS Collaboration, *E_T^{miss} performance in the ATLAS detector using 2015–2016 LHC pp collisions*, ATLAS-CONF-2018-023, 2018, URL: <https://cds.cern.ch/record/2625233>.
- [120] ATLAS Collaboration, *Performance of electron and photon triggers in ATLAS during LHC Run 2*, *Eur. Phys. J. C* **80** (2020) 47, arXiv: 1909.00761 [hep-ex].
- [121] ATLAS Collaboration, *Performance of the ATLAS muon triggers in Run 2*, *JINST* **15** (2020) P09015, arXiv: 2004.13447 [hep-ex].
- [122] ATLAS Collaboration, *Performance of the missing transverse momentum triggers for the ATLAS detector during Run-2 data taking*, *JHEP* **08** (2020) 080, arXiv: 2005.09554 [hep-ex].
- [123] ATLAS Collaboration, *Object-based missing transverse momentum significance in the ATLAS Detector*, ATLAS-CONF-2018-038, 2018, URL: <https://cds.cern.ch/record/2630948>.
- [124] ATLAS Collaboration, *Observation of electroweak $W^\pm Z$ boson pair production in association with two jets in pp collisions at $\sqrt{s} = 13$ TeV with the ATLAS detector*, *Phys. Lett. B* **793** (2019) 469, arXiv: 1812.09740 [hep-ex].
- [125] ATLAS Collaboration, *Measurement of $W^\pm Z$ production cross sections and gauge boson polarisation in pp collisions at $\sqrt{s} = 13$ TeV with the ATLAS detector*, *Eur. Phys. J. C* **79** (2019) 535, arXiv: 1902.05759 [hep-ex].
- [126] ATLAS Collaboration, *Observation of Higgs boson production in association with a top quark pair at the LHC with the ATLAS detector*, *Phys. Lett. B* **784** (2018) 173, arXiv: 1806.00425 [hep-ex].
- [127] ATLAS Collaboration, *Search for direct production of winos and higgsinos in events with two same-sign or three leptons in pp collision data at 13 TeV with the ATLAS detector*, ATLAS-CONF-2022-057, 2022, URL: <https://cds.cern.ch/record/2826603>.
- [128] D0 Collaboration, *Extraction of the width of the W boson from measurements of $\sigma(p\bar{p} \rightarrow W + X) \times B(W \rightarrow e\nu)$ and $\sigma(p\bar{p} \rightarrow Z + X) \times B(Z \rightarrow ee)$ and their ratio*, *Phys. Rev. D* **61** (2000) 072001, arXiv: hep-ex/9906025.
- [129] ATLAS Collaboration, *Tools for estimating fake/non-prompt lepton backgrounds with the ATLAS detector at the LHC*, (2022), arXiv: 2211.16178 [hep-ex].
- [130] ATLAS Collaboration, *Formulae for Estimating Significance*, ATLAS-PHYS-PUB-2020-025, 2020, URL: <https://cds.cern.ch/record/2736148>.
- [131] ATLAS Collaboration, *Electron reconstruction and identification in the ATLAS experiment using the 2015 and 2016 LHC proton–proton collision data at $\sqrt{s} = 13$ TeV*, *Eur. Phys. J. C* **79** (2019) 639, arXiv: 1902.04655 [hep-ex].
- [132] ATLAS Collaboration, *Electron efficiency measurements with the ATLAS detector using the 2015 LHC proton–proton collision data*, ATLAS-CONF-2016-024, 2016, URL: <https://cds.cern.ch/record/2157687>.

- [133] ATLAS Collaboration, *Forward jet vertex tagging using the particle flow algorithm*, ATL-PHYS-PUB-2019-026, 2019, URL: <https://cds.cern.ch/record/2683100>.
- [134] ATLAS Collaboration, *Jet energy scale measurements and their systematic uncertainties in proton–proton collisions at $\sqrt{s} = 13$ TeV with the ATLAS detector*, *Phys. Rev. D* **96** (2017) 072002, arXiv: [1703.09665](https://arxiv.org/abs/1703.09665) [[hep-ex](#)].
- [135] ATLAS Collaboration, *ATLAS b -jet identification performance and efficiency measurement with $t\bar{t}$ events in pp collisions at $\sqrt{s} = 13$ TeV*, *Eur. Phys. J. C* **79** (2019) 970, arXiv: [1907.05120](https://arxiv.org/abs/1907.05120) [[hep-ex](#)].
- [136] ATLAS Collaboration, *Measurement of the c -jet mistagging efficiency in $t\bar{t}$ events using pp collision data at $\sqrt{s} = 13$ TeV collected with the ATLAS detector*, *Eur. Phys. J. C* **82** (2021) 95, arXiv: [2109.10627](https://arxiv.org/abs/2109.10627) [[hep-ex](#)].
- [137] ATLAS Collaboration, *Calibration of light-flavour b -jet mistagging rates using ATLAS proton–proton collision data at $\sqrt{s} = 13$ TeV*, ATL-CONF-2018-006, 2018, URL: <https://cds.cern.ch/record/2314418>.
- [138] L. A. Harland-Lang, A. D. Martin, P. Motylinski and R. S. Thorne, *Parton distributions in the LHC era: MMHT 2014 PDFs*, *Eur. Phys. J. C* **75** (2015) 204, arXiv: [1412.3989](https://arxiv.org/abs/1412.3989) [[hep-ph](#)].
- [139] S. Dulat et al., *New parton distribution functions from a global analysis of quantum chromodynamics*, *Phys. Rev. D* **93** (2016) 033006, arXiv: [1506.07443](https://arxiv.org/abs/1506.07443) [[hep-ph](#)].
- [140] NNPDF Collaboration, R. D. Ball et al., *Parton distributions with LHC data*, *Nucl. Phys. B* **867** (2013) 244, arXiv: [1207.1303](https://arxiv.org/abs/1207.1303) [[hep-ph](#)].
- [141] M. Baak et al., *HistFitter software framework for statistical data analysis*, *Eur. Phys. J. C* **75** (2015) 153, arXiv: [1410.1280](https://arxiv.org/abs/1410.1280) [[hep-ex](#)].
- [142] T. Junk, *Confidence level computation for combining searches with small statistics*, *Nucl. Instrum. Meth. A* **434** (1999) 435, arXiv: [hep-ex/9902006](https://arxiv.org/abs/hep-ex/9902006).
- [143] A. L. Read, *Presentation of search results: the CL_S technique*, *J. Phys. G* **28** (2002) 2693.
- [144] G. Cowan, K. Cranmer, E. Gross and O. Vitells, *Asymptotic formulae for likelihood-based tests of new physics*, *Eur. Phys. J. C* **71** (2011) 1554, arXiv: [1007.1727](https://arxiv.org/abs/1007.1727) [[physics.data-an](#)], Erratum: *Eur. Phys. J. C* **73** (2013) 2501.
- [145] ATLAS Collaboration, *ATLAS Computing Acknowledgements*, ATL-SOFT-PUB-2021-003, 2021, URL: <https://cds.cern.ch/record/2776662>.

The ATLAS Collaboration

G. Aad ¹⁰², B. Abbott ¹²⁰, K. Abeling ⁵⁵, N.J. Abicht ⁴⁹, S.H. Abidi ²⁹, A. Aboulhorma ^{35e}, H. Abramowicz ¹⁵¹, H. Abreu ¹⁵⁰, Y. Abulaiti ¹¹⁷, A.C. Abusleme Hoffman ^{137a}, B.S. Acharya ^{69a,69b,n}, C. Adam Bourdarios ⁴, L. Adamczyk ^{86a}, L. Adamek ¹⁵⁵, S.V. Addepalli ²⁶, M.J. Addison ¹⁰¹, J. Adelman ¹¹⁵, A. Adiguzel ^{21c}, T. Adye ¹³⁴, A.A. Affolder ¹³⁶, Y. Afik ³⁶, M.N. Agaras ¹³, J. Agarwala ^{73a,73b}, A. Aggarwal ¹⁰⁰, C. Agheorghiesei ^{27c}, A. Ahmad ³⁶, F. Ahmadov ^{38,z}, W.S. Ahmed ¹⁰⁴, S. Ahuja ⁹⁵, X. Ai ^{62a}, G. Aielli ^{76a,76b}, M. Ait Tamliah ^{35e}, B. Aitbenkikh ^{35a}, I. Aizenberg ¹⁶⁹, M. Akbiyik ¹⁰⁰, T.P.A. Åkesson ⁹⁸, A.V. Akimov ³⁷, D. Akiyama ¹⁶⁸, N.N. Akolkar ²⁴, K. Al Houry ⁴¹, G.L. Alberghi ^{23b}, J. Albert ¹⁶⁵, P. Albicocco ⁵³, G.L. Albouy ⁶⁰, S. Alderweireldt ⁵², M. Aleksa ³⁶, I.N. Aleksandrov ³⁸, C. Alexa ^{27b}, T. Alexopoulos ¹⁰, A. Alfonsi ¹¹⁴, F. Alfonsi ^{23b}, M. Algren ⁵⁶, M. Alhroob ¹²⁰, B. Ali ¹³², H.M.J. Ali ⁹¹, S. Ali ¹⁴⁸, S.W. Alibocus ⁹², M. Aliev ³⁷, G. Alimonti ^{71a}, W. Alkahi ⁵⁵, C. Allaire ⁶⁶, B.M.M. Allbrooke ¹⁴⁶, J.F. Allen ⁵², C.A. Allendes Flores ^{137f}, P.P. Allport ²⁰, A. Aloisio ^{72a,72b}, F. Alonso ⁹⁰, C. Alpigiani ¹³⁸, M. Alvarez Estevez ⁹⁹, A. Alvarez Fernandez ¹⁰⁰, M. Alves Cardoso ⁵⁶, M.G. Alviggi ^{72a,72b}, M. Aly ¹⁰¹, Y. Amaral Coutinho ^{83b}, A. Ambler ¹⁰⁴, C. Amelung ³⁶, M. Amerl ¹⁰¹, C.G. Ames ¹⁰⁹, D. Amidei ¹⁰⁶, S.P. Amor Dos Santos ^{130a}, K.R. Amos ¹⁶³, V. Ananiev ¹²⁵, C. Anastopoulos ¹³⁹, T. Andeen ¹¹, J.K. Anders ³⁶, S.Y. Andreev ^{47a,47b}, A. Andreatta ^{71a,71b}, S. Angelidakis ⁹, A. Angerami ^{41,ac}, A.V. Anisenkov ³⁷, A. Annovi ^{74a}, C. Antel ⁵⁶, M.T. Anthony ¹³⁹, E. Antipov ¹⁴⁵, M. Antonelli ⁵³, D.J.A. Antrim ^{17a}, F. Anulli ^{75a}, M. Aoki ⁸⁴, T. Aoki ¹⁵³, J.A. Aparisi Pozo ¹⁶³, M.A. Aparo ¹⁴⁶, L. Aperio Bella ⁴⁸, C. Appelt ¹⁸, A. Apyan ²⁶, N. Aranzabal ³⁶, C. Arcangeletti ⁵³, A.T.H. Arce ⁵¹, E. Arena ⁹², J-F. Arguin ¹⁰⁸, S. Argyropoulos ⁵⁴, J.-H. Arling ⁴⁸, O. Arnaez ⁴, H. Arnold ¹¹⁴, Z.P. Arrubarrena Tame ¹⁰⁹, G. Artoni ^{75a,75b}, H. Asada ¹¹¹, K. Asai ¹¹⁸, S. Asai ¹⁵³, N.A. Asbah ⁶¹, K. Assamagan ²⁹, R. Astalos ^{28a}, S. Atashi ¹⁶⁰, R.J. Atkin ^{33a}, M. Atkinson ¹⁶², N.B. Atlay ¹⁸, H. Atmani ^{62b}, P.A. Atlasiddha ¹⁰⁶, K. Augsten ¹³², S. Auricchio ^{72a,72b}, A.D. Auriol ²⁰, V.A. Austrup ¹⁰¹, G. Avolio ³⁶, K. Axiotis ⁵⁶, G. Azuelos ^{108,ag}, D. Babal ^{28b}, H. Bachacou ¹³⁵, K. Bachas ^{152,q}, A. Bachiu ³⁴, F. Backman ^{47a,47b}, A. Badea ⁶¹, P. Bagnaia ^{75a,75b}, M. Bahmani ¹⁸, A.J. Bailey ¹⁶³, V.R. Bailey ¹⁶², J.T. Baines ¹³⁴, L. Baines ⁹⁴, C. Bakalis ¹⁰, O.K. Baker ¹⁷², E. Bakos ¹⁵, D. Bakshi Gupta ⁸, R. Balasubramanian ¹¹⁴, E.M. Baldin ³⁷, P. Balek ^{86a}, E. Ballabene ^{23b,23a}, F. Balli ¹³⁵, L.M. Baltes ^{63a}, W.K. Balunas ³², J. Balz ¹⁰⁰, E. Banas ⁸⁷, M. Bandieramonte ¹²⁹, A. Bandyopadhyay ²⁴, S. Bansal ²⁴, L. Barak ¹⁵¹, M. Barakat ⁴⁸, E.L. Barberio ¹⁰⁵, D. Barberis ^{57b,57a}, M. Barbero ¹⁰², G. Barbour ⁹⁶, K.N. Barends ^{33a}, T. Barillari ¹¹⁰, M-S. Barisits ³⁶, T. Barklow ¹⁴³, P. Baron ¹²², D.A. Baron Moreno ¹⁰¹, A. Baroncelli ^{62a}, G. Barone ²⁹, A.J. Barr ¹²⁶, J.D. Barr ⁹⁶, L. Barranco Navarro ^{47a,47b}, F. Barreiro ⁹⁹, J. Barreiro Guimarães da Costa ^{14a}, U. Barron ¹⁵¹, M.G. Barros Teixeira ^{130a}, S. Barsov ³⁷, F. Bartels ^{63a}, R. Bartoldus ¹⁴³, A.E. Barton ⁹¹, P. Bartos ^{28a}, A. Basan ¹⁰⁰, M. Baselga ⁴⁹, A. Bassalat ^{66,b}, M.J. Basso ^{156a}, C.R. Basson ¹⁰¹, R.L. Bates ⁵⁹, S. Batlamous ^{35e}, J.R. Batley ³², B. Batool ¹⁴¹, M. Battaglia ¹³⁶, D. Battulga ¹⁸, M. Baucé ^{75a,75b}, M. Bauer ³⁶, P. Bauer ²⁴, L.T. Bazzano Hurrell ³⁰, J.B. Beacham ⁵¹, T. Beau ¹²⁷, P.H. Beauchemin ¹⁵⁸, F. Becherer ⁵⁴, P. Bechtel ²⁴, H.P. Beck ^{19,p}, K. Becker ¹⁶⁷, A.J. Beddall ⁸², V.A. Bednyakov ³⁸, C.P. Bee ¹⁴⁵, L.J. Beemster ¹⁵, T.A. Beermann ³⁶, M. Begalli ^{83d}, M. Beger ²⁹, A. Behera ¹⁴⁵, J.K. Behr ⁴⁸, J.F. Beirer ⁵⁵, F. Beisiegel ²⁴, M. Belfkir ¹⁵⁹, G. Bella ¹⁵¹, L. Bellagamba ^{23b}, A. Bellerive ³⁴, P. Bellos ²⁰, K. Beloborodov ³⁷, N.L. Belyaev ³⁷, D. Bencheikroun ^{35a}, F. Bendebba ^{35a},

Y. Benhammou [ID151](#), M. Benoit [ID29](#), J.R. Bensingler [ID26](#), S. Bentvelsen [ID114](#), L. Beresford [ID48](#),
 M. Beretta [ID53](#), E. Bergeaas Kuutmann [ID161](#), N. Berger [ID4](#), B. Bergmann [ID132](#), J. Beringer [ID17a](#),
 G. Bernardi [ID5](#), C. Bernius [ID143](#), F.U. Bernlochner [ID24](#), F. Bernon [ID36,102](#), T. Berry [ID95](#), P. Berta [ID133](#),
 A. Berthold [ID50](#), I.A. Bertram [ID91](#), S. Bethke [ID110](#), A. Betti [ID75a,75b](#), A.J. Bevan [ID94](#), M. Bhamjee [ID33c](#),
 S. Bhatta [ID145](#), D.S. Bhattacharya [ID166](#), P. Bhattarai [ID26](#), V.S. Bhopatkar [ID121](#), R. Bi [ID29,ai](#),
 R.M. Bianchi [ID129](#), G. Bianco [ID23b,23a](#), O. Biebel [ID109](#), R. Bielski [ID123](#), M. Biglietti [ID77a](#),
 T.R.V. Billoud [ID132](#), M. Bindi [ID55](#), A. Bingul [ID21b](#), C. Bini [ID75a,75b](#), A. Biondini [ID92](#),
 C.J. Birch-sykes [ID101](#), G.A. Bird [ID20,134](#), M. Birman [ID169](#), M. Biros [ID133](#), T. Bisanz [ID49](#),
 E. Bisceglie [ID43b,43a](#), D. Biswas [ID141](#), A. Bitadze [ID101](#), K. Bjørke [ID125](#), I. Bloch [ID48](#), C. Blocker [ID26](#),
 A. Blue [ID59](#), U. Blumenschein [ID94](#), J. Blumenthal [ID100](#), G.J. Bobbink [ID114](#), V.S. Bobrovnikov [ID37](#),
 M. Boehler [ID54](#), B. Boehm [ID166](#), D. Bogavac [ID36](#), A.G. Bogdanchikov [ID37](#), C. Bohm [ID47a](#),
 V. Boisvert [ID95](#), P. Bokan [ID48](#), T. Bold [ID86a](#), M. Bomben [ID5](#), M. Bona [ID94](#), M. Boonekamp [ID135](#),
 C.D. Booth [ID95](#), A.G. Borbély [ID59](#), I.S. Bordulev [ID37](#), H.M. Borecka-Bielska [ID108](#), L.S. Borgna [ID96](#),
 G. Borissov [ID91](#), D. Bortoletto [ID126](#), D. Boscherini [ID23b](#), M. Bosman [ID13](#), J.D. Bossio Sola [ID36](#),
 K. Bouaouda [ID35a](#), N. Bouchhar [ID163](#), J. Boudreau [ID129](#), E.V. Bouhova-Thacker [ID91](#), D. Boumediene [ID40](#),
 R. Bouquet [ID5](#), A. Boveia [ID119](#), J. Boyd [ID36](#), D. Boye [ID29](#), I.R. Boyko [ID38](#), J. Bracinik [ID20](#),
 N. Brahim [ID62d](#), G. Brandt [ID171](#), O. Brandt [ID32](#), F. Braren [ID48](#), B. Brau [ID103](#), J.E. Brau [ID123](#),
 R. Brenner [ID169](#), L. Brenner [ID114](#), R. Brenner [ID161](#), S. Bressler [ID169](#), D. Britton [ID59](#), D. Britzger [ID110](#),
 I. Brock [ID24](#), G. Brooijmans [ID41](#), W.K. Brooks [ID137f](#), E. Brost [ID29](#), L.M. Brown [ID165](#), L.E. Bruce [ID61](#),
 T.L. Bruckler [ID126](#), P.A. Bruckman de Renstrom [ID87](#), B. Brüers [ID48](#), D. Bruncko [ID28b,*](#), A. Bruni [ID23b](#),
 G. Bruni [ID23b](#), M. Bruschi [ID23b](#), N. Bruscano [ID75a,75b](#), T. Buanes [ID16](#), Q. Buat [ID138](#), D. Buchin [ID110](#),
 A.G. Buckley [ID59](#), M.K. Bugge [ID125](#), O. Bulekov [ID37](#), B.A. Bullard [ID143](#), S. Burdin [ID92](#),
 C.D. Burgard [ID49](#), A.M. Burger [ID40](#), B. Burghgrave [ID8](#), O. Burlayenko [ID54](#), J.T.P. Burr [ID32](#),
 C.D. Burton [ID11](#), J.C. Burzynski [ID142](#), E.L. Busch [ID41](#), V. Büscher [ID100](#), P.J. Bussey [ID59](#),
 J.M. Butler [ID25](#), C.M. Buttar [ID59](#), J.M. Butterworth [ID96](#), W. Buttinger [ID134](#), C.J. Buxo Vazquez [ID107](#),
 A.R. Buzykaev [ID37](#), G. Cabras [ID23b](#), S. Cabrera Urbán [ID163](#), L. Cadamuro [ID66](#), D. Caforio [ID58](#),
 H. Cai [ID129](#), Y. Cai [ID14a,14e](#), V.M.M. Cairo [ID36](#), O. Cakir [ID3a](#), N. Calace [ID36](#), P. Calafiura [ID17a](#),
 G. Calderini [ID127](#), P. Calfayan [ID68](#), G. Callea [ID59](#), L.P. Caloba [ID83b](#), D. Calvet [ID40](#), S. Calvet [ID40](#),
 T.P. Calvet [ID102](#), M. Calvetti [ID74a,74b](#), R. Camacho Toro [ID127](#), S. Camarda [ID36](#), D. Camarero Munoz [ID26](#),
 P. Camarri [ID76a,76b](#), M.T. Camerlingo [ID72a,72b](#), D. Cameron [ID125](#), C. Camincher [ID165](#), M. Campanelli [ID96](#),
 A. Camplani [ID42](#), V. Canale [ID72a,72b](#), A. Canesse [ID104](#), M. Cano Bret [ID80](#), J. Cantero [ID163](#), Y. Cao [ID162](#),
 F. Capocasa [ID26](#), M. Capua [ID43b,43a](#), A. Carbone [ID71a,71b](#), R. Cardarelli [ID76a](#), J.C.J. Cardenas [ID8](#),
 F. Cardillo [ID163](#), T. Carli [ID36](#), G. Carlino [ID72a](#), J.I. Carlotta [ID13](#), B.T. Carlson [ID129,r](#),
 E.M. Carlson [ID165,156a](#), L. Carminati [ID71a,71b](#), A. Carnelli [ID135](#), M. Carnesale [ID75a,75b](#), S. Caron [ID113](#),
 E. Carquin [ID137f](#), S. Carrá [ID71a](#), G. Carratta [ID23b,23a](#), F. Carrio Argos [ID33g](#), J.W.S. Carter [ID155](#),
 T.M. Carter [ID52](#), M.P. Casado [ID13,i](#), M. Caspar [ID48](#), E.G. Castiglia [ID172](#), F.L. Castillo [ID4](#),
 L. Castillo Garcia [ID13](#), V. Castillo Gimenez [ID163](#), N.F. Castro [ID130a,130e](#), A. Catinaccio [ID36](#),
 J.R. Catmore [ID125](#), V. Cavaliere [ID29](#), N. Cavalli [ID23b,23a](#), V. Cavasinni [ID74a,74b](#), Y.C. Cekmecelioglu [ID48](#),
 E. Celebi [ID21a](#), F. Celli [ID126](#), M.S. Centonze [ID70a,70b](#), K. Cerny [ID122](#), A.S. Cerqueira [ID83a](#), A. Cerri [ID146](#),
 L. Cerrito [ID76a,76b](#), F. Cerutti [ID17a](#), B. Cervato [ID141](#), A. Cervelli [ID23b](#), G. Cesarini [ID53](#), S.A. Cetin [ID82](#),
 Z. Chadi [ID35a](#), D. Chakraborty [ID115](#), M. Chala [ID130f](#), J. Chan [ID170](#), W.Y. Chan [ID153](#), J.D. Chapman [ID32](#),
 E. Chapon [ID135](#), B. Chargeishvili [ID149b](#), D.G. Charlton [ID20](#), T.P. Charman [ID94](#), M. Chatterjee [ID19](#),
 C. Chauhan [ID133](#), S. Chekanov [ID6](#), S.V. Chekulaev [ID156a](#), G.A. Chelkov [ID38,a](#), A. Chen [ID106](#),
 B. Chen [ID151](#), B. Chen [ID165](#), H. Chen [ID14c](#), H. Chen [ID29](#), J. Chen [ID62c](#), J. Chen [ID142](#), M. Chen [ID126](#),
 S. Chen [ID153](#), S.J. Chen [ID14c](#), X. Chen [ID62c](#), X. Chen [ID14b,af](#), Y. Chen [ID62a](#), C.L. Cheng [ID170](#),
 H.C. Cheng [ID64a](#), S. Cheong [ID143](#), A. Cheplakov [ID38](#), E. Cheremushkina [ID48](#), E. Cherepanova [ID114](#),
 R. Cherkaoui El Moursli [ID35e](#), E. Cheu [ID7](#), K. Cheung [ID65](#), L. Chevalier [ID135](#), V. Chiarella [ID53](#),

G. Chiarelli ^{74a}, N. Chiedde ¹⁰², G. Chiodini ^{70a}, A.S. Chisholm ²⁰, A. Chitan ^{27b}, M. Chitishvili ¹⁶³, M.V. Chizhov ³⁸, K. Choi ¹¹, A.R. Chomont ^{75a,75b}, Y. Chou ¹⁰³, E.Y.S. Chow ¹¹⁴, T. Chowdhury ^{33g}, K.L. Chu ¹⁶⁹, M.C. Chu ^{64a}, X. Chu ^{14a,14e}, J. Chudoba ¹³¹, J.J. Chwastowski ⁸⁷, D. Cieri ¹¹⁰, K.M. Ciesla ^{86a}, V. Cindro ⁹³, A. Ciocio ^{17a}, F. Cirotto ^{72a,72b}, Z.H. Citron ^{169,1}, M. Citterio ^{71a}, D.A. Ciubotaru ^{27b}, B.M. Ciungu ¹⁵⁵, A. Clark ⁵⁶, P.J. Clark ⁵², J.M. Clavijo Columbie ⁴⁸, S.E. Clawson ⁴⁸, C. Clement ^{47a,47b}, J. Clercx ⁴⁸, L. Clissa ^{23b,23a}, Y. Coadou ¹⁰², M. Cobal ^{69a,69c}, A. Coccaro ^{57b}, R.F. Coelho Barrue ^{130a}, R. Coelho Lopes De Sa ¹⁰³, S. Coelli ^{71a}, H. Cohen ¹⁵¹, A.E.C. Coimbra ^{71a,71b}, B. Cole ⁴¹, J. Collot ⁶⁰, P. Conde Muiño ^{130a,130g}, M.P. Connell ^{33c}, S.H. Connell ^{33c}, I.A. Connelly ⁵⁹, E.I. Conroy ¹²⁶, F. Conventi ^{72a,ah}, H.G. Cooke ²⁰, A.M. Cooper-Sarkar ¹²⁶, A. Cordeiro Oudot Choi ¹²⁷, F. Cormier ¹⁶⁴, L.D. Corpe ⁴⁰, M. Corradi ^{75a,75b}, F. Corriveau ^{104,x}, A. Cortes-Gonzalez ¹⁸, M.J. Costa ¹⁶³, F. Costanza ⁴, D. Costanzo ¹³⁹, B.M. Cote ¹¹⁹, G. Cowan ⁹⁵, K. Cranmer ¹⁷⁰, D. Cremonini ^{23b,23a}, S. Crépe-Renaudin ⁶⁰, F. Crescioli ¹²⁷, M. Cristinziani ¹⁴¹, M. Cristoforetti ^{78a,78b}, V. Croft ¹¹⁴, J.E. Crosby ¹²¹, G. Crosetti ^{43b,43a}, A. Cueto ⁹⁹, T. Cuhadar Donszelmann ¹⁶⁰, H. Cui ^{14a,14e}, Z. Cui ⁷, W.R. Cunningham ⁵⁹, F. Curcio ^{43b,43a}, P. Czodrowski ³⁶, M.M. Czurylo ^{63b}, M.J. Da Cunha Sargedas De Sousa ^{62a}, J.V. Da Fonseca Pinto ^{83b}, C. Da Via ¹⁰¹, W. Dabrowski ^{86a}, T. Dado ⁴⁹, S. Dahbi ^{33g}, T. Dai ¹⁰⁶, C. Dallapiccola ¹⁰³, M. Dam ⁴², G. D'amen ²⁹, V. D'Amico ¹⁰⁹, J. Damp ¹⁰⁰, J.R. Dandoy ¹²⁸, M.F. Daneri ³⁰, M. Danninger ¹⁴², V. Dao ³⁶, G. Darbo ^{57b}, S. Darmora ⁶, S.J. Das ^{29,ai}, S. D'Auria ^{71a,71b}, C. David ^{156b}, T. Davidek ¹³³, B. Davis-Purcell ³⁴, I. Dawson ⁹⁴, H.A. Day-hall ¹³², K. De ⁸, R. De Asmundis ^{72a}, N. De Biase ⁴⁸, S. De Castro ^{23b,23a}, N. De Groot ¹¹³, P. de Jong ¹¹⁴, H. De la Torre ¹⁰⁷, A. De Maria ^{14c}, A. De Salvo ^{75a}, U. De Sanctis ^{76a,76b}, A. De Santo ¹⁴⁶, J.B. De Vivie De Regie ⁶⁰, D.V. Dedovich ³⁸, J. Degens ¹¹⁴, A.M. Deiana ⁴⁴, F. Del Corso ^{23b,23a}, J. Del Peso ⁹⁹, F. Del Rio ^{63a}, F. Deliot ¹³⁵, C.M. Delitzsch ⁴⁹, M. Della Pietra ^{72a,72b}, D. Della Volpe ⁵⁶, A. Dell'Acqua ³⁶, L. Dell'Asta ^{71a,71b}, M. Delmastro ⁴, P.A. Delsart ⁶⁰, S. Demers ¹⁷², M. Demichev ³⁸, S.P. Denisov ³⁷, L. D'Eramo ⁴⁰, D. Derendarz ⁸⁷, F. Derue ¹²⁷, P. Dervan ⁹², K. Desch ²⁴, C. Deutsch ²⁴, F.A. Di Bello ^{57b,57a}, A. Di Ciaccio ^{76a,76b}, L. Di Ciaccio ⁴, A. Di Domenico ^{75a,75b}, C. Di Donato ^{72a,72b}, A. Di Girolamo ³⁶, G. Di Gregorio ⁵, A. Di Luca ^{78a,78b}, B. Di Micco ^{77a,77b}, R. Di Nardo ^{77a,77b}, C. Diaconu ¹⁰², M. Diamantopoulou ³⁴, F.A. Dias ¹¹⁴, T. Dias Do Vale ¹⁴², M.A. Diaz ^{137a,137b}, F.G. Diaz Capriles ²⁴, M. Didenko ¹⁶³, E.B. Diehl ¹⁰⁶, L. Diehl ⁵⁴, S. Díez Cornell ⁴⁸, C. Diez Pardos ¹⁴¹, C. Dimitriadi ^{161,24,161}, A. Dimitrievska ^{17a}, J. Dingfelder ²⁴, I-M. Dinu ^{27b}, S.J. Dittmeier ^{63b}, F. Dittus ³⁶, F. Djama ¹⁰², T. Djobava ^{149b}, J.I. Djuvsland ¹⁶, C. Doglioni ^{101,98}, J. Dolejsi ¹³³, Z. Dolezal ¹³³, M. Donadelli ^{83c}, B. Dong ¹⁰⁷, J. Donini ⁴⁰, A. D'Onofrio ^{77a,77b}, M. D'Onofrio ⁹², J. Dopke ¹³⁴, A. Doria ^{72a}, N. Dos Santos Fernandes ^{130a}, M.T. Dova ⁹⁰, A.T. Doyle ⁵⁹, M.A. Draguet ¹²⁶, E. Dreyer ¹⁶⁹, I. Drivas-koulouris ¹⁰, A.S. Drobac ¹⁵⁸, M. Drozdova ⁵⁶, D. Du ^{62a}, T.A. du Pree ¹¹⁴, F. Dubinin ³⁷, M. Dubovsky ^{28a}, E. Duchovni ¹⁶⁹, G. Duckeck ¹⁰⁹, O.A. Ducu ^{27b}, D. Duda ⁵², A. Dudarev ³⁶, E.R. Duden ²⁶, M. D'uffizi ¹⁰¹, L. Duflot ⁶⁶, M. Dührssen ³⁶, C. Dülsen ¹⁷¹, A.E. Dumitriu ^{27b}, M. Dunford ^{63a}, S. Dungs ⁴⁹, K. Dunne ^{47a,47b}, A. Duperrin ¹⁰², H. Duran Yildiz ^{3a}, M. Düren ⁵⁸, A. Durglishvili ^{149b}, B.L. Dwyer ¹¹⁵, G.I. Dyckes ^{17a}, M. Dyndal ^{86a}, S. Dysch ¹⁰¹, B.S. Dziedzic ⁸⁷, Z.O. Earnshaw ¹⁴⁶, G.H. Eberwein ¹²⁶, B. Eckerova ^{28a}, S. Eggebrecht ⁵⁵, M.G. Eggleston ⁵¹, E. Egidio Purcino De Souza ¹²⁷, L.F. Ehrke ⁵⁶, G. Eigen ¹⁶, K. Einsweiler ^{17a}, T. Ekelof ¹⁶¹, P.A. Ekman ⁹⁸, S. El Farkh ^{35b}, Y. El Ghazali ^{35b}, H. El Jarrari ^{35e,148}, A. El Moussaouy ^{35a}, V. Ellajosyula ¹⁶¹, M. Ellert ¹⁶¹, F. Ellinghaus ¹⁷¹, A.A. Elliot ⁹⁴, N. Ellis ³⁶, J. Elmsheuser ²⁹, M. Elsing ³⁶, D. Emelianov ¹³⁴, Y. Enari ¹⁵³, I. Ene ^{17a},

S. Epari [ID13](#), J. Erdmann [ID49](#), P.A. Erland [ID87](#), M. Errenst [ID171](#), M. Escalier [ID66](#), C. Escobar [ID163](#), E. Etzion [ID151](#), G. Evans [ID130a](#), H. Evans [ID68](#), L.S. Evans [ID95](#), M.O. Evans [ID146](#), A. Ezhilov [ID37](#), S. Ezzarqtouni [ID35a](#), F. Fabbri [ID59](#), L. Fabbri [ID23b,23a](#), G. Facini [ID96](#), V. Fadeyev [ID136](#), R.M. Fakhrutdinov [ID37](#), S. Falciano [ID75a](#), L.F. Falda Ulhoa Coelho [ID36](#), P.J. Falke [ID24](#), J. Faltova [ID133](#), C. Fan [ID162](#), Y. Fan [ID14a](#), Y. Fang [ID14a,14e](#), M. Fanti [ID71a,71b](#), M. Faraj [ID69a,69b](#), Z. Farazpay [ID97](#), A. Farbin [ID8](#), A. Farilla [ID77a](#), T. Farooque [ID107](#), S.M. Farrington [ID52](#), F. Fassi [ID35e](#), D. Fassouliotis [ID9](#), M. Faucci Giannelli [ID76a,76b](#), W.J. Fawcett [ID32](#), L. Fayard [ID66](#), P. Federic [ID133](#), P. Federicova [ID131](#), O.L. Fedin [ID37,a](#), G. Fedotov [ID37](#), M. Feickert [ID170](#), L. Feligioni [ID102](#), D.E. Fellers [ID123](#), C. Feng [ID62b](#), M. Feng [ID14b](#), Z. Feng [ID114](#), M.J. Fenton [ID160](#), A.B. Fenyuk [ID37](#), L. Ferencz [ID48](#), R.A.M. Ferguson [ID91](#), S.I. Fernandez Luengo [ID137f](#), M.J.V. Fernoux [ID102](#), J. Ferrando [ID48](#), A. Ferrari [ID161](#), P. Ferrari [ID114,113](#), R. Ferrari [ID73a](#), D. Ferrere [ID56](#), C. Ferretti [ID106](#), F. Fiedler [ID100](#), A. Filipčić [ID93](#), E.K. Filmer [ID1](#), F. Filthaut [ID113](#), M.C.N. Fiolhais [ID130a,130c,c](#), L. Fiorini [ID163](#), W.C. Fisher [ID107](#), T. Fitschen [ID101](#), P.M. Fitzhugh [ID135](#), I. Fleck [ID141](#), P. Fleischmann [ID106](#), T. Flick [ID171](#), L. Flores [ID128](#), M. Flores [ID33d,ad](#), L.R. Flores Castillo [ID64a](#), L. Flores Sanz De Acedo [ID36](#), F.M. Follega [ID78a,78b](#), N. Fomin [ID16](#), J.H. Foo [ID155](#), B.C. Forland [ID68](#), A. Formica [ID135](#), A.C. Forti [ID101](#), E. Fortin [ID36](#), A.W. Fortman [ID61](#), M.G. Foti [ID17a](#), L. Fountas [ID9,j](#), D. Fournier [ID66](#), H. Fox [ID91](#), P. Francavilla [ID74a,74b](#), S. Francescato [ID61](#), S. Franchellucci [ID56](#), M. Franchini [ID23b,23a](#), S. Franchino [ID63a](#), D. Francis [ID36](#), L. Franco [ID113](#), L. Franconi [ID48](#), M. Franklin [ID61](#), G. Frattari [ID26](#), A.C. Freegard [ID94](#), W.S. Freund [ID83b](#), Y.Y. Frid [ID151](#), N. Fritzsche [ID50](#), A. Froch [ID54](#), D. Froidevaux [ID36](#), J.A. Frost [ID126](#), Y. Fu [ID62a](#), M. Fujimoto [ID118](#), E. Fullana Torregrosa [ID163,*](#), K.Y. Fung [ID64a](#), E. Furtado De Simas Filho [ID83b](#), M. Furukawa [ID153](#), J. Fuster [ID163](#), A. Gabrielli [ID23b,23a](#), A. Gabrielli [ID155](#), P. Gadow [ID36](#), G. Gagliardi [ID57b,57a](#), L.G. Gagnon [ID17a](#), E.J. Gallas [ID126](#), B.J. Gallop [ID134](#), K.K. Gan [ID119](#), S. Ganguly [ID153](#), J. Gao [ID62a](#), Y. Gao [ID52](#), F.M. Garay Walls [ID137a,137b](#), B. Garcia [ID29](#), C. García [ID163](#), A. Garcia Alonso [ID114](#), A.G. Garcia Caffaro [ID172](#), J.E. García Navarro [ID163](#), M. Garcia-Sciveres [ID17a](#), G.L. Gardner [ID128](#), R.W. Gardner [ID39](#), N. Garelli [ID158](#), D. Garg [ID80](#), R.B. Garg [ID143,o](#), J.M. Gargan [ID52](#), C.A. Garner [ID155](#), S.J. Gasiorowski [ID138](#), P. Gaspar [ID83b](#), G. Gaudio [ID73a](#), V. Gautam [ID13](#), P. Gauzzi [ID75a,75b](#), I.L. Gavrilenko [ID37](#), A. Gavriyuk [ID37](#), C. Gay [ID164](#), G. Gaycken [ID48](#), E.N. Gazis [ID10](#), A.A. Geanta [ID27b](#), C.M. Gee [ID136](#), C. Gemme [ID57b](#), M.H. Genest [ID60](#), S. Gentile [ID75a,75b](#), S. George [ID95](#), W.F. George [ID20](#), T. Geralis [ID46](#), P. Gessinger-Befurt [ID36](#), M.E. Geyik [ID171](#), M. Ghneimat [ID141](#), K. Ghorbanian [ID94](#), A. Ghosal [ID141](#), A. Ghosh [ID160](#), A. Ghosh [ID7](#), B. Giacobbe [ID23b](#), S. Giagu [ID75a,75b](#), P. Giannetti [ID74a](#), A. Giannini [ID62a](#), S.M. Gibson [ID95](#), M. Gignac [ID136](#), D.T. Gil [ID86b](#), A.K. Gilbert [ID86a](#), B.J. Gilbert [ID41](#), D. Gillberg [ID34](#), G. Gilles [ID114](#), N.E.K. Gillwald [ID48](#), L. Ginabat [ID127](#), D.M. Gingrich [ID2,ag](#), M.P. Giordani [ID69a,69c](#), P.F. Giraud [ID135](#), G. Giugliarelli [ID69a,69c](#), D. Giugni [ID71a](#), F. Giuli [ID36](#), I. Gkialas [ID9,j](#), L.K. Gladilin [ID37](#), C. Glasman [ID99](#), G.R. Gledhill [ID123](#), G. Glemža [ID48](#), M. Glisic [ID123](#), I. Gnesi [ID43b,f](#), Y. Go [ID29,ai](#), M. Goblirsch-Kolb [ID36](#), B. Gocke [ID49](#), D. Godin [ID108](#), B. Gokturk [ID21a](#), S. Goldfarb [ID105](#), T. Golling [ID56](#), M.G.D. Gololo [ID33g](#), D. Golubkov [ID37](#), J.P. Gombas [ID107](#), A. Gomes [ID130a,130b](#), G. Gomes Da Silva [ID141](#), A.J. Gomez Delegido [ID163](#), R. Gonçalves [ID130a,130c](#), G. Gonella [ID123](#), L. Gonella [ID20](#), A. Gongadze [ID149c](#), F. Gonnella [ID20](#), J.L. Gonski [ID41](#), R.Y. González Andana [ID52](#), S. González de la Hoz [ID163](#), S. Gonzalez Fernandez [ID13](#), R. Gonzalez Lopez [ID92](#), C. Gonzalez Renteria [ID17a](#), R. Gonzalez Suarez [ID161](#), S. Gonzalez-Sevilla [ID56](#), G.R. Gonzalvo Rodriguez [ID163](#), L. Goossens [ID36](#), P.A. Gorbounov [ID37](#), B. Gorini [ID36](#), E. Gorini [ID70a,70b](#), A. Gorišek [ID93](#), T.C. Gosart [ID128](#), A.T. Goshaw [ID51](#), M.I. Gostkin [ID38](#), S. Goswami [ID121](#), C.A. Gottardo [ID36](#), M. Goughri [ID35b](#), V. Goumarre [ID48](#), A.G. Goussiou [ID138](#), N. Govender [ID33c](#), I. Grabowska-Bold [ID86a](#), K. Graham [ID34](#), E. Gramstad [ID125](#), S. Grancagnolo [ID70a,70b](#), M. Grandi [ID146](#), P.M. Gravila [ID27f](#), F.G. Gravili [ID70a,70b](#), H.M. Gray [ID17a](#), M. Greco [ID70a,70b](#), C. Grefe [ID24](#), I.M. Gregor [ID48](#), P. Grenier [ID143](#), C. Grieco [ID13](#), A.A. Grillo [ID136](#), K. Grimm [ID31](#), S. Grinstein [ID13,t](#), J.-F. Grivaz [ID66](#), E. Gross [ID169](#), J. Grosse-Knetter [ID55](#), C. Grud [ID106](#), J.C. Grundy [ID126](#), L. Guan [ID106](#),

W. Guan ²⁹, C. Gubbels ¹⁶⁴, J.G.R. Guerrero Rojas ¹⁶³, G. Guerrieri ^{69a,69c}, F. Guescini ¹¹⁰,
 R. Gugel ¹⁰⁰, J.A.M. Guhit ¹⁰⁶, A. Guida ¹⁸, T. Guillemain ⁴, E. Guilloton ^{167,134}, S. Guindon ³⁶,
 F. Guo ^{14a,14e}, J. Guo ^{62c}, L. Guo ⁴⁸, Y. Guo ¹⁰⁶, R. Gupta ⁴⁸, S. Gurbuz ²⁴, S.S. Gurdasani ⁵⁴,
 G. Gustavino ³⁶, M. Guth ⁵⁶, P. Gutierrez ¹²⁰, L.F. Gutierrez Zagazeta ¹²⁸, C. Gutschow ⁹⁶,
 C. Gwenlan ¹²⁶, C.B. Gwilliam ⁹², E.S. Haaland ¹²⁵, A. Haas ¹¹⁷, M. Habedank ⁴⁸,
 C. Haber ^{17a}, H.K. Hadavand ⁸, A. Hadeef ¹⁰⁰, S. Hadzic ¹¹⁰, J.J. Hahn ¹⁴¹, E.H. Haines ⁹⁶,
 M. Haleem ¹⁶⁶, J. Haley ¹²¹, J.J. Hall ¹³⁹, G.D. Hallowell ¹⁰², L. Halser ¹⁹, K. Hamano ¹⁶⁵,
 H. Hamdaoui ^{35e}, M. Hamer ²⁴, G.N. Hamity ⁵², E.J. Hampshire ⁹⁵, J. Han ^{62b}, K. Han ^{62a},
 L. Han ^{14c}, L. Han ^{62a}, S. Han ^{17a}, Y.F. Han ¹⁵⁵, K. Hanagaki ⁸⁴, M. Hance ¹³⁶,
 D.A. Hangal ^{41,ac}, H. Hanif ¹⁴², M.D. Hank ¹²⁸, R. Hankache ¹⁰¹, J.B. Hansen ⁴²,
 J.D. Hansen ⁴², P.H. Hansen ⁴², K. Hara ¹⁵⁷, D. Harada ⁵⁶, T. Harenberg ¹⁷¹, S. Harkusha ³⁷,
 M.L. Harris ¹⁰³, Y.T. Harris ¹²⁶, J. Harrison ¹³, N.M. Harrison ¹¹⁹, P.F. Harrison ¹⁶⁷,
 N.M. Hartman ¹¹⁰, N.M. Hartmann ¹⁰⁹, Y. Hasegawa ¹⁴⁰, A. Hasib ⁵², S. Haug ¹⁹,
 R. Hauser ¹⁰⁷, C.M. Hawkes ²⁰, R.J. Hawkins ³⁶, Y. Hayashi ¹⁵³, S. Hayashida ¹¹¹,
 D. Hayden ¹⁰⁷, C. Hayes ¹⁰⁶, R.L. Hayes ¹¹⁴, C.P. Hays ¹²⁶, J.M. Hays ⁹⁴, H.S. Hayward ⁹²,
 F. He ^{62a}, M. He ^{14a,14e}, Y. He ¹⁵⁴, Y. He ¹²⁷, N.B. Heatley ⁹⁴, V. Hedberg ⁹⁸,
 A.L. Heggelund ¹²⁵, N.D. Hehir ^{94,*}, C. Heidegger ⁵⁴, K.K. Heidegger ⁵⁴, W.D. Heidorn ⁸¹,
 J. Heilman ³⁴, S. Heim ⁴⁸, T. Heim ^{17a}, J.G. Heinlein ¹²⁸, J.J. Heinrich ¹²³, L. Heinrich ^{110,ae},
 J. Hejbal ¹³¹, L. Helary ⁴⁸, A. Held ¹⁷⁰, S. Hellesund ¹⁶, C.M. Helling ¹⁶⁴, S. Hellman ^{47a,47b},
 R.C.W. Henderson ⁹¹, L. Henkelmann ³², A.M. Henriques Correia ³⁶, H. Herde ⁹⁸,
 Y. Hernández Jiménez ¹⁴⁵, L.M. Herrmann ²⁴, T. Herrmann ⁵⁰, G. Herten ⁵⁴, R. Hertenberger ¹⁰⁹,
 L. Hervas ³⁶, M.E. Hespings ¹⁰⁰, N.P. Hessey ^{156a}, H. Hibi ⁸⁵, S.J. Hillier ²⁰, J.R. Hinds ¹⁰⁷,
 F. Hinterkeuser ²⁴, M. Hirose ¹²⁴, S. Hirose ¹⁵⁷, D. Hirschbuehl ¹⁷¹, T.G. Hitchings ¹⁰¹,
 B. Hiti ⁹³, J. Hobbs ¹⁴⁵, R. Hobincu ^{27e}, N. Hod ¹⁶⁹, M.C. Hodgkinson ¹³⁹, B.H. Hodgkinson ³²,
 A. Hoecker ³⁶, J. Hofer ⁴⁸, T. Holm ²⁴, M. Holzbock ¹¹⁰, L.B.A.H. Hommels ³², B.P. Honan ¹⁰¹,
 J. Hong ^{62c}, T.M. Hong ¹²⁹, B.H. Hooberman ¹⁶², W.H. Hopkins ⁶, Y. Horii ¹¹¹, S. Hou ¹⁴⁸,
 A.S. Howard ⁹³, J. Howarth ⁵⁹, J. Hoya ⁶, M. Hrabovsky ¹²², A. Hrynevich ⁴⁸, T. Hryn'ova ⁴,
 P.J. Hsu ⁶⁵, S.-C. Hsu ¹³⁸, Q. Hu ⁴¹, Y.F. Hu ^{14a,14e}, S. Huang ^{64b}, X. Huang ^{14c}, Y. Huang ¹³⁹,
 Y. Huang ^{14a}, Z. Huang ¹⁰¹, Z. Hubacek ¹³², M. Huebner ²⁴, F. Huegging ²⁴, T.B. Huffman ¹²⁶,
 C.A. Hugli ⁴⁸, M. Huhtinen ³⁶, S.K. Huiberts ¹⁶, R. Hulsken ¹⁰⁴, N. Huseynov ^{12,a},
 J. Huston ¹⁰⁷, J. Huth ⁶¹, R. Hyneman ¹⁴³, G. Iacobucci ⁵⁶, G. Iakovidis ²⁹, I. Ibragimov ¹⁴¹,
 L. Iconomidou-Fayard ⁶⁶, P. Iengo ^{72a,72b}, R. Iguchi ¹⁵³, T. Iizawa ⁸⁴, Y. Ikegami ⁸⁴, N. Ilic ¹⁵⁵,
 H. Imam ^{35a}, M. Ince Lezki ⁵⁶, T. Ingebretsen Carlson ^{47a,47b}, G. Introzzi ^{73a,73b}, M. Iodice ^{77a},
 V. Ippolito ^{75a,75b}, R.K. Irwin ⁹², M. Ishino ¹⁵³, W. Islam ¹⁷⁰, C. Issever ^{18,48}, S. Istin ^{21a,ak},
 H. Ito ¹⁶⁸, J.M. Iturbe Ponce ^{64a}, R. Iuppa ^{78a,78b}, A. Ivina ¹⁶⁹, J.M. Izen ⁴⁵, V. Izzo ^{72a},
 P. Jacka ^{131,132}, P. Jackson ¹, R.M. Jacobs ⁴⁸, B.P. Jaeger ¹⁴², C.S. Jagfeld ¹⁰⁹, P. Jain ⁵⁴,
 G. Jäkel ¹⁷¹, K. Jakobs ⁵⁴, T. Jakoubek ¹⁶⁹, J. Jamieson ⁵⁹, K.W. Janas ^{86a}, A.E. Jaspán ⁹²,
 M. Javurkova ¹⁰³, F. Jeanneau ¹³⁵, L. Jeanty ¹²³, J. Jejelava ^{149a,aa}, P. Jenni ^{54,g},
 C.E. Jessiman ³⁴, S. Jézéquel ⁴, C. Jia ^{62b}, J. Jia ¹⁴⁵, X. Jia ⁶¹, X. Jia ^{14a,14e}, Z. Jia ^{14c},
 Y. Jiang ^{62a}, S. Jiggins ⁴⁸, J. Jimenez Pena ¹³, S. Jin ^{14c}, A. Jinaru ^{27b}, O. Jinnouchi ¹⁵⁴,
 P. Johansson ¹³⁹, K.A. Johns ⁷, J.W. Johnson ¹³⁶, D.M. Jones ³², E. Jones ⁴⁸, P. Jones ³²,
 R.W.L. Jones ⁹¹, T.J. Jones ⁹², R. Joshi ¹¹⁹, J. Jovicevic ¹⁵, X. Ju ^{17a}, J.J. Junggeburth ³⁶,
 T. Junkermann ^{63a}, A. Juste Rozas ^{13,t}, M.K. Juzek ⁸⁷, S. Kabana ^{137e}, A. Kaczmarzka ⁸⁷,
 M. Kado ¹¹⁰, H. Kagan ¹¹⁹, M. Kagan ¹⁴³, A. Kahn ⁴¹, A. Kahn ¹²⁸, C. Kahra ¹⁰⁰, T. Kaji ¹⁶⁸,
 E. Kajomovitz ¹⁵⁰, N. Kakati ¹⁶⁹, I. Kalaitzidou ⁵⁴, C.W. Kalderon ²⁹, A. Kamenshchikov ¹⁵⁵,
 S. Kanayama ¹⁵⁴, N.J. Kang ¹³⁶, D. Kar ^{33g}, K. Karava ¹²⁶, M.J. Kareem ^{156b}, E. Karentzos ⁵⁴,
 I. Karknias ¹⁵², O. Karkout ¹¹⁴, S.N. Karpov ³⁸, Z.M. Karpova ³⁸, V. Kartvelishvili ⁹¹,

A.N. Karyukhin ³⁷, E. Kasimi ¹⁵², J. Katzy ⁴⁸, S. Kaur ³⁴, K. Kawade ¹⁴⁰, M.P. Kawale ¹²⁰,
 T. Kawamoto ¹³⁵, E.F. Kay ³⁶, F.I. Kaya ¹⁵⁸, S. Kazakos ¹⁰⁷, V.F. Kazanin ³⁷, Y. Ke ¹⁴⁵,
 J.M. Keaveney ^{33a}, R. Keeler ¹⁶⁵, G.V. Kehris ⁶¹, J.S. Keller ³⁴, A.S. Kelly ⁹⁶, J.J. Kempster ¹⁴⁶,
 K.E. Kennedy ⁴¹, P.D. Kennedy ¹⁰⁰, O. Kepka ¹³¹, B.P. Kerridge ¹⁶⁷, S. Kersten ¹⁷¹,
 B.P. Kerševan ⁹³, S. Keshri ⁶⁶, L. Keszeghova ^{28a}, S. Ketabchi Haghghat ¹⁵⁵, M. Khandoga ¹²⁷,
 A. Khanov ¹²¹, A.G. Kharlamov ³⁷, T. Kharlamova ³⁷, E.E. Khoda ¹³⁸, T.J. Khoo ¹⁸,
 G. Khoriauli ¹⁶⁶, J. Khubua ^{149b}, Y.A.R. Khwaira ⁶⁶, A. Kilgallon ¹²³, D.W. Kim ^{47a,47b},
 Y.K. Kim ³⁹, N. Kimura ⁹⁶, A. Kirchhoff ⁵⁵, C. Kirfel ²⁴, F. Kirfel ²⁴, J. Kirk ¹³⁴,
 A.E. Kiryunin ¹¹⁰, C. Kitsaki ¹⁰, O. Kivernyk ²⁴, M. Klassen ^{63a}, C. Klein ³⁴, L. Klein ¹⁶⁶,
 M.H. Klein ¹⁰⁶, M. Klein ⁹², S.B. Klein ⁵⁶, U. Klein ⁹², P. Klimek ³⁶, A. Klimentov ²⁹,
 T. Klioutchnikova ³⁶, P. Kluit ¹¹⁴, S. Kluth ¹¹⁰, E. Kneringer ⁷⁹, T.M. Knight ¹⁵⁵, A. Knue ⁵⁴,
 R. Kobayashi ⁸⁸, S.F. Koch ¹²⁶, M. Kocian ¹⁴³, P. Kodyš ¹³³, D.M. Koeck ¹²³, P.T. Koenig ²⁴,
 T. Koffas ³⁴, M. Kolb ¹³⁵, I. Koletsou ⁴, T. Komarek ¹²², K. Köneke ⁵⁴, A.X.Y. Kong ¹,
 T. Kono ¹¹⁸, N. Konstantinidis ⁹⁶, B. Konya ⁹⁸, R. Kopeliansky ⁶⁸, S. Koperny ^{86a}, K. Korcyl ⁸⁷,
 K. Kordas ^{152,e}, G. Koren ¹⁵¹, A. Korn ⁹⁶, S. Korn ⁵⁵, I. Korolkov ¹³, N. Korotkova ³⁷,
 B. Kortman ¹¹⁴, O. Kortner ¹¹⁰, S. Kortner ¹¹⁰, W.H. Kostecka ¹¹⁵, V.V. Kostyukhin ¹⁴¹,
 A. Kotsokechagia ¹³⁵, A. Kotwal ⁵¹, A. Koulouris ³⁶, A. Kourkoumeli-Charalampidi ^{73a,73b},
 C. Kourkoumelis ⁹, E. Kourlitis ^{110,ae}, O. Kovanda ¹⁴⁶, R. Kowalewski ¹⁶⁵, W. Kozanecki ¹³⁵,
 A.S. Kozhin ³⁷, V.A. Kramarenko ³⁷, G. Kramberger ⁹³, P. Kramer ¹⁰⁰, M.W. Krasny ¹²⁷,
 A. Krasznahorkay ³⁶, J.W. Kraus ¹⁷¹, J.A. Kremer ¹⁰⁰, T. Kresse ⁵⁰, J. Kretschmar ⁹²,
 K. Kreul ¹⁸, P. Krieger ¹⁵⁵, S. Krishnamurthy ¹⁰³, M. Krivos ¹³³, K. Krizka ²⁰,
 K. Kroeninger ⁴⁹, H. Kroha ¹¹⁰, J. Kroll ¹³¹, J. Kroll ¹²⁸, K.S. Krowpman ¹⁰⁷, U. Kruchonak ³⁸,
 H. Krüger ²⁴, N. Krumnack ⁸¹, M.C. Kruse ⁵¹, J.A. Krzysiak ⁸⁷, O. Kuchinskaia ³⁷, S. Kuday ^{3a},
 S. Kuehn ³⁶, R. Kuesters ⁵⁴, T. Kuhl ⁴⁸, V. Kukhtin ³⁸, Y. Kulchitsky ^{37,a}, S. Kuleshov ^{137d,137b},
 M. Kumar ^{33g}, N. Kumari ¹⁰², A. Kupco ¹³¹, T. Kupfer ⁴⁹, A. Kupich ³⁷, O. Kuprash ⁵⁴,
 H. Kurashige ⁸⁵, L.L. Kurchaninov ^{156a}, O. Kurdysh ⁶⁶, Y.A. Kurochkin ³⁷, A. Kurova ³⁷,
 M. Kuze ¹⁵⁴, A.K. Kvam ¹⁰³, J. Kvita ¹²², T. Kwan ¹⁰⁴, N.G. Kyriacou ¹⁰⁶, L.A.O. Laatu ¹⁰²,
 C. Lacasta ¹⁶³, F. Lacava ^{75a,75b}, H. Lacker ¹⁸, D. Lacour ¹²⁷, N.N. Lad ⁹⁶, E. Ladygin ³⁸,
 B. Laforge ¹²⁷, T. Lagouri ^{137e}, S. Lai ⁵⁵, I.K. Lakomic ^{86a}, N. Lalloue ⁶⁰, J.E. Lambert ¹⁶⁵,
 S. Lammers ⁶⁸, W. Lampl ⁷, C. Lampoudis ^{152,e}, A.N. Lancaster ¹¹⁵, E. Lançon ²⁹,
 U. Landgraf ⁵⁴, M.P.J. Landon ⁹⁴, V.S. Lang ⁵⁴, R.J. Langenberg ¹⁰³, O.K.B. Langrekken ¹²⁵,
 A.J. Lankford ¹⁶⁰, F. Lanni ³⁶, K. Lantzsch ²⁴, A. Lanza ^{73a}, A. Lapertosa ^{57b,57a},
 J.F. Laporte ¹³⁵, T. Lari ^{71a}, F. Lasagni Manghi ^{23b}, M. Lassnig ³⁶, V. Latonova ¹³¹,
 A. Laudrain ¹⁰⁰, A. Laurier ¹⁵⁰, S.D. Lawlor ⁹⁵, Z. Lawrence ¹⁰¹, M. Lazzaroni ^{71a,71b}, B. Le ¹⁰¹,
 E.M. Le Boulicaut ⁵¹, B. Leban ⁹³, A. Lebedev ⁸¹, M. LeBlanc ³⁶, F. Ledroit-Guillon ⁶⁰,
 A.C.A. Lee ⁹⁶, S.C. Lee ¹⁴⁸, S. Lee ^{47a,47b}, T.F. Lee ⁹², L.L. Leeuw ^{33c}, H.P. Lefebvre ⁹⁵,
 M. Lefebvre ¹⁶⁵, C. Leggett ^{17a}, G. Lehmann Miotto ³⁶, M. Leigh ⁵⁶, W.A. Leight ¹⁰³,
 W. Leinonen ¹¹³, A. Leisos ^{152,s}, M.A.L. Leite ^{83c}, C.E. Leitgeb ⁴⁸, R. Leitner ¹³³,
 K.J.C. Leney ⁴⁴, T. Lenz ²⁴, S. Leone ^{74a}, C. Leonidopoulos ⁵², A. Leopold ¹⁴⁴, C. Leroy ¹⁰⁸,
 R. Les ¹⁰⁷, C.G. Lester ³², M. Levchenko ³⁷, J. Levêque ⁴, D. Levin ¹⁰⁶, L.J. Levinson ¹⁶⁹,
 M.P. Lewicki ⁸⁷, D.J. Lewis ⁴, A. Li ⁵, B. Li ^{62b}, C. Li ^{62a}, C-Q. Li ^{62c}, H. Li ^{62a}, H. Li ^{62b},
 H. Li ^{14c}, H. Li ^{62b}, K. Li ¹³⁸, L. Li ^{62c}, M. Li ^{14a,14e}, Q.Y. Li ^{62a}, S. Li ^{14a,14e}, S. Li ^{62d,62c,d},
 T. Li ⁵, X. Li ¹⁰⁴, Z. Li ¹²⁶, Z. Li ¹⁰⁴, Z. Li ⁹², Z. Li ^{14a,14e}, Z. Liang ^{14a}, M. Liberatore ¹³⁵,
 B. Liberti ^{76a}, K. Lie ^{64c}, J. Lieber Marin ^{83b}, H. Lien ⁶⁸, K. Lin ¹⁰⁷, R.E. Lindley ⁷,
 J.H. Lindon ², A. Linss ⁴⁸, E. Lipeles ¹²⁸, A. Lipniacka ¹⁶, A. Lister ¹⁶⁴, J.D. Little ⁴,
 B. Liu ^{14a}, B.X. Liu ¹⁴², D. Liu ^{62d,62c}, J.B. Liu ^{62a}, J.K.K. Liu ³², K. Liu ^{62d,62c}, M. Liu ^{62a},
 M.Y. Liu ^{62a}, P. Liu ^{14a}, Q. Liu ^{62d,138,62c}, X. Liu ^{62a}, Y. Liu ^{14d,14e}, Y.L. Liu ¹⁰⁶, Y.W. Liu ^{62a},

J. Llorente Merino ¹⁴², S.L. Lloyd ⁹⁴, E.M. Lobodzinska ⁴⁸, P. Loch ⁷, S. Loffredo ^{76a,76b},
 T. Lohse ¹⁸, K. Lohwasser ¹³⁹, E. Loiacono ⁴⁸, M. Lokajicek ^{131,*}, J.D. Lomas ²⁰,
 J.D. Long ¹⁶², I. Longarini ¹⁶⁰, L. Longo ^{70a,70b}, R. Longo ¹⁶², I. Lopez Paz ⁶⁷,
 A. Lopez Solis ⁴⁸, J. Lorenz ¹⁰⁹, N. Lorenzo Martinez ⁴, A.M. Lory ¹⁰⁹,
 G. Löschke Centeno ¹⁴⁶, O. Loseva ³⁷, X. Lou ^{47a,47b}, X. Lou ^{14a,14e}, A. Lounis ⁶⁶, J. Love ⁶,
 P.A. Love ⁹¹, G. Lu ^{14a,14e}, M. Lu ⁸⁰, S. Lu ¹²⁸, Y.J. Lu ⁶⁵, H.J. Lubatti ¹³⁸, C. Luci ^{75a,75b},
 F.L. Lucio Alves ^{14c}, A. Lucotte ⁶⁰, F. Luehring ⁶⁸, I. Luise ¹⁴⁵, O. Lukianchuk ⁶⁶,
 O. Lundberg ¹⁴⁴, B. Lund-Jensen ¹⁴⁴, N.A. Luongo ¹²³, M.S. Lutz ¹⁵¹, D. Lynn ²⁹, H. Lyons ⁹²,
 R. Lysak ¹³¹, E. Lytken ⁹⁸, V. Lyubushkin ³⁸, T. Lyubushkina ³⁸, M.M. Lyukova ¹⁴⁵, H. Ma ²⁹,
 K. Ma ^{62a}, L.L. Ma ^{62b}, Y. Ma ¹²¹, D.M. Mac Donell ¹⁶⁵, G. Maccarrone ⁵³, J.C. MacDonald ¹⁰⁰,
 R. Madar ⁴⁰, W.F. Mader ⁵⁰, J. Maeda ⁸⁵, T. Maeno ²⁹, M. Maerker ⁵⁰, H. Maguire ¹³⁹,
 V. Maiboroda ¹³⁵, A. Maio ^{130a,130b,130d}, K. Maj ^{86a}, O. Majersky ⁴⁸, S. Majewski ¹²³,
 N. Makovec ⁶⁶, V. Maksimovic ¹⁵, B. Malaescu ¹²⁷, Pa. Malecki ⁸⁷, V.P. Maleev ³⁷,
 F. Malek ⁶⁰, M. Mali ⁹³, D. Malito ⁹⁵, U. Mallik ⁸⁰, S. Maltezos ¹⁰, S. Malyukov ³⁸, J. Mamuzic ¹³,
 G. Mancini ⁵³, G. Manco ^{73a,73b}, J.P. Mandalia ⁹⁴, I. Mandić ⁹³,
 L. Manhaes de Andrade Filho ^{83a}, I.M. Maniatis ¹⁶⁹, J. Manjarres Ramos ^{102,ab}, D.C. Mankad ¹⁶⁹,
 A. Mann ¹⁰⁹, B. Mansoulie ¹³⁵, S. Manzoni ³⁶, A. Marantis ^{152,s}, G. Marchiori ⁵,
 M. Marcisovsky ¹³¹, C. Marcon ^{71a}, M. Marinescu ²⁰, M. Marjanovic ¹²⁰, E.J. Marshall ⁹¹,
 Z. Marshall ^{17a}, S. Marti-Garcia ¹⁶³, T.A. Martin ¹⁶⁷, V.J. Martin ⁵², B. Martin dit Latour ¹⁶,
 L. Martinelli ^{75a,75b}, M. Martinez ^{13,t}, P. Martinez Agullo ¹⁶³, V.I. Martinez Outschoorn ¹⁰³,
 P. Martinez Suarez ¹³, S. Martin-Haugh ¹³⁴, V.S. Martoiu ^{27b}, A.C. Martyniuk ⁹⁶, A. Marzin ³⁶,
 D. Mascione ^{78a,78b}, L. Masetti ¹⁰⁰, T. Mashimo ¹⁵³, J. Masik ¹⁰¹, A.L. Maslennikov ³⁷,
 L. Massa ^{23b}, P. Massarotti ^{72a,72b}, P. Mastrandrea ^{74a,74b}, A. Mastroberardino ^{43b,43a},
 T. Masubuchi ¹⁵³, T. Mathisen ¹⁶¹, J. Matousek ¹³³, N. Matsuzawa ¹⁵³, J. Maurer ^{27b}, B. Maček ⁹³,
 D.A. Maximov ³⁷, R. Mazini ¹⁴⁸, I. Maznas ¹⁵², M. Mazza ¹⁰⁷, S.M. Mazza ¹³⁶,
 E. Mazzeo ^{71a,71b}, C. Mc Ginn ²⁹, J.P. Mc Gowan ¹⁰⁴, S.P. Mc Kee ¹⁰⁶, E.F. McDonald ¹⁰⁵,
 A.E. McDougall ¹¹⁴, J.A. Mcfayden ¹⁴⁶, R.P. McGovern ¹²⁸, G. Mchedlidze ^{149b},
 R.P. Mckenzie ^{33g}, T.C. Mclachlan ⁴⁸, D.J. Mclaughlin ⁹⁶, K.D. McLean ¹⁶⁵, S.J. McMahon ¹³⁴,
 P.C. McNamara ¹⁰⁵, C.M. Mcpartland ⁹², R.A. McPherson ^{165,x}, S. Mehlhase ¹⁰⁹, A. Mehta ⁹²,
 D. Melini ¹⁵⁰, B.R. Mellado Garcia ^{33g}, A.H. Melo ⁵⁵, F. Meloni ⁴⁸,
 A.M. Mendes Jacques Da Costa ¹⁰¹, H.Y. Meng ¹⁵⁵, L. Meng ⁹¹, S. Menke ¹¹⁰, M. Mentink ³⁶,
 E. Meoni ^{43b,43a}, C. Merlassino ¹²⁶, L. Merola ^{72a,72b}, C. Meroni ^{71a,71b}, G. Merz ¹⁰⁶,
 O. Meshkov ³⁷, J. Metcalfe ⁶, A.S. Mete ⁶, C. Meyer ⁶⁸, J-P. Meyer ¹³⁵, R.P. Middleton ¹³⁴,
 L. Mijović ⁵², G. Mikenberg ¹⁶⁹, M. Mikestikova ¹³¹, M. Mikuž ⁹³, H. Mildner ¹⁰⁰, A. Milic ³⁶,
 C.D. Milke ⁴⁴, D.W. Miller ³⁹, L.S. Miller ³⁴, A. Milov ¹⁶⁹, D.A. Milstead ^{47a,47b}, T. Min ^{14c},
 A.A. Minaenko ³⁷, I.A. Minashvili ^{149b}, L. Mince ⁵⁹, A.I. Mincer ¹¹⁷, B. Mindur ^{86a},
 M. Mineev ³⁸, Y. Mino ⁸⁸, L.M. Mir ¹³, M. Miralles Lopez ¹⁶³, M. Mironova ^{17a}, A. Mishima ¹⁵³,
 M.C. Missio ¹¹³, T. Mitani ¹⁶⁸, A. Mitra ¹⁶⁷, V.A. Mitsou ¹⁶³, O. Miu ¹⁵⁵, P.S. Miyagawa ⁹⁴,
 Y. Miyazaki ⁸⁹, A. Mizukami ⁸⁴, T. Mkrtychyan ^{63a}, M. Mlinarevic ⁹⁶, T. Mlinarevic ⁹⁶,
 M. Mlynarikova ³⁶, S. Mobius ¹⁹, K. Mochizuki ¹⁰⁸, P. Moder ⁴⁸, P. Mogg ¹⁰⁹,
 A.F. Mohammed ^{14a,14e}, S. Mohapatra ⁴¹, G. Mokgatitwane ^{33g}, L. Moleri ¹⁶⁹, B. Mondal ¹⁴¹,
 S. Mondal ¹³², K. Mönig ⁴⁸, E. Monnier ¹⁰², L. Monsonis Romero ¹⁶³, J. Montejó Berlingen ^{13,84},
 M. Montella ¹¹⁹, F. Montekali ^{77a,77b}, F. Monticelli ⁹⁰, S. Monzani ^{69a,69c}, N. Morange ⁶⁶,
 A.L. Moreira De Carvalho ^{130a}, M. Moreno Llácer ¹⁶³, C. Moreno Martinez ⁵⁶, P. Morettini ^{57b},
 S. Morgenstern ³⁶, M. Morii ⁶¹, M. Morinaga ¹⁵³, A.K. Morley ³⁶, F. Morodei ^{75a,75b},
 L. Morvaj ³⁶, P. Moschovakos ³⁶, B. Moser ³⁶, M. Mosidze ^{149b}, T. Moskalets ⁵⁴,
 P. Moskvitina ¹¹³, J. Moss ^{31,m}, E.J.W. Moyses ¹⁰³, O. Mtintsilana ^{33g}, S. Muanza ¹⁰²,

J. Mueller ¹²⁹, D. Muenstermann ⁹¹, R. Müller ¹⁹, G.A. Mullier ¹⁶¹, A.J. Mullin³², J.J. Mullin¹²⁸, D.P. Mungo ¹⁵⁵, D. Munoz Perez ¹⁶³, F.J. Munoz Sanchez ¹⁰¹, M. Murin ¹⁰¹, W.J. Murray ^{167,134}, A. Murrone ^{71a,71b}, J.M. Muse ¹²⁰, M. Muškinja ^{17a}, C. Mwewa ²⁹, A.G. Myagkov ^{37,a}, A.J. Myers ⁸, A.A. Myers¹²⁹, G. Myers ⁶⁸, M. Myska ¹³², B.P. Nachman ^{17a}, O. Nackenhorst ⁴⁹, A. Nag ⁵⁰, K. Nagai ¹²⁶, K. Nagano ⁸⁴, J.L. Nagle ^{29,ai}, E. Nagy ¹⁰², A.M. Nairz ³⁶, Y. Nakahama ⁸⁴, K. Nakamura ⁸⁴, K. Nakkalil ⁵, H. Nanjo ¹²⁴, R. Narayan ⁴⁴, E.A. Narayanan ¹¹², I. Naryshkin ³⁷, M. Naseri ³⁴, S. Nasri ¹⁵⁹, C. Nass ²⁴, G. Navarro ^{22a}, J. Navarro-Gonzalez ¹⁶³, R. Nayak ¹⁵¹, A. Nayaz ¹⁸, P.Y. Nechaeva ³⁷, F. Nechansky ⁴⁸, L. Nedic ¹²⁶, T.J. Neep ²⁰, A. Negri ^{73a,73b}, M. Negrini ^{23b}, C. Nellist ¹¹⁴, C. Nelson ¹⁰⁴, K. Nelson ¹⁰⁶, S. Nemecek ¹³¹, M. Nessi ^{36,h}, M.S. Neubauer ¹⁶², F. Neuhaus ¹⁰⁰, J. Neundorf ⁴⁸, R. Newhouse ¹⁶⁴, P.R. Newman ²⁰, C.W. Ng ¹²⁹, Y.W.Y. Ng ⁴⁸, B. Ngair ^{35e}, H.D.N. Nguyen ¹⁰⁸, R.B. Nickerson ¹²⁶, R. Nicolaidou ¹³⁵, J. Nielsen ¹³⁶, M. Niemeyer ⁵⁵, J. Niermann ^{55,36}, N. Nikiforou ³⁶, V. Nikolaenko ^{37,a}, I. Nikolic-Audit ¹²⁷, K. Nikolopoulos ²⁰, P. Nilsson ²⁹, I. Ninca ⁴⁸, H.R. Nindhito ⁵⁶, G. Ninio ¹⁵¹, A. Nisati ^{75a}, N. Nishu ², R. Nisius ¹¹⁰, J-E. Nitschke ⁵⁰, E.K. Nkadimeng ^{33g}, S.J. Noacco Rosende ⁹⁰, T. Nobe ¹⁵³, D.L. Noel ³², T. Nommensen ¹⁴⁷, M.B. Norfolk ¹³⁹, R.R.B. Norisam ⁹⁶, B.J. Norman ³⁴, J. Novak ⁹³, T. Novak ⁴⁸, L. Novotny ¹³², R. Novotny ¹¹², L. Nozka ¹²², K. Ntekas ¹⁶⁰, N.M.J. Nunes De Moura Junior ^{83b}, E. Nurse⁹⁶, J. Ocariz ¹²⁷, A. Ochi ⁸⁵, I. Ochoa ^{130a}, S. Oerde ¹⁶¹, J.T. Offermann ³⁹, A. Ogrodnik ¹³³, A. Oh ¹⁰¹, C.C. Ohm ¹⁴⁴, H. Oide ⁸⁴, R. Oishi ¹⁵³, M.L. Ojeda ⁴⁸, Y. Okazaki ⁸⁸, M.W. O'Keefe⁹², Y. Okumura ¹⁵³, L.F. Oleiro Seabra ^{130a}, S.A. Olivares Pino ^{137d}, D. Oliveira Damazio ²⁹, D. Oliveira Goncalves ^{83a}, J.L. Oliver ¹⁶⁰, A. Olszewski ⁸⁷, Ö.O. Öncel ⁵⁴, D.C. O'Neil ¹⁴², A.P. O'Neill ¹⁹, A. Onofre ^{130a,130e}, P.U.E. Onyisi ¹¹, M.J. Oreglia ³⁹, G.E. Orellana ⁹⁰, D. Orestano ^{77a,77b}, N. Orlando ¹³, R.S. Orr ¹⁵⁵, V. O'Shea ⁵⁹, L.M. Osojnak ¹²⁸, R. Ospanov ^{62a}, G. Otero y Garzon ³⁰, H. Otono ⁸⁹, P.S. Ott ^{63a}, G.J. Ottino ^{17a}, M. Ouchrif ^{35d}, J. Ouellette ²⁹, F. Ould-Saada ¹²⁵, M. Owen ⁵⁹, R.E. Owen ¹³⁴, K.Y. Oyulmaz ^{21a}, V.E. Ozcan ^{21a}, N. Ozturk ⁸, S. Ozturk ⁸², H.A. Pacey ³², A. Pacheco Pages ¹³, C. Padilla Aranda ¹³, G. Padovano ^{75a,75b}, S. Pagan Griso ^{17a}, G. Palacino ⁶⁸, A. Palazzo ^{70a,70b}, S. Palestini ³⁶, J. Pan ¹⁷², T. Pan ^{64a}, D.K. Panchal ¹¹, C.E. Pandini ¹¹⁴, J.G. Panduro Vazquez ⁹⁵, H. Pang ^{14b}, P. Pani ⁴⁸, G. Panizzo ^{69a,69c}, L. Paolozzi ⁵⁶, C. Papadatos ¹⁰⁸, S. Parajuli ⁴⁴, A. Paramonov ⁶, C. Paraskevopoulos ¹⁰, D. Paredes Hernandez ^{64b}, T.H. Park ¹⁵⁵, M.A. Parker ³², F. Parodi ^{57b,57a}, E.W. Parrish ¹¹⁵, V.A. Parrish ⁵², J.A. Parsons ⁴¹, U. Parzefall ⁵⁴, B. Pascual Dias ¹⁰⁸, L. Pascual Dominguez ¹⁵¹, F. Pasquali ¹¹⁴, E. Pasqualucci ^{75a}, S. Passaggio ^{57b}, F. Pastore ⁹⁵, P. Pasuwan ^{47a,47b}, P. Patel ⁸⁷, U.M. Patel ⁵¹, J.R. Pater ¹⁰¹, T. Pauly ³⁶, J. Pearkes ¹⁴³, M. Pedersen ¹²⁵, R. Pedro ^{130a}, S.V. Peleganchuk ³⁷, O. Penc ³⁶, E.A. Pender ⁵², H. Peng ^{62a}, K.E. Pensi ¹⁰⁹, M. Penzin ³⁷, B.S. Peralva ^{83d}, A.P. Pereira Peixoto ⁶⁰, L. Pereira Sanchez ^{47a,47b}, D.V. Perepelitsa ^{29,ai}, E. Perez Codina ^{156a}, M. Perganti ¹⁰, L. Perini ^{71a,71b,*}, H. Pernegger ³⁶, O. Perrin ⁴⁰, K. Peters ⁴⁸, R.F.Y. Peters ¹⁰¹, B.A. Petersen ³⁶, T.C. Petersen ⁴², E. Petit ¹⁰², V. Petousis ¹³², C. Petridou ^{152,e}, A. Petrukhin ¹⁴¹, M. Pettee ^{17a}, N.E. Pettersson ³⁶, A. Petukhov ³⁷, K. Petukhova ¹³³, A. Peyaud ¹³⁵, R. Pezoa ^{137f}, L. Pezzotti ³⁶, G. Pezzullo ¹⁷², T.M. Pham ¹⁷⁰, T. Pham ¹⁰⁵, P.W. Phillips ¹³⁴, G. Piacquadio ¹⁴⁵, E. Pianori ^{17a}, F. Piazza ^{71a,71b}, R. Piegaia ³⁰, D. Pietreanu ^{27b}, A.D. Pilkington ¹⁰¹, M. Pinamonti ^{69a,69c}, J.L. Pinfeld ², B.C. Pinheiro Pereira ^{130a}, A.E. Pinto Pinoargote ¹³⁵, K.M. Piper ¹⁴⁶, A. Pirttikoski ⁵⁶, C. Pitman Donaldson⁹⁶, D.A. Pizzi ³⁴, L. Pizzimento ^{64b}, A. Pizzini ¹¹⁴, M.-A. Pleier ²⁹, V. Plesanovs⁵⁴, V. Pleskot ¹³³, E. Plotnikova³⁸, G. Poddar ⁴, R. Poettgen ⁹⁸, L. Poggioli ¹²⁷, I. Pokharel ⁵⁵, S. Polacek ¹³³, G. Polesello ^{73a}, A. Poley ^{142,156a}, R. Polifka ¹³², A. Polini ^{23b}, C.S. Pollard ¹⁶⁷, Z.B. Pollock ¹¹⁹, V. Polychronakos ²⁹, E. Pompa Pacchi ^{75a,75b},

D. Ponomarenko ¹¹³, L. Pontecorvo ³⁶, S. Popa ^{27a}, G.A. Popeneciu ^{27d}, A. Poreba ³⁶,
 D.M. Portillo Quintero ^{156a}, S. Pospisil ¹³², M.A. Postill ¹³⁹, P. Postolache ^{27c}, K. Potamianos ¹⁶⁷,
 P.A. Potepa ^{86a}, I.N. Potrap ³⁸, C.J. Potter ³², H. Potti ¹, T. Poulsen ⁴⁸, J. Poveda ¹⁶³,
 M.E. Pozo Astigarraga ³⁶, A. Prades Ibanez ¹⁶³, J. Pretel ⁵⁴, D. Price ¹⁰¹, M. Primavera ^{70a},
 M.A. Principe Martin ⁹⁹, R. Privara ¹²², T. Procter ⁵⁹, M.L. Proffitt ¹³⁸, N. Proklova ¹²⁸,
 K. Prokofiev ^{64c}, G. Proto ¹¹⁰, S. Protopopescu ²⁹, J. Proudfoot ⁶, M. Przybycien ^{86a},
 W.W. Przygoda ^{86b}, J.E. Puddefoot ¹³⁹, D. Pudzha ³⁷, D. Pyatiiizbyantseva ³⁷, J. Qian ¹⁰⁶,
 D. Qichen ¹⁰¹, Y. Qin ¹⁰¹, T. Qiu ⁵², A. Quadt ⁵⁵, M. Queitsch-Maitland ¹⁰¹, G. Quetant ⁵⁶,
 G. Rabanal Bolanos ⁶¹, D. Rafanoharana ⁵⁴, F. Ragusa ^{71a,71b}, J.L. Rainbolt ³⁹, J.A. Raine ⁵⁶,
 S. Rajagopalan ²⁹, E. Ramakoti ³⁷, K. Ran ^{48,14e}, N.P. Rapheeha ^{33g}, H. Rasheed ^{27b},
 V. Raskina ¹²⁷, D.F. Rassloff ^{63a}, S. Rave ¹⁰⁰, B. Ravina ⁵⁵, I. Ravinovich ¹⁶⁹, M. Raymond ³⁶,
 A.L. Read ¹²⁵, N.P. Readioff ¹³⁹, D.M. Rebutzi ^{73a,73b}, G. Redlinger ²⁹, A.S. Reed ¹¹⁰,
 K. Reeves ²⁶, J.A. Reidelsturz ¹⁷¹, D. Reikher ¹⁵¹, A. Rej ¹⁴¹, C. Rembser ³⁶, A. Renardi ⁴⁸,
 M. Renda ^{27b}, M.B. Rendel ¹¹⁰, F. Renner ⁴⁸, A.G. Rennie ⁵⁹, S. Resconi ^{71a},
 M. Ressegotti ^{57b,57a}, S. Rettie ³⁶, J.G. Reyes Rivera ¹⁰⁷, B. Reynolds ¹¹⁹, E. Reynolds ^{17a},
 O.L. Rezanova ³⁷, P. Reznicek ¹³³, N. Ribaric ⁹¹, E. Ricci ^{78a,78b}, R. Richter ¹¹⁰,
 S. Richter ^{47a,47b}, E. Richter-Was ^{86b}, M. Ridel ¹²⁷, S. Ridouani ^{35d}, P. Rieck ¹¹⁷, P. Riedler ³⁶,
 M. Rijssenbeek ¹⁴⁵, A. Rimoldi ^{73a,73b}, M. Rimoldi ⁴⁸, L. Rinaldi ^{23b,23a}, T.T. Rinn ²⁹,
 M.P. Rinnagel ¹⁰⁹, G. Ripellino ¹⁶¹, I. Riu ¹³, P. Rivadeneira ⁴⁸, J.C. Rivera Vergara ¹⁶⁵,
 F. Rizatdinova ¹²¹, E. Rizvi ⁹⁴, B.A. Roberts ¹⁶⁷, B.R. Roberts ^{17a}, S.H. Robertson ^{104,x},
 M. Robin ⁴⁸, D. Robinson ³², C.M. Robles Gajardo ^{137f}, M. Robles Manzano ¹⁰⁰, A. Robson ⁵⁹,
 A. Rocchi ^{76a,76b}, C. Roda ^{74a,74b}, S. Rodriguez Bosca ^{63a}, Y. Rodriguez Garcia ^{22a},
 A. Rodriguez Rodriguez ⁵⁴, A.M. Rodríguez Vera ^{156b}, S. Roe ³⁶, J.T. Roemer ¹⁶⁰,
 A.R. Roepe-Gier ¹³⁶, J. Roggel ¹⁷¹, O. Røhne ¹²⁵, R.A. Rojas ¹⁰³, C.P.A. Roland ⁶⁸, J. Roloff ²⁹,
 A. Romaniouk ³⁷, E. Romano ^{73a,73b}, M. Romano ^{23b}, A.C. Romero Hernandez ¹⁶²,
 N. Rompotis ⁹², L. Roos ¹²⁷, S. Rosati ^{75a}, B.J. Rosser ³⁹, E. Rossi ¹²⁶, E. Rossi ^{72a,72b},
 L.P. Rossi ^{57b}, L. Rossini ⁴⁸, R. Rosten ¹¹⁹, M. Rotaru ^{27b}, B. Rottler ⁵⁴, C. Rougier ^{102,ab},
 D. Rousseau ⁶⁶, D. Rousso ³², A. Roy ¹⁶², S. Roy-Garand ¹⁵⁵, A. Rozanov ¹⁰², Y. Rozen ¹⁵⁰,
 X. Ruan ^{33g}, A. Rubio Jimenez ¹⁶³, A.J. Ruby ⁹², V.H. Ruelas Rivera ¹⁸, T.A. Ruggeri ¹,
 A. Ruggiero ¹²⁶, A. Ruiz-Martinez ¹⁶³, A. Rummler ³⁶, Z. Rurikova ⁵⁴, N.A. Rusakovich ³⁸,
 H.L. Russell ¹⁶⁵, G. Russo ^{75a,75b}, J.P. Rutherford ⁷, S. Rutherford Colmenares ³², K. Rybacki ⁹¹,
 M. Rybar ¹³³, E.B. Rye ¹²⁵, A. Ryzhov ⁴⁴, J.A. Sabater Iglesias ⁵⁶, P. Sabatini ¹⁶³,
 L. Sabetta ^{75a,75b}, H.F-W. Sadrozinski ¹³⁶, F. Safai Tehrani ^{75a}, B. Safarzadeh Samani ¹⁴⁶,
 M. Safdari ¹⁴³, S. Saha ¹⁶⁵, M. Sahinsoy ¹¹⁰, M. Saimpert ¹³⁵, M. Saito ¹⁵³, T. Saito ¹⁵³,
 D. Salamani ³⁶, A. Salnikov ¹⁴³, J. Salt ¹⁶³, A. Salvador Salas ¹³, D. Salvatore ^{43b,43a},
 F. Salvatore ¹⁴⁶, A. Salzburger ³⁶, D. Sammel ⁵⁴, D. Sampsonidis ^{152,e}, D. Sampsonidou ¹²³,
 J. Sánchez ¹⁶³, A. Sanchez Pineda ⁴, V. Sanchez Sebastian ¹⁶³, H. Sandaker ¹²⁵, C.O. Sander ⁴⁸,
 J.A. Sandesara ¹⁰³, M. Sandhoff ¹⁷¹, C. Sandoval ^{22b}, D.P.C. Sankey ¹³⁴, T. Sano ⁸⁸,
 A. Sansoni ⁵³, L. Santi ^{75a,75b}, C. Santoni ⁴⁰, H. Santos ^{130a,130b}, S.N. Santpur ^{17a}, A. Santra ¹⁶⁹,
 K.A. Saoucha ¹³⁹, J.G. Saraiva ^{130a,130d}, J. Sardain ⁷, O. Sasaki ⁸⁴, K. Sato ¹⁵⁷, C. Sauer ^{63b},
 F. Sauerburger ⁵⁴, E. Sauvan ⁴, P. Savard ^{155,ag}, R. Sawada ¹⁵³, C. Sawyer ¹³⁴, L. Sawyer ⁹⁷,
 I. Sayago Galvan ¹⁶³, C. Sbarra ^{23b}, A. Sbrizzi ^{23b,23a}, T. Scanlon ⁹⁶, J. Schaarschmidt ¹³⁸,
 P. Schacht ¹¹⁰, D. Schaefer ³⁹, U. Schäfer ¹⁰⁰, A.C. Schaffer ^{66,44}, D. Schaile ¹⁰⁹,
 R.D. Schamberger ¹⁴⁵, C. Scharf ¹⁸, M.M. Schefer ¹⁹, V.A. Schegelsky ³⁷, D. Scheirich ¹³³,
 F. Schenck ¹⁸, M. Schernau ¹⁶⁰, C. Scheulen ⁵⁵, C. Schiavi ^{57b,57a}, E.J. Schioppa ^{70a,70b},
 M. Schioppa ^{43b,43a}, B. Schlag ^{143,o}, K.E. Schleicher ⁵⁴, S. Schlenker ³⁶, J. Schmeing ¹⁷¹,
 M.A. Schmidt ¹⁷¹, K. Schmieden ¹⁰⁰, C. Schmitt ¹⁰⁰, S. Schmitt ⁴⁸, L. Schoeffel ¹³⁵,

A. Schoening [id](#)^{63b}, P.G. Scholer [id](#)⁵⁴, E. Schopf [id](#)¹²⁶, M. Schott [id](#)¹⁰⁰, J. Schovancova [id](#)³⁶,
 S. Schramm [id](#)⁵⁶, F. Schroeder [id](#)¹⁷¹, T. Schroer [id](#)⁵⁶, H-C. Schultz-Coulon [id](#)^{63a}, M. Schumacher [id](#)⁵⁴,
 B.A. Schumm [id](#)¹³⁶, Ph. Schune [id](#)¹³⁵, A.J. Schuy [id](#)¹³⁸, H.R. Schwartz [id](#)¹³⁶, A. Schwartzman [id](#)¹⁴³,
 T.A. Schwarz [id](#)¹⁰⁶, Ph. Schwemling [id](#)¹³⁵, R. Schwienhorst [id](#)¹⁰⁷, A. Sciandra [id](#)¹³⁶, G. Sciolla [id](#)²⁶,
 F. Scuri [id](#)^{74a}, C.D. Sebastiani [id](#)⁹², K. Sedlaczek [id](#)¹¹⁵, P. Seema [id](#)¹⁸, S.C. Seidel [id](#)¹¹², A. Seiden [id](#)¹³⁶,
 B.D. Seidlitz [id](#)⁴¹, C. Seitz [id](#)⁴⁸, J.M. Seixas [id](#)^{83b}, G. Sekhniadze [id](#)^{72a}, S.J. Sekula [id](#)⁴⁴, L. Selem [id](#)⁶⁰,
 N. Semprini-Cesari [id](#)^{23b,23a}, D. Sengupta [id](#)⁵⁶, V. Senthilkumar [id](#)¹⁶³, L. Serin [id](#)⁶⁶, L. Serkin [id](#)^{69a,69b},
 M. Sessa [id](#)^{76a,76b}, H. Severini [id](#)¹²⁰, F. Sforza [id](#)^{57b,57a}, A. Sfyrla [id](#)⁵⁶, E. Shabalina [id](#)⁵⁵, R. Shaheen [id](#)¹⁴⁴,
 J.D. Shahinian [id](#)¹²⁸, D. Shaked Renous [id](#)¹⁶⁹, L.Y. Shan [id](#)^{14a}, M. Shapiro [id](#)^{17a}, A. Sharma [id](#)³⁶,
 A.S. Sharma [id](#)¹⁶⁴, P. Sharma [id](#)⁸⁰, S. Sharma [id](#)⁴⁸, P.B. Shatalov [id](#)³⁷, K. Shaw [id](#)¹⁴⁶, S.M. Shaw [id](#)¹⁰¹,
 A. Shcherbakova [id](#)³⁷, Q. Shen [id](#)^{62c,5}, P. Sherwood [id](#)⁹⁶, L. Shi [id](#)⁹⁶, X. Shi [id](#)^{14a}, C.O. Shimmin [id](#)¹⁷²,
 Y. Shimogama [id](#)¹⁶⁸, J.D. Shinner [id](#)⁹⁵, I.P.J. Shipsey [id](#)¹²⁶, S. Shirabe [id](#)^{56,h}, M. Shiyakova [id](#)^{38,v},
 J. Shlomi [id](#)¹⁶⁹, M.J. Shochet [id](#)³⁹, J. Shojaii [id](#)¹⁰⁵, D.R. Shope [id](#)¹²⁵, B. Shrestha [id](#)¹²⁰, S. Shrestha [id](#)^{119,aj},
 E.M. Shrif [id](#)^{33g}, M.J. Shroff [id](#)¹⁶⁵, P. Sicho [id](#)¹³¹, A.M. Sickles [id](#)¹⁶², E. Sideras Haddad [id](#)^{33g},
 A. Sidoti [id](#)^{23b}, F. Siegert [id](#)⁵⁰, Dj. Sijacki [id](#)¹⁵, R. Sikora [id](#)^{86a}, F. Sili [id](#)⁹⁰, J.M. Silva [id](#)²⁰,
 M.V. Silva Oliveira [id](#)²⁹, S.B. Silverstein [id](#)^{47a}, S. Simion [id](#)⁶⁶, R. Simoniello [id](#)³⁶, E.L. Simpson [id](#)⁵⁹,
 H. Simpson [id](#)¹⁴⁶, L.R. Simpson [id](#)¹⁰⁶, N.D. Simpson [id](#)⁹⁸, S. Simsek [id](#)⁸², S. Sindhu [id](#)⁵⁵, P. Sinervo [id](#)¹⁵⁵,
 S. Singh [id](#)¹⁵⁵, S. Sinha [id](#)⁴⁸, S. Sinha [id](#)¹⁰¹, M. Sioli [id](#)^{23b,23a}, I. Siral [id](#)³⁶, E. Sitnikova [id](#)⁴⁸,
 S.Yu. Sivoklokov [id](#)^{37,*}, J. Sjölin [id](#)^{47a,47b}, A. Skaf [id](#)⁵⁵, E. Skorda [id](#)²⁰, P. Skubic [id](#)¹²⁰, M. Slawinska [id](#)⁸⁷,
 V. Smakhtin [id](#)¹⁶⁹, B.H. Smart [id](#)¹³⁴, J. Smiesko [id](#)³⁶, S.Yu. Smirnov [id](#)³⁷, Y. Smirnov [id](#)³⁷,
 L.N. Smirnova [id](#)^{37,a}, O. Smirnova [id](#)⁹⁸, A.C. Smith [id](#)⁴¹, E.A. Smith [id](#)³⁹, H.A. Smith [id](#)¹²⁶,
 J.L. Smith [id](#)⁹², R. Smith [id](#)¹⁴³, M. Smizanska [id](#)⁹¹, K. Smolek [id](#)¹³², A.A. Snesarev [id](#)³⁷, S.R. Snider [id](#)¹⁵⁵,
 H.L. Snoek [id](#)¹¹⁴, S. Snyder [id](#)²⁹, R. Sobie [id](#)^{165,x}, A. Soffer [id](#)¹⁵¹, C.A. Solans Sanchez [id](#)³⁶,
 E.Yu. Soldatov [id](#)³⁷, U. Soldevila [id](#)¹⁶³, A.A. Solodkov [id](#)³⁷, S. Solomon [id](#)²⁶, A. Soloshenko [id](#)³⁸,
 K. Solovieva [id](#)⁵⁴, O.V. Solovyanov [id](#)⁴⁰, V. Solovyev [id](#)³⁷, P. Sommer [id](#)³⁶, A. Sonay [id](#)¹³,
 W.Y. Song [id](#)^{156b}, J.M. Sonneveld [id](#)¹¹⁴, A. Sopczak [id](#)¹³², A.L. Soppio [id](#)⁹⁶, F. Sopkova [id](#)^{28b},
 V. Sothilingam [id](#)^{63a}, S. Sottocornola [id](#)⁶⁸, R. Soualah [id](#)^{116b}, Z. Soumami [id](#)^{35e}, D. South [id](#)⁴⁸,
 S. Spagnolo [id](#)^{70a,70b}, M. Spalla [id](#)¹¹⁰, D. Sperlich [id](#)⁵⁴, G. Spigo [id](#)³⁶, M. Spina [id](#)¹⁴⁶, S. Spinali [id](#)⁹¹,
 D.P. Spiteri [id](#)⁵⁹, M. Spousta [id](#)¹³³, E.J. Staats [id](#)³⁴, A. Stabile [id](#)^{71a,71b}, R. Stamen [id](#)^{63a},
 M. Stamenkovic [id](#)¹¹⁴, A. Stampekis [id](#)²⁰, M. Standke [id](#)²⁴, E. Stanecka [id](#)⁸⁷, M.V. Stange [id](#)⁵⁰,
 B. Stanislaus [id](#)^{17a}, M.M. Stanitzki [id](#)⁴⁸, B. Stapf [id](#)⁴⁸, E.A. Starchenko [id](#)³⁷, G.H. Stark [id](#)¹³⁶,
 J. Stark [id](#)^{102,ab}, D.M. Starko [id](#)^{156b}, P. Staroba [id](#)¹³¹, P. Starovoitov [id](#)^{63a}, S. Stärz [id](#)¹⁰⁴, R. Staszewski [id](#)⁸⁷,
 G. Stavropoulos [id](#)⁴⁶, J. Steentoft [id](#)¹⁶¹, P. Steinberg [id](#)²⁹, B. Stelzer [id](#)^{142,156a}, H.J. Stelzer [id](#)¹²⁹,
 O. Stelzer-Chilton [id](#)^{156a}, H. Stenzel [id](#)⁵⁸, T.J. Stevenson [id](#)¹⁴⁶, G.A. Stewart [id](#)³⁶, J.R. Stewart [id](#)¹²¹,
 M.C. Stockton [id](#)³⁶, G. Stoicea [id](#)^{27b}, M. Stolarski [id](#)^{130a}, S. Stonjek [id](#)¹¹⁰, A. Straessner [id](#)⁵⁰,
 J. Strandberg [id](#)¹⁴⁴, S. Strandberg [id](#)^{47a,47b}, M. Strauss [id](#)¹²⁰, T. Strebler [id](#)¹⁰², P. Strizenec [id](#)^{28b},
 R. Ströhmer [id](#)¹⁶⁶, D.M. Strom [id](#)¹²³, L.R. Strom [id](#)⁴⁸, R. Stroynowski [id](#)⁴⁴, A. Strubig [id](#)^{47a,47b},
 S.A. Stucci [id](#)²⁹, B. Stugu [id](#)¹⁶, J. Stupak [id](#)¹²⁰, N.A. Styles [id](#)⁴⁸, D. Su [id](#)¹⁴³, S. Su [id](#)^{62a}, W. Su [id](#)^{62d},
 X. Su [id](#)^{62a,66}, K. Sugizaki [id](#)¹⁵³, V.V. Sulin [id](#)³⁷, M.J. Sullivan [id](#)⁹², D.M.S. Sultan [id](#)^{78a,78b},
 L. Sultanliyeva [id](#)³⁷, S. Sultansoy [id](#)^{3b}, T. Sumida [id](#)⁸⁸, S. Sun [id](#)¹⁰⁶, S. Sun [id](#)¹⁷⁰,
 O. Sunneborn Gudnadottir [id](#)¹⁶¹, N. Sur [id](#)¹⁰², M.R. Sutton [id](#)¹⁴⁶, H. Suzuki [id](#)¹⁵⁷, M. Svatos [id](#)¹³¹,
 M. Swiatlowski [id](#)^{156a}, T. Swirski [id](#)¹⁶⁶, I. Sykora [id](#)^{28a}, M. Sykora [id](#)¹³³, T. Sykora [id](#)¹³³, D. Ta [id](#)¹⁰⁰,
 K. Tackmann [id](#)^{48,u}, A. Taffard [id](#)¹⁶⁰, R. Tafirout [id](#)^{156a}, J.S. Tafoya Vargas [id](#)⁶⁶, E.P. Takeva [id](#)⁵²,
 Y. Takubo [id](#)⁸⁴, M. Talby [id](#)¹⁰², A.A. Talyshev [id](#)³⁷, K.C. Tam [id](#)^{64b}, N.M. Tamir [id](#)¹⁵¹, A. Tanaka [id](#)¹⁵³,
 J. Tanaka [id](#)¹⁵³, R. Tanaka [id](#)⁶⁶, M. Tanasini [id](#)^{57b,57a}, Z. Tao [id](#)¹⁶⁴, S. Tapia Araya [id](#)^{137f},
 S. Tapprogge [id](#)¹⁰⁰, A. Tarek Abouelfadl Mohamed [id](#)¹⁰⁷, S. Tarem [id](#)¹⁵⁰, K. Tariq [id](#)^{14a}, G. Tarna [id](#)^{102,27b},
 G.F. Tartarelli [id](#)^{71a}, P. Tas [id](#)¹³³, M. Tasevsky [id](#)¹³¹, E. Tassi [id](#)^{43b,43a}, A.C. Tate [id](#)¹⁶², G. Tateno [id](#)¹⁵³,

Y. Tayalati ^{35e,w}, G.N. Taylor ¹⁰⁵, W. Taylor ^{156b}, H. Teagle ⁹², A.S. Tee ¹⁷⁰,
 R. Teixeira De Lima ¹⁴³, P. Teixeira-Dias ⁹⁵, J.J. Teoh ¹⁵⁵, K. Terashi ¹⁵³, J. Terron ⁹⁹,
 S. Terzo ¹³, M. Testa ⁵³, R.J. Teuscher ^{155,x}, A. Thaler ⁷⁹, O. Theiner ⁵⁶, N. Themistokleous ⁵²,
 T. Thevenaux-Pelzer ¹⁰², O. Thielmann ¹⁷¹, D.W. Thomas ⁹⁵, J.P. Thomas ²⁰, E.A. Thompson ^{17a},
 P.D. Thompson ²⁰, E. Thomson ¹²⁸, Y. Tian ⁵⁵, V. Tikhomirov ^{37,a}, Yu.A. Tikhonov ³⁷,
 S. Timoshenko ³⁷, D. Timoshyn ¹³³, E.X.L. Ting ¹, P. Tipton ¹⁷², S.H. Tlou ^{33g}, A. Tnourji ⁴⁰,
 K. Todome ^{23b,23a}, S. Todorova-Nova ¹³³, S. Todt ⁵⁰, M. Togawa ⁸⁴, J. Tojo ⁸⁹, S. Tokár ^{28a},
 K. Tokushuku ⁸⁴, O. Toldaiev ⁶⁸, R. Tombs ³², M. Tomoto ^{84,111}, L. Tompkins ^{143,o},
 K.W. Topolnicki ^{86b}, E. Torrence ¹²³, H. Torres ^{102,ab}, E. Torró Pastor ¹⁶³, M. Toscani ³⁰,
 C. Tosciri ³⁹, M. Tost ¹¹, D.R. Tovey ¹³⁹, A. Traeet ¹⁶, I.S. Trandafir ^{27b}, T. Trefzger ¹⁶⁶,
 A. Tricoli ²⁹, I.M. Trigger ^{156a}, S. Trincaz-Duvoid ¹²⁷, D.A. Trischuk ²⁶, B. Trocmé ⁶⁰,
 C. Troncon ^{71a}, L. Truong ^{33c}, M. Trzebinski ⁸⁷, A. Trzupek ⁸⁷, F. Tsai ¹⁴⁵, M. Tsai ¹⁰⁶,
 A. Tsiamis ^{152,e}, P.V. Tsiarehka ³⁷, S. Tsigaridas ^{156a}, A. Tsirigotis ^{152,s}, V. Tsiskaridze ¹⁵⁵,
 E.G. Tskhadadze ^{149a}, M. Tsopoulou ^{152,e}, Y. Tsujikawa ⁸⁸, I.I. Tsukerman ³⁷, V. Tsulaia ^{17a},
 S. Tsuno ⁸⁴, O. Tsur ¹⁵⁰, K. Tsurii ¹¹⁸, D. Tsybychev ¹⁴⁵, Y. Tu ^{64b}, A. Tudorache ^{27b},
 V. Tudorache ^{27b}, A.N. Tuna ³⁶, S. Turchikhin ³⁸, I. Turk Cakir ^{3a}, R. Turra ^{71a},
 T. Turtuvshin ^{38,y}, P.M. Tuts ⁴¹, S. Tzamarias ^{152,e}, P. Tzanis ¹⁰, E. Tzovara ¹⁰⁰, K. Uchida ¹⁵³,
 F. Ukegawa ¹⁵⁷, P.A. Ulloa Poblete ^{137c,137b}, E.N. Umaka ²⁹, G. Unal ³⁶, M. Unal ¹¹,
 A. Undrus ²⁹, G. Unel ¹⁶⁰, J. Urban ^{28b}, P. Urquijo ¹⁰⁵, G. Usai ⁸, R. Ushioda ¹⁵⁴,
 M. Usman ¹⁰⁸, Z. Uysal ^{21b}, L. Vacavant ¹⁰², V. Vacek ¹³², B. Vachon ¹⁰⁴, K.O.H. Vadla ¹²⁵,
 T. Vafeiadis ³⁶, A. Vaitkus ⁹⁶, C. Valderanis ¹⁰⁹, E. Valdes Santurio ^{47a,47b}, M. Valente ^{156a},
 S. Valentinetti ^{23b,23a}, A. Valero ¹⁶³, E. Valiente Moreno ¹⁶³, A. Vallier ^{102,ab},
 J.A. Valls Ferrer ¹⁶³, D.R. Van Arneman ¹¹⁴, T.R. Van Daalen ¹³⁸, A. Van Der Graaf ⁴⁹,
 P. Van Gemmeren ⁶, M. Van Rijnbach ^{125,36}, S. Van Stroud ⁹⁶, I. Van Vulpen ¹¹⁴,
 M. Vanadia ^{76a,76b}, W. Vandelli ³⁶, M. Vandenbroucke ¹³⁵, E.R. Vandewall ¹²¹, D. Vannicola ¹⁵¹,
 L. Vannoli ^{57b,57a}, R. Vari ^{75a}, E.W. Varnes ⁷, C. Varni ^{17b}, T. Varol ¹⁴⁸, D. Varouchas ⁶⁶,
 L. Varriale ¹⁶³, K.E. Varvell ¹⁴⁷, M.E. Vasile ^{27b}, L. Vaslin ⁴⁰, G.A. Vasquez ¹⁶⁵, F. Vazeille ⁴⁰,
 T. Vazquez Schroeder ³⁶, J. Veatch ³¹, V. Vecchio ¹⁰¹, M.J. Veen ¹⁰³, I. Veliscek ¹²⁶,
 L.M. Veloce ¹⁵⁵, F. Veloso ^{130a,130c}, S. Veneziano ^{75a}, A. Ventura ^{70a,70b}, A. Verbytskyi ¹¹⁰,
 M. Verducci ^{74a,74b}, C. Vergis ²⁴, M. Verissimo De Araujo ^{83b}, W. Verkerke ¹¹⁴,
 J.C. Vermeulen ¹¹⁴, C. Vernieri ¹⁴³, M. Vessella ¹⁰³, M.C. Vetterli ^{142,ag}, A. Vgenopoulos ^{152,e},
 N. Viaux Maira ^{137f}, T. Vickey ¹³⁹, O.E. Vickey Boeriu ¹³⁹, G.H.A. Viehhauser ¹²⁶, L. Viganì ^{63b},
 M. Villa ^{23b,23a}, M. Villaplana Perez ¹⁶³, E.M. Villhauer ⁵², E. Vilucchi ⁵³, M.G. Vincier ³⁴,
 G.S. Virdee ²⁰, A. Vishwakarma ⁵², A. Visibile ¹¹⁴, C. Vittori ³⁶, I. Vivarelli ¹⁴⁶, V. Vladimirov ¹⁶⁷,
 E. Voevodina ¹¹⁰, F. Vogel ¹⁰⁹, P. Vokac ¹³², J. Von Ahnen ⁴⁸, E. Von Toerne ²⁴,
 B. Vormwald ³⁶, V. Vorobel ¹³³, K. Vorobev ³⁷, M. Vos ¹⁶³, K. Voss ¹⁴¹, J.H. Vossebeld ⁹²,
 M. Vozak ¹¹⁴, L. Vozdecky ⁹⁴, N. Vranjes ¹⁵, M. Vranjes Milosavljevic ¹⁵, M. Vreeswijk ¹¹⁴,
 R. Vuillermet ³⁶, O. Vujinovic ¹⁰⁰, I. Vukotic ³⁹, S. Wada ¹⁵⁷, C. Wagner ¹⁰³, J.M. Wagner ^{17a},
 W. Wagner ¹⁷¹, S. Wahdan ¹⁷¹, H. Wahlberg ⁹⁰, R. Wakasa ¹⁵⁷, M. Wakida ¹¹¹, J. Walder ¹³⁴,
 R. Walker ¹⁰⁹, W. Walkowiak ¹⁴¹, A. Wall ¹²⁸, T. Wamorkar ⁶, A.Z. Wang ¹⁷⁰, C. Wang ¹⁰⁰,
 C. Wang ^{62c}, H. Wang ^{17a}, J. Wang ^{64a}, R.-J. Wang ¹⁰⁰, R. Wang ⁶¹, R. Wang ⁶,
 S.M. Wang ¹⁴⁸, S. Wang ^{62b}, T. Wang ^{62a}, W.T. Wang ⁸⁰, W. Wang ^{14a}, X. Wang ^{14c},
 X. Wang ¹⁶², X. Wang ^{62c}, Y. Wang ^{62d}, Y. Wang ^{14c}, Z. Wang ¹⁰⁶, Z. Wang ^{62d,51,62c},
 Z. Wang ¹⁰⁶, A. Warburton ¹⁰⁴, R.J. Ward ²⁰, N. Warrack ⁵⁹, A.T. Watson ²⁰, H. Watson ⁵⁹,
 M.F. Watson ²⁰, E. Watton ^{59,134}, G. Watts ¹³⁸, B.M. Waugh ⁹⁶, C. Weber ²⁹, H.A. Weber ¹⁸,
 M.S. Weber ¹⁹, S.M. Weber ^{63a}, C. Wei ^{62a}, Y. Wei ¹²⁶, A.R. Weidberg ¹²⁶, E.J. Weik ¹¹⁷,
 J. Weingarten ⁴⁹, M. Weirich ¹⁰⁰, C. Weiser ⁵⁴, C.J. Wells ⁴⁸, T. Wenaus ²⁹, B. Wendland ⁴⁹,

T. Wengler ³⁶, N.S. Wenke ¹¹⁰, N. Wermes ²⁴, M. Wessels ^{63a}, K. Whalen ¹²³, A.M. Wharton ⁹¹, A.S. White ⁶¹, A. White ⁸, M.J. White ¹, D. Whiteson ¹⁶⁰, L. Wickremasinghe ¹²⁴, W. Wiedenmann ¹⁷⁰, C. Wiel ⁵⁰, M. Wielers ¹³⁴, C. Wiglesworth ⁴², D.J. Wilbern ¹²⁰, H.G. Wilkens ³⁶, D.M. Williams ⁴¹, H.H. Williams ¹²⁸, S. Williams ³², S. Willocq ¹⁰³, B.J. Wilson ¹⁰¹, P.J. Windischhofer ³⁹, F.I. Winkel ³⁰, F. Winklmeier ¹²³, B.T. Winter ⁵⁴, J.K. Winter ¹⁰¹, M. Wittgen ¹⁴³, M. Wobisch ⁹⁷, Z. Wolffs ¹¹⁴, R. Wölker ¹²⁶, J. Wollrath ¹⁶⁰, M.W. Wolter ⁸⁷, H. Wolters ^{130a,130c}, A.F. Wongel ⁴⁸, S.D. Worm ⁴⁸, B.K. Wosiek ⁸⁷, K.W. Woźniak ⁸⁷, S. Wozniewski ⁵⁵, K. Wraight ⁵⁹, C. Wu ²⁰, J. Wu ^{14a,14e}, M. Wu ^{64a}, M. Wu ¹¹³, S.L. Wu ¹⁷⁰, X. Wu ⁵⁶, Y. Wu ^{62a}, Z. Wu ¹³⁵, J. Wuerzinger ^{110,ae}, T.R. Wyatt ¹⁰¹, B.M. Wynne ⁵², S. Xella ⁴², L. Xia ^{14c}, M. Xia ^{14b}, J. Xiang ^{64c}, X. Xiao ¹⁰⁶, M. Xie ^{62a}, X. Xie ^{62a}, S. Xin ^{14a,14e}, J. Xiong ^{17a}, D. Xu ^{14a}, H. Xu ^{62a}, L. Xu ^{62a}, R. Xu ¹²⁸, T. Xu ¹⁰⁶, Y. Xu ^{14b}, Z. Xu ⁵², Z. Xu ^{14a}, B. Yabsley ¹⁴⁷, S. Yacoub ^{33a}, N. Yamaguchi ⁸⁹, Y. Yamaguchi ¹⁵⁴, E. Yamashita ¹⁵³, H. Yamauchi ¹⁵⁷, T. Yamazaki ^{17a}, Y. Yamazaki ⁸⁵, J. Yan ^{62c}, S. Yan ¹²⁶, Z. Yan ²⁵, H.J. Yang ^{62c,62d}, H.T. Yang ^{62a}, S. Yang ^{62a}, T. Yang ^{64c}, X. Yang ^{62a}, X. Yang ^{14a}, Y. Yang ⁴⁴, Y. Yang ^{62a}, Z. Yang ^{62a}, W-M. Yao ^{17a}, Y.C. Yap ⁴⁸, H. Ye ^{14c}, H. Ye ⁵⁵, J. Ye ⁴⁴, S. Ye ²⁹, X. Ye ^{62a}, Y. Yeh ⁹⁶, I. Yeletsikh ³⁸, B.K. Yeo ^{17b}, M.R. Yexley ⁹⁶, P. Yin ⁴¹, K. Yorita ¹⁶⁸, S. Younas ^{27b}, C.J.S. Young ³⁶, C. Young ¹⁴³, Y. Yu ^{62a}, M. Yuan ¹⁰⁶, R. Yuan ^{62b,k}, L. Yue ⁹⁶, M. Zaazoua ^{62a}, B. Zabinski ³⁷, E. Zaid ⁵², T. Zakareishvili ^{149b}, N. Zakharchuk ³⁴, S. Zambito ⁵⁶, J.A. Zamora Saa ^{137d,137b}, J. Zang ¹⁵³, D. Zanzi ⁵⁴, O. Zaplatilek ¹³², C. Zeitnitz ¹⁷¹, H. Zeng ^{14a}, J.C. Zeng ¹⁶², D.T. Zenger Jr ²⁶, O. Zenin ³⁷, T. Ženiš ^{28a}, S. Zenz ⁹⁴, S. Zerradi ^{35a}, D. Zerwas ⁶⁶, M. Zhai ^{14a,14e}, B. Zhang ^{14c}, D.F. Zhang ¹³⁹, J. Zhang ^{62b}, J. Zhang ⁶, K. Zhang ^{14a,14e}, L. Zhang ^{14c}, P. Zhang ^{14a,14e}, R. Zhang ¹⁷⁰, S. Zhang ¹⁰⁶, T. Zhang ¹⁵³, X. Zhang ^{62c}, X. Zhang ^{62b}, Y. Zhang ^{62c,5}, Y. Zhang ⁹⁶, Z. Zhang ^{17a}, Z. Zhang ⁶⁶, H. Zhao ¹³⁸, P. Zhao ⁵¹, T. Zhao ^{62b}, Y. Zhao ¹³⁶, Z. Zhao ^{62a}, A. Zhemchugov ³⁸, K. Zheng ¹⁶², X. Zheng ^{62a}, Z. Zheng ¹⁴³, D. Zhong ¹⁶², B. Zhou ¹⁰⁶, H. Zhou ⁷, N. Zhou ^{62c}, Y. Zhou ⁷, C.G. Zhu ^{62b}, J. Zhu ¹⁰⁶, Y. Zhu ^{62c}, Y. Zhu ^{62a}, X. Zhuang ^{14a}, K. Zhukov ³⁷, V. Zhulanov ³⁷, N.I. Zimine ³⁸, J. Zinsser ^{63b}, M. Ziolkowski ¹⁴¹, L. Živković ¹⁵, A. Zoccoli ^{23b,23a}, K. Zoch ⁵⁶, T.G. Zorbas ¹³⁹, O. Zormpa ⁴⁶, W. Zou ⁴¹, L. Zwalinski ³⁶.

¹Department of Physics, University of Adelaide, Adelaide; Australia.

²Department of Physics, University of Alberta, Edmonton AB; Canada.

³(^a) Department of Physics, Ankara University, Ankara; (^b) Division of Physics, TOBB University of Economics and Technology, Ankara; Türkiye.

⁴LAPP, Université Savoie Mont Blanc, CNRS/IN2P3, Annecy; France.

⁵APC, Université Paris Cité, CNRS/IN2P3, Paris; France.

⁶High Energy Physics Division, Argonne National Laboratory, Argonne IL; United States of America.

⁷Department of Physics, University of Arizona, Tucson AZ; United States of America.

⁸Department of Physics, University of Texas at Arlington, Arlington TX; United States of America.

⁹Physics Department, National and Kapodistrian University of Athens, Athens; Greece.

¹⁰Physics Department, National Technical University of Athens, Zografou; Greece.

¹¹Department of Physics, University of Texas at Austin, Austin TX; United States of America.

¹²Institute of Physics, Azerbaijan Academy of Sciences, Baku; Azerbaijan.

¹³Institut de Física d'Altes Energies (IFAE), Barcelona Institute of Science and Technology, Barcelona; Spain.

¹⁴(^a) Institute of High Energy Physics, Chinese Academy of Sciences, Beijing; (^b) Physics Department, Tsinghua University, Beijing; (^c) Department of Physics, Nanjing University, Nanjing; (^d) School of Science,

Shenzhen Campus of Sun Yat-sen University;^(e)University of Chinese Academy of Science (UCAS), Beijing; China.

¹⁵Institute of Physics, University of Belgrade, Belgrade; Serbia.

¹⁶Department for Physics and Technology, University of Bergen, Bergen; Norway.

¹⁷(^a)Physics Division, Lawrence Berkeley National Laboratory, Berkeley CA;^(b)University of California, Berkeley CA; United States of America.

¹⁸Institut für Physik, Humboldt Universität zu Berlin, Berlin; Germany.

¹⁹Albert Einstein Center for Fundamental Physics and Laboratory for High Energy Physics, University of Bern, Bern; Switzerland.

²⁰School of Physics and Astronomy, University of Birmingham, Birmingham; United Kingdom.

²¹(^a)Department of Physics, Bogazici University, Istanbul;^(b)Department of Physics Engineering, Gaziantep University, Gaziantep;^(c)Department of Physics, Istanbul University, Istanbul; Türkiye.

²²(^a)Facultad de Ciencias y Centro de Investigaciones, Universidad Antonio Nariño, Bogotá;^(b)Departamento de Física, Universidad Nacional de Colombia, Bogotá; Colombia.

²³(^a)Dipartimento di Fisica e Astronomia A. Righi, Università di Bologna, Bologna;^(b)INFN Sezione di Bologna; Italy.

²⁴Physikalisches Institut, Universität Bonn, Bonn; Germany.

²⁵Department of Physics, Boston University, Boston MA; United States of America.

²⁶Department of Physics, Brandeis University, Waltham MA; United States of America.

²⁷(^a)Transilvania University of Brasov, Brasov;^(b)Horia Hulubei National Institute of Physics and Nuclear Engineering, Bucharest;^(c)Department of Physics, Alexandru Ioan Cuza University of Iasi, Iasi;^(d)National Institute for Research and Development of Isotopic and Molecular Technologies, Physics Department, Cluj-Napoca;^(e)University Politehnica Bucharest, Bucharest;^(f)West University in Timisoara, Timisoara;^(g)Faculty of Physics, University of Bucharest, Bucharest; Romania.

²⁸(^a)Faculty of Mathematics, Physics and Informatics, Comenius University, Bratislava;^(b)Department of Subnuclear Physics, Institute of Experimental Physics of the Slovak Academy of Sciences, Kosice; Slovak Republic.

²⁹Physics Department, Brookhaven National Laboratory, Upton NY; United States of America.

³⁰Universidad de Buenos Aires, Facultad de Ciencias Exactas y Naturales, Departamento de Física, y CONICET, Instituto de Física de Buenos Aires (IFIBA), Buenos Aires; Argentina.

³¹California State University, CA; United States of America.

³²Cavendish Laboratory, University of Cambridge, Cambridge; United Kingdom.

³³(^a)Department of Physics, University of Cape Town, Cape Town;^(b)iThemba Labs, Western Cape;^(c)Department of Mechanical Engineering Science, University of Johannesburg, Johannesburg;

^(d)National Institute of Physics, University of the Philippines Diliman (Philippines);^(e)University of South Africa, Department of Physics, Pretoria;^(f)University of Zululand, KwaDlangezwa;^(g)School of Physics, University of the Witwatersrand, Johannesburg; South Africa.

³⁴Department of Physics, Carleton University, Ottawa ON; Canada.

³⁵(^a)Faculté des Sciences Ain Chock, Réseau Universitaire de Physique des Hautes Energies - Université Hassan II, Casablanca;^(b)Faculté des Sciences, Université Ibn-Tofail, Kénitra;^(c)Faculté des Sciences Semlalia, Université Cadi Ayyad, LPHEA-Marrakech;^(d)LPMR, Faculté des Sciences, Université Mohamed Premier, Oujda;^(e)Faculté des sciences, Université Mohammed V, Rabat;^(f)Institute of Applied Physics, Mohammed VI Polytechnic University, Ben Guerir; Morocco.

³⁶CERN, Geneva; Switzerland.

³⁷Affiliated with an institute covered by a cooperation agreement with CERN.

³⁸Affiliated with an international laboratory covered by a cooperation agreement with CERN.

³⁹Enrico Fermi Institute, University of Chicago, Chicago IL; United States of America.

- ⁴⁰LPC, Université Clermont Auvergne, CNRS/IN2P3, Clermont-Ferrand; France.
- ⁴¹Nevis Laboratory, Columbia University, Irvington NY; United States of America.
- ⁴²Niels Bohr Institute, University of Copenhagen, Copenhagen; Denmark.
- ⁴³(^a)Dipartimento di Fisica, Università della Calabria, Rende; (^b)INFN Gruppo Collegato di Cosenza, Laboratori Nazionali di Frascati; Italy.
- ⁴⁴Physics Department, Southern Methodist University, Dallas TX; United States of America.
- ⁴⁵Physics Department, University of Texas at Dallas, Richardson TX; United States of America.
- ⁴⁶National Centre for Scientific Research "Demokritos", Agia Paraskevi; Greece.
- ⁴⁷(^a)Department of Physics, Stockholm University; (^b)Oskar Klein Centre, Stockholm; Sweden.
- ⁴⁸Deutsches Elektronen-Synchrotron DESY, Hamburg and Zeuthen; Germany.
- ⁴⁹Fakultät Physik , Technische Universität Dortmund, Dortmund; Germany.
- ⁵⁰Institut für Kern- und Teilchenphysik, Technische Universität Dresden, Dresden; Germany.
- ⁵¹Department of Physics, Duke University, Durham NC; United States of America.
- ⁵²SUPA - School of Physics and Astronomy, University of Edinburgh, Edinburgh; United Kingdom.
- ⁵³INFN e Laboratori Nazionali di Frascati, Frascati; Italy.
- ⁵⁴Physikalisches Institut, Albert-Ludwigs-Universität Freiburg, Freiburg; Germany.
- ⁵⁵II. Physikalisches Institut, Georg-August-Universität Göttingen, Göttingen; Germany.
- ⁵⁶Département de Physique Nucléaire et Corpusculaire, Université de Genève, Genève; Switzerland.
- ⁵⁷(^a)Dipartimento di Fisica, Università di Genova, Genova; (^b)INFN Sezione di Genova; Italy.
- ⁵⁸II. Physikalisches Institut, Justus-Liebig-Universität Giessen, Giessen; Germany.
- ⁵⁹SUPA - School of Physics and Astronomy, University of Glasgow, Glasgow; United Kingdom.
- ⁶⁰LPSC, Université Grenoble Alpes, CNRS/IN2P3, Grenoble INP, Grenoble; France.
- ⁶¹Laboratory for Particle Physics and Cosmology, Harvard University, Cambridge MA; United States of America.
- ⁶²(^a)Department of Modern Physics and State Key Laboratory of Particle Detection and Electronics, University of Science and Technology of China, Hefei; (^b)Institute of Frontier and Interdisciplinary Science and Key Laboratory of Particle Physics and Particle Irradiation (MOE), Shandong University, Qingdao; (^c)School of Physics and Astronomy, Shanghai Jiao Tong University, Key Laboratory for Particle Astrophysics and Cosmology (MOE), SKLPPC, Shanghai; (^d)Tsung-Dao Lee Institute, Shanghai; China.
- ⁶³(^a)Kirchhoff-Institut für Physik, Ruprecht-Karls-Universität Heidelberg, Heidelberg; (^b)Physikalisches Institut, Ruprecht-Karls-Universität Heidelberg, Heidelberg; Germany.
- ⁶⁴(^a)Department of Physics, Chinese University of Hong Kong, Shatin, N.T., Hong Kong; (^b)Department of Physics, University of Hong Kong, Hong Kong; (^c)Department of Physics and Institute for Advanced Study, Hong Kong University of Science and Technology, Clear Water Bay, Kowloon, Hong Kong; China.
- ⁶⁵Department of Physics, National Tsing Hua University, Hsinchu; Taiwan.
- ⁶⁶IJCLab, Université Paris-Saclay, CNRS/IN2P3, 91405, Orsay; France.
- ⁶⁷Centro Nacional de Microelectrónica (IMB-CNM-CSIC), Barcelona; Spain.
- ⁶⁸Department of Physics, Indiana University, Bloomington IN; United States of America.
- ⁶⁹(^a)INFN Gruppo Collegato di Udine, Sezione di Trieste, Udine; (^b)ICTP, Trieste; (^c)Dipartimento Politecnico di Ingegneria e Architettura, Università di Udine, Udine; Italy.
- ⁷⁰(^a)INFN Sezione di Lecce; (^b)Dipartimento di Matematica e Fisica, Università del Salento, Lecce; Italy.
- ⁷¹(^a)INFN Sezione di Milano; (^b)Dipartimento di Fisica, Università di Milano, Milano; Italy.
- ⁷²(^a)INFN Sezione di Napoli; (^b)Dipartimento di Fisica, Università di Napoli, Napoli; Italy.
- ⁷³(^a)INFN Sezione di Pavia; (^b)Dipartimento di Fisica, Università di Pavia, Pavia; Italy.
- ⁷⁴(^a)INFN Sezione di Pisa; (^b)Dipartimento di Fisica E. Fermi, Università di Pisa, Pisa; Italy.
- ⁷⁵(^a)INFN Sezione di Roma; (^b)Dipartimento di Fisica, Sapienza Università di Roma, Roma; Italy.
- ⁷⁶(^a)INFN Sezione di Roma Tor Vergata; (^b)Dipartimento di Fisica, Università di Roma Tor Vergata,

Roma; Italy.

^{77(a)}INFN Sezione di Roma Tre; ^(b)Dipartimento di Matematica e Fisica, Università Roma Tre, Roma; Italy.

^{78(a)}INFN-TIFPA; ^(b)Università degli Studi di Trento, Trento; Italy.

⁷⁹Universität Innsbruck, Department of Astro and Particle Physics, Innsbruck; Austria.

⁸⁰University of Iowa, Iowa City IA; United States of America.

⁸¹Department of Physics and Astronomy, Iowa State University, Ames IA; United States of America.

⁸²Istinye University, Sariyer, Istanbul; Türkiye.

^{83(a)}Departamento de Engenharia Elétrica, Universidade Federal de Juiz de Fora (UFJF), Juiz de Fora; ^(b)Universidade Federal do Rio De Janeiro COPPE/EE/IF, Rio de Janeiro; ^(c)Instituto de Física, Universidade de São Paulo, São Paulo; ^(d)Rio de Janeiro State University, Rio de Janeiro; Brazil.

⁸⁴KEK, High Energy Accelerator Research Organization, Tsukuba; Japan.

⁸⁵Graduate School of Science, Kobe University, Kobe; Japan.

^{86(a)}AGH University of Krakow, Faculty of Physics and Applied Computer Science, Krakow; ^(b)Marian Smoluchowski Institute of Physics, Jagiellonian University, Krakow; Poland.

⁸⁷Institute of Nuclear Physics Polish Academy of Sciences, Krakow; Poland.

⁸⁸Faculty of Science, Kyoto University, Kyoto; Japan.

⁸⁹Research Center for Advanced Particle Physics and Department of Physics, Kyushu University, Fukuoka ; Japan.

⁹⁰Instituto de Física La Plata, Universidad Nacional de La Plata and CONICET, La Plata; Argentina.

⁹¹Physics Department, Lancaster University, Lancaster; United Kingdom.

⁹²Oliver Lodge Laboratory, University of Liverpool, Liverpool; United Kingdom.

⁹³Department of Experimental Particle Physics, Jožef Stefan Institute and Department of Physics, University of Ljubljana, Ljubljana; Slovenia.

⁹⁴School of Physics and Astronomy, Queen Mary University of London, London; United Kingdom.

⁹⁵Department of Physics, Royal Holloway University of London, Egham; United Kingdom.

⁹⁶Department of Physics and Astronomy, University College London, London; United Kingdom.

⁹⁷Louisiana Tech University, Ruston LA; United States of America.

⁹⁸Fysiska institutionen, Lunds universitet, Lund; Sweden.

⁹⁹Departamento de Física Teórica C-15 and CIAFF, Universidad Autónoma de Madrid, Madrid; Spain.

¹⁰⁰Institut für Physik, Universität Mainz, Mainz; Germany.

¹⁰¹School of Physics and Astronomy, University of Manchester, Manchester; United Kingdom.

¹⁰²CPPM, Aix-Marseille Université, CNRS/IN2P3, Marseille; France.

¹⁰³Department of Physics, University of Massachusetts, Amherst MA; United States of America.

¹⁰⁴Department of Physics, McGill University, Montreal QC; Canada.

¹⁰⁵School of Physics, University of Melbourne, Victoria; Australia.

¹⁰⁶Department of Physics, University of Michigan, Ann Arbor MI; United States of America.

¹⁰⁷Department of Physics and Astronomy, Michigan State University, East Lansing MI; United States of America.

¹⁰⁸Group of Particle Physics, University of Montreal, Montreal QC; Canada.

¹⁰⁹Fakultät für Physik, Ludwig-Maximilians-Universität München, München; Germany.

¹¹⁰Max-Planck-Institut für Physik (Werner-Heisenberg-Institut), München; Germany.

¹¹¹Graduate School of Science and Kobayashi-Maskawa Institute, Nagoya University, Nagoya; Japan.

¹¹²Department of Physics and Astronomy, University of New Mexico, Albuquerque NM; United States of America.

¹¹³Institute for Mathematics, Astrophysics and Particle Physics, Radboud University/Nikhef, Nijmegen; Netherlands.

- ¹¹⁴Nikhef National Institute for Subatomic Physics and University of Amsterdam, Amsterdam; Netherlands.
- ¹¹⁵Department of Physics, Northern Illinois University, DeKalb IL; United States of America.
- ¹¹⁶(^a)New York University Abu Dhabi, Abu Dhabi;(^b)University of Sharjah, Sharjah; United Arab Emirates.
- ¹¹⁷Department of Physics, New York University, New York NY; United States of America.
- ¹¹⁸Ochanomizu University, Otsuka, Bunkyo-ku, Tokyo; Japan.
- ¹¹⁹Ohio State University, Columbus OH; United States of America.
- ¹²⁰Homer L. Dodge Department of Physics and Astronomy, University of Oklahoma, Norman OK; United States of America.
- ¹²¹Department of Physics, Oklahoma State University, Stillwater OK; United States of America.
- ¹²²Palacký University, Joint Laboratory of Optics, Olomouc; Czech Republic.
- ¹²³Institute for Fundamental Science, University of Oregon, Eugene, OR; United States of America.
- ¹²⁴Graduate School of Science, Osaka University, Osaka; Japan.
- ¹²⁵Department of Physics, University of Oslo, Oslo; Norway.
- ¹²⁶Department of Physics, Oxford University, Oxford; United Kingdom.
- ¹²⁷LPNHE, Sorbonne Université, Université Paris Cité, CNRS/IN2P3, Paris; France.
- ¹²⁸Department of Physics, University of Pennsylvania, Philadelphia PA; United States of America.
- ¹²⁹Department of Physics and Astronomy, University of Pittsburgh, Pittsburgh PA; United States of America.
- ¹³⁰(^a)Laboratório de Instrumentação e Física Experimental de Partículas - LIP, Lisboa;(^b)Departamento de Física, Faculdade de Ciências, Universidade de Lisboa, Lisboa;(^c)Departamento de Física, Universidade de Coimbra, Coimbra;(^d)Centro de Física Nuclear da Universidade de Lisboa, Lisboa;(^e)Departamento de Física, Universidade do Minho, Braga;(^f)Departamento de Física Teórica y del Cosmos, Universidad de Granada, Granada (Spain);(^g)Departamento de Física, Instituto Superior Técnico, Universidade de Lisboa, Lisboa; Portugal.
- ¹³¹Institute of Physics of the Czech Academy of Sciences, Prague; Czech Republic.
- ¹³²Czech Technical University in Prague, Prague; Czech Republic.
- ¹³³Charles University, Faculty of Mathematics and Physics, Prague; Czech Republic.
- ¹³⁴Particle Physics Department, Rutherford Appleton Laboratory, Didcot; United Kingdom.
- ¹³⁵IRFU, CEA, Université Paris-Saclay, Gif-sur-Yvette; France.
- ¹³⁶Santa Cruz Institute for Particle Physics, University of California Santa Cruz, Santa Cruz CA; United States of America.
- ¹³⁷(^a)Departamento de Física, Pontificia Universidad Católica de Chile, Santiago;(^b)Millennium Institute for Subatomic physics at high energy frontier (SAPHIR), Santiago;(^c)Instituto de Investigación Multidisciplinario en Ciencia y Tecnología, y Departamento de Física, Universidad de La Serena;(^d)Universidad Andres Bello, Department of Physics, Santiago;(^e)Instituto de Alta Investigación, Universidad de Tarapacá, Arica;(^f)Departamento de Física, Universidad Técnica Federico Santa María, Valparaíso; Chile.
- ¹³⁸Department of Physics, University of Washington, Seattle WA; United States of America.
- ¹³⁹Department of Physics and Astronomy, University of Sheffield, Sheffield; United Kingdom.
- ¹⁴⁰Department of Physics, Shinshu University, Nagano; Japan.
- ¹⁴¹Department Physik, Universität Siegen, Siegen; Germany.
- ¹⁴²Department of Physics, Simon Fraser University, Burnaby BC; Canada.
- ¹⁴³SLAC National Accelerator Laboratory, Stanford CA; United States of America.
- ¹⁴⁴Department of Physics, Royal Institute of Technology, Stockholm; Sweden.
- ¹⁴⁵Departments of Physics and Astronomy, Stony Brook University, Stony Brook NY; United States of

America.

¹⁴⁶Department of Physics and Astronomy, University of Sussex, Brighton; United Kingdom.

¹⁴⁷School of Physics, University of Sydney, Sydney; Australia.

¹⁴⁸Institute of Physics, Academia Sinica, Taipei; Taiwan.

¹⁴⁹^(a)E. Andronikashvili Institute of Physics, Iv. Javakhishvili Tbilisi State University, Tbilisi; ^(b)High Energy Physics Institute, Tbilisi State University, Tbilisi; ^(c)University of Georgia, Tbilisi; Georgia.

¹⁵⁰Department of Physics, Technion, Israel Institute of Technology, Haifa; Israel.

¹⁵¹Raymond and Beverly Sackler School of Physics and Astronomy, Tel Aviv University, Tel Aviv; Israel.

¹⁵²Department of Physics, Aristotle University of Thessaloniki, Thessaloniki; Greece.

¹⁵³International Center for Elementary Particle Physics and Department of Physics, University of Tokyo, Tokyo; Japan.

¹⁵⁴Department of Physics, Tokyo Institute of Technology, Tokyo; Japan.

¹⁵⁵Department of Physics, University of Toronto, Toronto ON; Canada.

¹⁵⁶^(a)TRIUMF, Vancouver BC; ^(b)Department of Physics and Astronomy, York University, Toronto ON; Canada.

¹⁵⁷Division of Physics and Tomonaga Center for the History of the Universe, Faculty of Pure and Applied Sciences, University of Tsukuba, Tsukuba; Japan.

¹⁵⁸Department of Physics and Astronomy, Tufts University, Medford MA; United States of America.

¹⁵⁹United Arab Emirates University, Al Ain; United Arab Emirates.

¹⁶⁰Department of Physics and Astronomy, University of California Irvine, Irvine CA; United States of America.

¹⁶¹Department of Physics and Astronomy, University of Uppsala, Uppsala; Sweden.

¹⁶²Department of Physics, University of Illinois, Urbana IL; United States of America.

¹⁶³Instituto de Física Corpuscular (IFIC), Centro Mixto Universidad de Valencia - CSIC, Valencia; Spain.

¹⁶⁴Department of Physics, University of British Columbia, Vancouver BC; Canada.

¹⁶⁵Department of Physics and Astronomy, University of Victoria, Victoria BC; Canada.

¹⁶⁶Fakultät für Physik und Astronomie, Julius-Maximilians-Universität Würzburg, Würzburg; Germany.

¹⁶⁷Department of Physics, University of Warwick, Coventry; United Kingdom.

¹⁶⁸Waseda University, Tokyo; Japan.

¹⁶⁹Department of Particle Physics and Astrophysics, Weizmann Institute of Science, Rehovot; Israel.

¹⁷⁰Department of Physics, University of Wisconsin, Madison WI; United States of America.

¹⁷¹Fakultät für Mathematik und Naturwissenschaften, Fachgruppe Physik, Bergische Universität Wuppertal, Wuppertal; Germany.

¹⁷²Department of Physics, Yale University, New Haven CT; United States of America.

^a Also Affiliated with an institute covered by a cooperation agreement with CERN.

^b Also at An-Najah National University, Nablus; Palestine.

^c Also at Borough of Manhattan Community College, City University of New York, New York NY; United States of America.

^d Also at Center for High Energy Physics, Peking University; China.

^e Also at Center for Interdisciplinary Research and Innovation (CIRI-AUTH), Thessaloniki; Greece.

^f Also at Centro Studi e Ricerche Enrico Fermi; Italy.

^g Also at CERN, Geneva; Switzerland.

^h Also at Département de Physique Nucléaire et Corpusculaire, Université de Genève, Genève; Switzerland.

ⁱ Also at Departament de Física de la Universitat Autònoma de Barcelona, Barcelona; Spain.

^j Also at Department of Financial and Management Engineering, University of the Aegean, Chios; Greece.

^k Also at Department of Physics and Astronomy, Michigan State University, East Lansing MI; United

States of America.

^l Also at Department of Physics, Ben Gurion University of the Negev, Beer Sheva; Israel.

^m Also at Department of Physics, California State University, Sacramento; United States of America.

ⁿ Also at Department of Physics, King's College London, London; United Kingdom.

^o Also at Department of Physics, Stanford University, Stanford CA; United States of America.

^p Also at Department of Physics, University of Fribourg, Fribourg; Switzerland.

^q Also at Department of Physics, University of Thessaly; Greece.

^r Also at Department of Physics, Westmont College, Santa Barbara; United States of America.

^s Also at Hellenic Open University, Patras; Greece.

^t Also at Institutio Catalana de Recerca i Estudis Avancats, ICREA, Barcelona; Spain.

^u Also at Institut für Experimentalphysik, Universität Hamburg, Hamburg; Germany.

^v Also at Institute for Nuclear Research and Nuclear Energy (INRNE) of the Bulgarian Academy of Sciences, Sofia; Bulgaria.

^w Also at Institute of Applied Physics, Mohammed VI Polytechnic University, Ben Guerir; Morocco.

^x Also at Institute of Particle Physics (IPP); Canada.

^y Also at Institute of Physics and Technology, Ulaanbaatar; Mongolia.

^z Also at Institute of Physics, Azerbaijan Academy of Sciences, Baku; Azerbaijan.

^{aa} Also at Institute of Theoretical Physics, Iliia State University, Tbilisi; Georgia.

^{ab} Also at L2IT, Université de Toulouse, CNRS/IN2P3, UPS, Toulouse; France.

^{ac} Also at Lawrence Livermore National Laboratory, Livermore; United States of America.

^{ad} Also at National Institute of Physics, University of the Philippines Diliman (Philippines); Philippines.

^{ae} Also at Technical University of Munich, Munich; Germany.

^{af} Also at The Collaborative Innovation Center of Quantum Matter (CICQM), Beijing; China.

^{ag} Also at TRIUMF, Vancouver BC; Canada.

^{ah} Also at Università di Napoli Parthenope, Napoli; Italy.

^{ai} Also at University of Colorado Boulder, Department of Physics, Colorado; United States of America.

^{aj} Also at Washington College, Chestertown, MD; United States of America.

^{ak} Also at Yeditepe University, Physics Department, Istanbul; Türkiye.

* Deceased